

UNIVERSITA' DEGLI STUDI DI NAPOLI

FEDERICO II



Ph.D. School in Chemical Sciences

XXVI course

**DNA repair and protection mechanisms in  
*Escherichia coli* and *Mycobacterium  
tuberculosis***

**Pamela di Pasquale**

Tutors:

Prof. Piero Pucci

Prof. Angela Duilio

Supervisor:

Prof. Filomena Sica

Coordinator:

Prof. Luigi Paduano

**Ai miei genitori,  
a mia sorella**

# Table of Contents

<b>Summary.....</b>	<b>1</b>
<b>Chapter 1: Introduction .....</b>	<b>3</b>
1. Alkylating stress and DNA response.....	4
1.1 Alkylating molecules.....	4
1.2 Analyses of DNA adducts.....	9
1.3 DNA alkylation response of <i>Escherichia coli</i> and Ada dependent system .....	10
1.4 AidB protein .....	13
2. Alkylation and tuberculosis .....	15
2.1 Tuberculosis overview .....	15
2.2 Mycobacterial infection and current therapies.....	16
2.3 Mycobacterium tuberculosis and alkylation response .....	17
3. Aims.....	19
<b>Chapter 2: Experimental section .....</b>	<b>21</b>
1. Identification of AidB molecular partners .....	22
1.1 <i>E. coli</i> Growths and Cell Extraction Preparation .....	22
1.2 Pull-Down Experiments .....	22
1.3 In Situ Digestion and LC-MS/MS Analyses.....	23
1.4 Construction of Expression Vectors, production and Purification of Recombinant Proteins .....	24
1.5 Co-Immunoprecipitation and Western Blotting.....	25
2. DIGE analyses .....	25
2.1 <i>E. coli</i> growths .....	25
2.2 2D DIGE and image analysis .....	26
2.3 LC-MS/MS analyses .....	27
3. Biofilm production and Adhesion capability .....	28
3.1 Static biofilm assay .....	28
3.2 Invasion assay .....	28
3.3 adhesion assay.....	29
4. Mycobacterial growths .....	29
4.1 <i>M. smegmatis</i> growths.....	29
4.2 Mtb growths .....	29
4.3 Construction of expression vectors.....	30
4.4 Production and purification of recombinant FadE8.....	30
4.5 Isovaleryl-CoA dehydrogenase activity assay.....	31
4.6 Electrophoretic shift mobility assays.....	31
5. Ethenobases analyses .....	32
5.1 DNA extraction .....	32
5.2 DNA hydrolyses and LC-MS/MS analyses.....	33
6. Methylated bases analyses .....	33
<b>Chapter 3: <i>Escherichia coli</i> and methylation stress.....</b>	<b>35</b>

1. Molecular partners of <i>Escherichia coli</i> transcriptional regulator AidB .....	36
1.1 Isolation of AidB Complexes in <i>E. coli</i> Upon Exposure to MMS .....	36
1.2 Identification of Proteins Specifically Interacting with AidB .....	37
1.3 Validation of Protein - protein Interactions by Co - immunoprecipitation Experiments ...	40
2. Differential proteomic approach to the study of <i>E.coli</i> upon exposure to methylating agent.	41
3. Effect of methylating agent on bacterial biofilms formation and adhesion capability .....	46
<b>Chapter 4: <i>Mycobacterium tuberculosis</i> and alkylation stress .....</b>	<b>49</b>
1. Effect of alkylating agent on <i>Mtb</i> growth and morphology.....	50
1.1 MMS on <i>Mycobacterium smegmatis</i> cells.....	50
1.2 MMS on <i>Mtb</i> clinical strains .....	51
1.3 Busulfan on <i>M. smegmatis</i> cells .....	53
2. Study of a <i>Mtb</i> protein potentially involved in alkylation response.....	54
2.1 <i>In silico</i> analysis of <i>Mtb</i> putative AidB homologue .....	54
2.2 Heterologous expression of fadE8 in <i>E. coli</i> and protein purification.....	56
2.3 FadE8 refolding processes.....	58
2.4 In vivo assisted FadE8 folding by GroEL/GroES complex .....	59
2.5 Recombinant FadE8 characterization.....	60
<b>Chapter 5: Qualitative and quantitative analyses of DNA alkylation in vivo .....</b>	<b>63</b>
1. Quantitative analysis of DNA ethenobases by LC-MS/MS.....	64
2. Quantitative analysis of methylated DNA by LC-MS/MS .....	66
<b>Chapter 6: Discussion.....</b>	<b>72</b>
<b>References .....</b>	<b>79</b>
<b>Appendix A.....</b>	<b>88</b>
<b>Appendix B.....</b>	<b>97</b>

## Summary

## Summary

Alkylating molecules are exogenous or endogenous chemicals commonly capable to modify nucleic acids in all living organisms causing dangerous and toxic effects. Several repair systems were developed by all organisms to avoid DNA alkylating modifications. In *Escherichia coli* AidB protein is involved in the adaptive response to alkylation stress in a still obscure fashion [1]. The same mechanism is also present in *Mycobacterium tuberculosis* (Mtb), the causing agent of tuberculosis. Human immune response usually targets bacterial systems which are essential for cells survival like DNA alkylating response [2]. All the information concerning these mechanisms are deeply interesting objects in order to understand molecular mechanism of MTB infection and to lead the identification of new putative therapeutic drugs.

In this biological contest, the study of DNA alkylation response processes in *E.coli* and *MTB* was the main interest in this PhD thesis. The first part was principally addressed to obtain a comprehensive description of *E.coli* response to alkylation stress while the second part was entirely focused on the Mtb response to methylating molecules. Finally in the third part a new tandem MS approach was set up to detect and quantify methylating DNA extracted from complex matrices. A complete elucidation of DNA response to alkylation damages in *E.coli*, a model organism for all bacteria was performed. Proteomic approaches were designed in order to identify and functionally analyze all the proteins differentially expressed in the presence and in the absence of methylating molecules.

Subsequently the project focused on the exploration of MTB response to alkylation stress. Different clinical tubercular and not tubercular strains were treated with alkylating agents in order to analyze sensitivity and morphological alterations. The results obtained showed the occurrence of a DNA response mechanism in MTB similar to that found in *E.coli*. *In silico* investigations revealed the presence of FadE8, a putative DNA protection protein homologous to *E.coli* AidB. The corresponding gene was cloned in several plasmidic vectors and expressed in *E.coli*. The recombinant FadE8 protein was structurally and functionally characterized.

A Multiple Reaction Monitoring (MRM) tandem MS procedure was used to qualitative and quantitative analyze DNA modifications. Through this approach *E.coli* and MTB systems were eventually compared and the functional roles of homologue proteins involved were highlighted.

## **Chapter 1:**

### **Introduction**



## **1. Alkylating stress and DNA response**

### **1.1 Alkylating molecules**

Living organisms are continuously subjected to alkylating conditions caused by both endogenous and exogenous species. Biological macromolecules, containing a large number of nucleophilic sites including DNA, RNA, proteins and lipids are sensitive to electrophilic species permeating cellular defenses and then subjected to alkylation damages. Due to its cellular long half-life, its singular copy in a cell and its biological role, DNA is the most dangerous target for cells survival. Reactive species like radicals, one-electron oxidants and chemicals such as various nitrating and alkylating agents can affect genetic information [3]. Specifically, alkylating molecules are species having one or more alkyl group which can react with nucleophilic sites on DNA bases causing covalent modifications known as adducts [4]. The most reactive sites to be attacked by alkylating molecules are the ring nitrogens (N) and the extracyclic oxygen (O) atoms of DNA bases.

The chemical lesions pattern depends on the molecular characteristic of alkyl agents i.e. the number of reactive sites, the type of group added (methyl, chloroethyl, etc.) and its reactivity (type of nucleophilic substitution) [5]. Sometimes alkylating molecules are not directly reactive with DNA, because they are not electrophilic but they can become mutagenic upon metabolic activation. Notably, the cytochrome P450 superfamily of monooxygenases is a group of enzymes that catalyze the oxidation of organic substances such as metabolic intermediates, as well as xenobiotic substances, drugs and other toxic chemicals. This system is capable to convert alkenes to electrophilic epoxides which may cause carcinogenic adducts [6]. As an example vinyl chloride an important industrial chemical commonly used in the production of polyvinyl chloride, is converted into chloroethylene oxide by cytochrome P450. This alkylating molecule is very unstable and it is transformed in the more stable chloroacetaldehyde (CAA) by chemical rearrangement as shown in Figure 1. CAA bifunctional alkylating agent produces etheno DNA adducts including 1,N6-

ethenoadenosine and 1,N2-ethenoguanosine which were shown to possess miscoding properties [7].

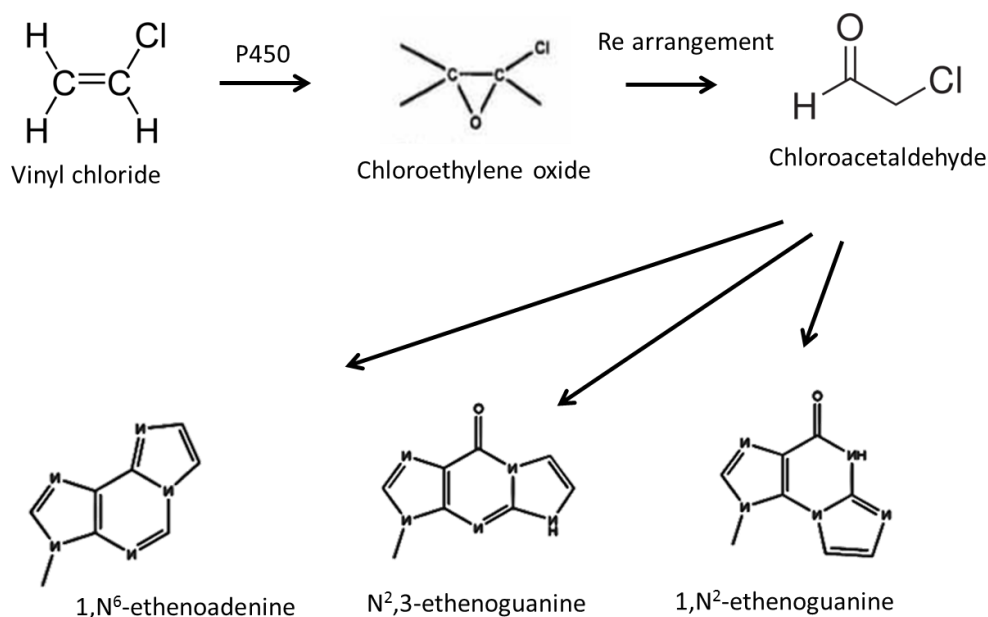
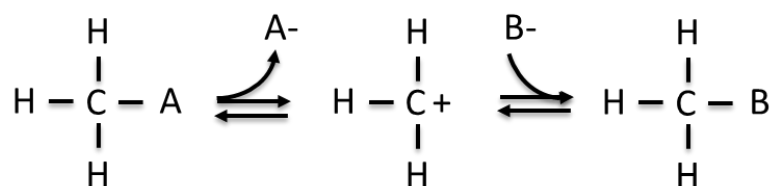
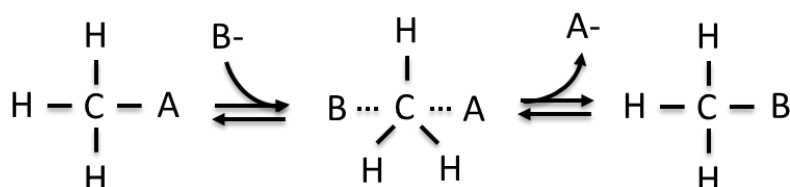


**Figure 1.** Activation of vinyl chloride by metabolic action of cytochrome P450 and formation of ethenobases *in vivo*.

Alkylating agents containing one active chemical moiety can modify DNA in a single site while bifunctional species possessing two reactive groups can bind simultaneously two sites generating intra- or inter-strand crosslinks. Alkylating molecules can attack the DNA reactive groups according to both  $S_N2$  mechanism by targeting ring nitrogen atoms and  $S_N1$  mechanism modifying nitrogen and extra cyclic oxygen groups. Both mechanisms are schematically represented in Figure 2. Amongst alkylating species, monofunctional methylating agents induce preferentially the formation of N-7-methylguanine (7MeG) at a rate of 60-80% of the total alkylation lesions because of the high nucleophilic reactivity of the N7 position of guanine. Mono-methylating agents can also produce N-3-methyladenine (3MeA) with an amount of 10-20% of total methyl adducts. In addition oxygen at position 6 of guanine is the most reactive oxygen in DNA and it is modified by  $S_N1$  alkylating agent to form O6-methylguanine (O6MeG).



SN1: Monomolecular mechanism  
Alkylation at N and O atoms



SN2: Bimolecular mechanism  
Alkylation at N atom

**Figure 2.** Schematic mechanism of DNA alkylation through nucleophilic substitutions: B is the nucleophilic base while the leaving group is donated by the alkylating agent.

Other nitrogen and oxygen atoms in DNA are modified by methylating agents to produce mutagenic lesions at very low levels. A typical monofunctional methylating molecule is methyl methane sulfonate (MMS) reported in Figure 3.

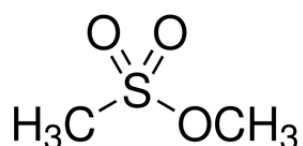


**Figure 3.** Methyl methane sulphonate chemical structure

7MeG and 3MeA are not directly mutagenic but they are hydrolytically unstable and undergo spontaneous depurination to produce apurinic sites. These sites can potentially cause transversion mutations (G-to-T for N 7-MeG and A-to-T for N 3-MeA). [8]. The most likely modified base positions and their dangerous implications are reported in Figure 4.

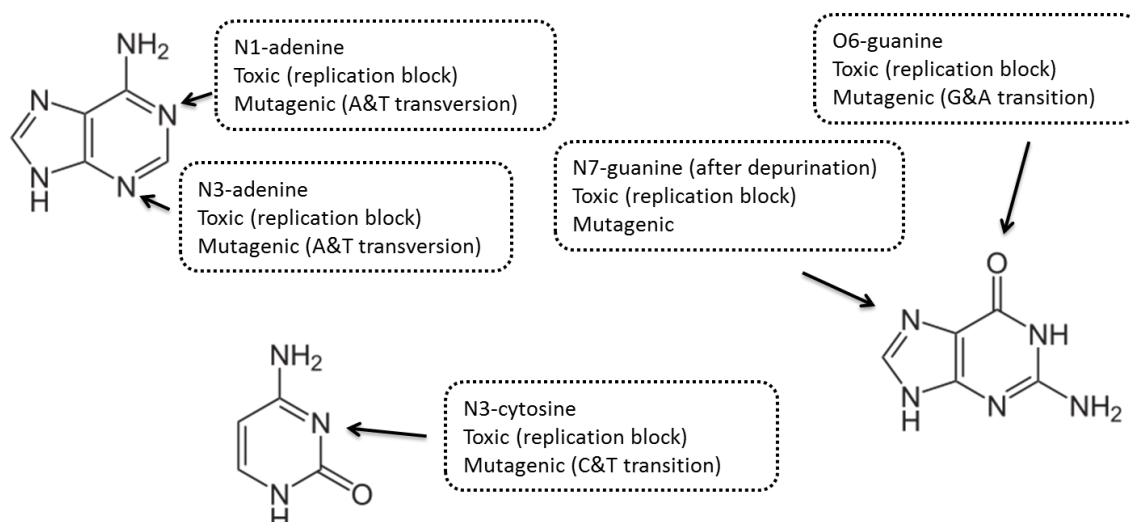


**Figure 4.** Base atoms usually modified by alkylating agent through nucleophilic substitution and their implication on cellular life.

Depending on their position DNA adducts can induce mutagenesis and/or cells death by blocking essential biological processes such as DNA replication and transcription [9]. Alkylated adducts can cause mutations by affecting DNA structural forces into two different ways: modification of the canonical Watson-Crick pairings and alteration in the strength of the hydrogen bonding, stacking and hydrophobic interactions. Causes of mutation are illustrated in Figure 5.

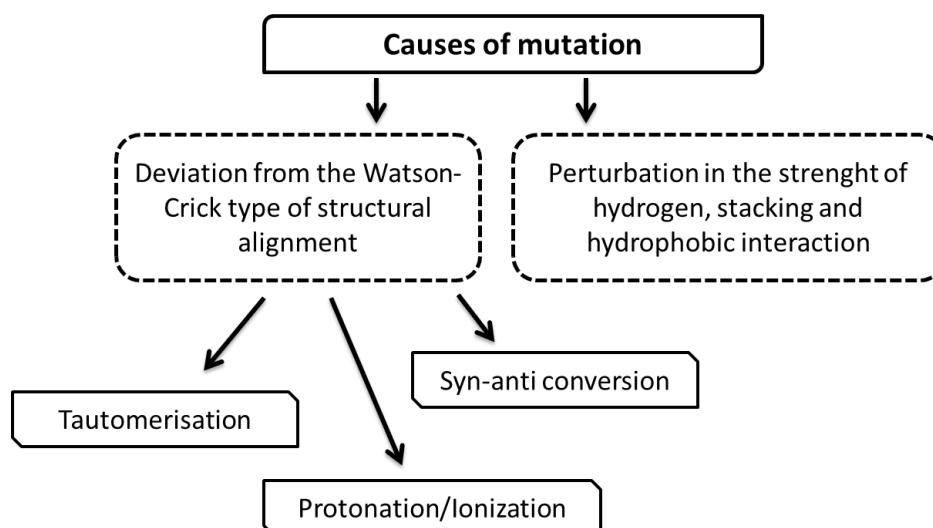


**Figure 5.** DNA damages by reactive species cause mutations influencing both Watson-Crick pairings and secondary interactions.

The study of alkylating molecules effects is interesting not only for the possibility of DNA damages but also for chemotherapeutics generated modifications. Indeed alkylating molecules are not only dangerous chemicals occurring in the environment but they are currently used as drugs in multiple anti-cancer therapies. The capacity of alkylating species to chemically modify DNA causing mutations is in fact used to target cancer cells more than normal cells. Cancer cell growing proceeds into two phases, graphically represented by Gompertz curve in Figure 6: an exponential phase followed by a plateau (similar to bacterial growing profile). As the tumor grows, cells inside lose afflux of oxygen so they reach necrosis until the size of tumor becomes constant with the same number of living and dead cells. As a consequence, alkylating agents have their mutagenic and cytotoxic effect more rapidly on fast growing cancer cells rather than normal cells [10].

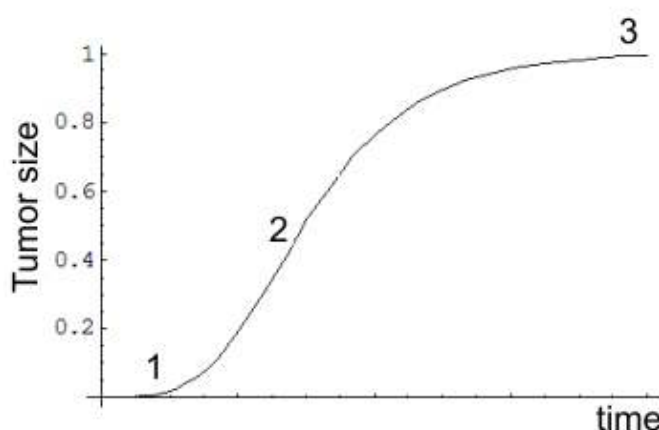


**Figure 6.** Gompertz curve representing tumor growing versus time increasing.

Most of the chemotherapeutic alkylating drugs used in anticancer chemotherapy are either monofunctional or bifunctional  $SN_1$  alkylating agents. One of the most common bifunctional alkylating molecules used in cancer chemotherapy is 1,4-butanediol dimethanesulfonate known as busulfan, reported in Figure 7.

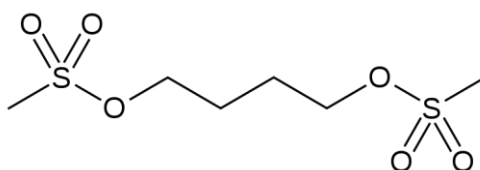


**Figure 7.** Chemical structure of Busulfan, one of the most common anti-cancer drug.

This bifunctional alkylating agent contains two methanesulfonate groups linked by a 4-carbon alkyl chain. Busulfan can be hydrolyzed to produce carbonium ions that can alkylate DNA [11].

## 1.2 Analyses of DNA adducts

DNA adducts represent outstanding biomarkers to evaluate the amount of DNA damage and then to appreciate the complex mechanisms involved in carcinogenesis. Moreover quantification of DNA adducts is an important tool to estimate the extent of cancer risk linked to a particular chemical agent or process. Detection and quantification of a specific methylation profiles caused by a definite agent permit to obtain comparative information about damage extent and its evolution in time. For these reasons accurate quantitative and qualitative measurement of DNA modification is an interesting and essential information to investigate multiple cellular problems.

Analytical techniques commonly used to quantify DNA methylation comprise  $^{32}\text{P}$  post-labeling, HPLC with UV, electrochemical or fluorescence detection, immunochemical methods, gas chromatography mass spectrometry and accelerated mass spectrometry [12]. One group is represented by more sensitive techniques such as  $^{32}\text{P}$  post-labeling and accelerated mass spectrometry while the other group comprise the most specific procedures like tandem mass spectrometry approaches coupled with liquid chromatography [13]. Despite lower sensitivity than the first group of techniques, mass spectrometry (MS) methodologies represent the most promising approaches for studying DNA modification. Indeed MS applications improve every day thanks to technological advances to allow short run time, enhanced sensitivity and selectivity and less ion suppression [14].

Some recent analytical approaches are based on the coupling between HPLC and tandem mass spectrometry working in multiple reaction monitoring (MRM) [15]. This methodology is commonly based on the use of liquid chromatography interfaced to an electrospray ionization source and a triple quadrupole (QQQ) mass spectrometer, schematically represented in Figure 8.

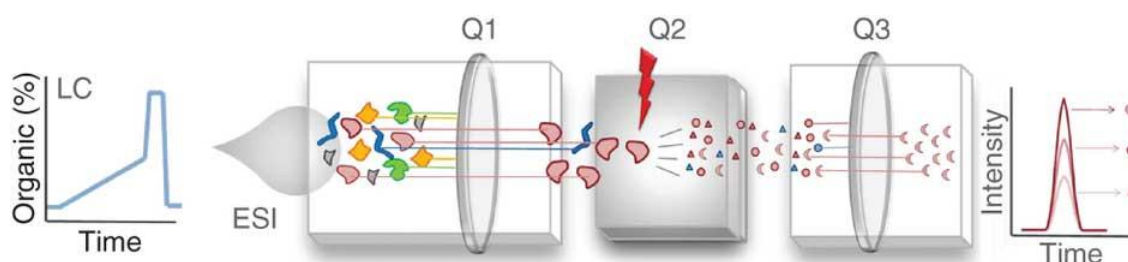


**Figure 8.** An MRM triple quadrupole analyses is shown. HPLC injects directly in the ESI source to perform Multiple Reaction Monitoring for all the selected transitions.

In a QQQ mass spectrometer operating in Multiple Reaction Monitoring (MRM) mode, the analysis proceeds through a two steps mass filtering. In the first phase the precursor ion of interest is selected by the Q1 and induced to fragment in the collision cell (Q2). Fragmentation of the pre-selected ion occurs by collision induced dissociation (CID) using an inert gas. In the second phase the third quadrupole (Q3) is used to select only a small number of specific fragment ions. This approach allows a specific molecule to be monitored, identified and quantified in a complex mixture. Ion counts in fact are directly proportional to the concentration of species present in the sample and can be measured by using an internal standard or by applying an external calibration. As a consequence this targeted MS approach permits to obtain qualitative and quantitative analyses of modified DNA bases even in the presence of a large amount of unmodified nucleotides. DNA samples are digested by enzymes or chemicals to obtain a mix of free normal and modified nucleosides or bases and the mixture is directly analyzed by LC-MS/MS.

### 1.3 DNA alkylation response of *Escherichia coli* and Ada dependent system

All cells developed several response systems in order to counteract damaging stress as a result of pro-mutagenicity, mutagenicity and cytotoxicity of alkyl lesions. Essentially, cells respond to these damages either repairing the DNA molecule or degrading the alkylating molecules. Proteins and RNAs are normally subjected to degradation and replacement pathways for their physiologic turnover in the cell. In case of damaged molecules, they can be replaced through new synthesis and only in

few and rare examples they are repaired rather than replenish with new molecules. In contrast genomic nucleic acid is a single copy molecule and its information is uniquely conserved. The only possible cellular choice is then to repair the DNA molecule following alkyl damages. Nevertheless, DNA alkylation lesions are often so extensive that cellular mechanisms are not capable to restore genetic information and the cell is driven to apoptotic pathways. In this way DNA and all the other cellular constituents are degraded in order to be used as simple building blocks minimizing damages to the entire organism [16].

Both multicellular, complex and unicellular simpler organisms have evolved multiple response mechanisms that can be essentially divided into four categories: direct repair mediated by methyltransferases or oxidative demethylases, base excision repair (BER) carried out by DNA glycosylases, mismatch repair system and nucleotide excision repair (NER) [17].

The genetic responses to alkylation damages in *Escherichia coli* are schematically presented in Table 1.

Genetic responses to DNA damage				
Stimulus	Signal	Sensor	Regulatory protein	Response
UV damaged DNA	Single stranded DNA	RecA	RecA*	SOS
Methyl damaged DNA	Methylphosphotriesters	Ada	<sup>me</sup> Ada	Adaptive
Superoxide	Superoxide and nitric acid	SoxRS	Oxidized SoxR	Superoxide resistance
Peroxide	Peroxide	OxyR	Oxidized OxyR	OxyR

**Table 1.** Summary of *E.coli* stress responses

Cells respond fundamentally to two classes of signals: the presence of a damaging specie or a DNA lesion. The presence of one of these events can be recognized by a specific sensor protein that induces the transcription of a definite repair response [1]. Activation of regulatory sensor depends on the kind of protein



involved: SoxR and OxyR are activated directly by the DNA damaging agent, RecA by the DNA damage and Ada by its own repair activity. This last protein belongs to the complex of adaptive response to alkylation damages of *Escherichia coli*. Ada working as a bifunctional enzyme possesses two cysteine residues that act as methyl acceptors from methylated DNA: the first one is required to demethylate phosphomethyltriester in the sugar phosphate backbone and the second one to remove methyl groups from either O6-methylguanine or O4-methylthymine. Both sites can be methylated from the specific substrates but only methylation by phosphates produces Ada conformational changes that induce the transcriptional regulator activity of the protein. Even though methylated phosphates are less dangerous than other lesions, these sites are the most quickly modified by methylating agents and thereby represent a sensitive regulatory signal leading to Ada operon induction. As a consequence, in the presence of sub-lethal concentrations of alkylating agents, *E. coli* enhances cellular response with increasing doses of damaging molecules. This mechanism known as the adaptive response consists of four genes included in the *ada* operon: *ada*, *alkA*, *alkB* and *aidB* as schematized in Figure 9.

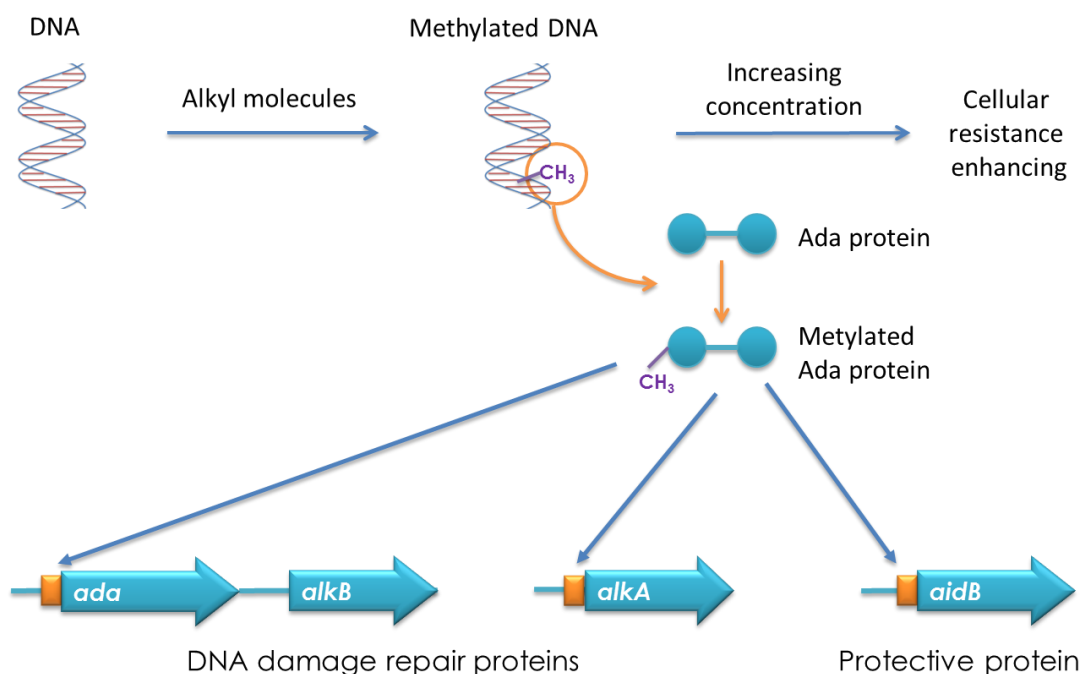


**Figure 9.** *E. coli* adaptive response to alkylation damages

AlkA protein is a glycosylase that repair several damages such as N7-methylguanine and N3-methyl purines and O2-methyl pyrimidines. The mechanism of action comprises the removal of a damaged base from the sugar phosphate backbone through cleavage of the glycosylic bond leading to an abasic site.

AlkB protein is an oxidative demethylase capable of removing 1-methyladenine and 3-methylcytosine from DNA using an  $\alpha$  ketoglutarate/Fe(II)-dependent mechanism coupled with the release of CO<sub>2</sub>, succinate and formaldehyde. Despite the large amount of available data, the function of AidB is still obscure and it will be discussed below.

In human cells the alkyltransferase expressed by MGMT presents a similar sequence to Ada and it is capable to remove alkyl adducts from O6 methylguanine in contrast to bacterial protein. AlkB has 9 different homologues in human cells capable to repair RNA, single strand and double strands DNA and presenting similar fold to the bacterial protein [18].

Definitely Ada, AlkA and AlkB show one or more homologs proteins in humans, all involved in DNA repair processes whereas no homologous of AidB have been reported so far.

#### 1.4 AidB protein

Acyl-CoA dehydrogenase AidB is the fourth protein involved in the Ada depending adaptive response of *E.coli*. Crystal structure reveals a homotetrameric organization associated as a dimer of dimers having identical DNA binding surfaces at the interface. Each subunit consists of two domains, the N-terminal region containing the dehydrogenase enzymatic site able to bind the FAD molecule and a positively charged C-terminal domain exhibiting DNA binding capability. The dehydrogenase activity binding site is smaller than typical acyl-CoA dehydrogenase and it presumably can accommodate different substrates [19]. In addition, the N-terminal domain of AidB shows an activity versus isovaleryl-CoA substrate about two orders of magnitude lower than human acyl-CoA dehydrogenase supporting the hypothesis that fatty acyl-CoAs are too large to fit the AidB active site and cannot represent its specific substrate [20].

Other structural experiments demonstrate that the presence of a FAD molecule is essential for the correct tetramerization of AidB otherwise deflavinated AidB is dimeric [21].

Recent work elucidated the ability of AidB to bind not only single and double strands DNA but also RNA suggesting the possible involvement of the protein in RNA defense mechanisms [22].

Our previous data demonstrated that AidB prevents DNA damage by alkylating agents and counteracts the block to transcription resulting from exposure to alkylating agents, preferentially acting on genes that are transcribed from promoters containing upstream (UP) elements. These protection effects were observed after treatment with MMS, MNNG and ENNG, three alkylating agents that produce different DNA lesions. Preventing of ENNG damage is especially interesting since ENNG lesions are repaired not only by the adaptive response system, but also by nucleotide excision repair in *E. coli*. Additionally, in the presence of methylating agents, AidB allows efficient transcription from UP element [2]. Therefore, unlike all the other protein belonging to the adaptive response, AidB might elicit a putative pathway of degradation of alkylating agents through its FAD dependent dehydrogenase activity. Alternatively, AidB might protect these DNA regions by physically interact with them thus impairing the dangerous action of alkylating agents.

The transcription of *aidb* gene under normal conditions of growth in the presence of oxygen is induced by Ada protein but in contrast to other adaptive response genes, it is also activated without alkylation stress as a result of anaerobic conditions or pH alteration. Moreover this gene is regulated by the universal anaerobiosis protein Fnr during anaerobic culturing with an increasing in the *aidB* expression. However in the presence of nitric oxide an extensive inhibition of expression is observed during incubation under anaerobic but not aerobic conditions [23].

## 2. Alkylation and tuberculosis

### 2.1 Tuberculosis overview

Alkylation response mechanisms are widespread in the majority of bacteria including *Mycobacterium tuberculosis*. This pathogenic bacterium causes the tuberculosis disease also known as the White Plague, one of the most ancient infection in the world. The earliest finding of mycobacterial traces infecting animals is dated at 17000 years before present, whereas the origin of tuberculosis infected humans is probably restricted to 4000-3000 BC [24]. In ancient Greece, pulmonary tuberculosis was broadly diffused and called Phthisis a Greek word for consumption. Around 460 BC Hippocrates described tubercular manifestations involving fever and the coughing up of blood, almost always fatal. In the 1800s sanatoria, medical facilities for long term illness, opened in association with treatment of tuberculosis but only in 1882 Robert Koch identified in *M.tuberculosis* the unique causative agent of the disease.

In the 1943, Schatz Waksman and colleagues identified streptomycin and they demonstrated its efficacy against tuberculosis in humans, leading to the “era” of antibiotic treatment of this bacterial infection [25].

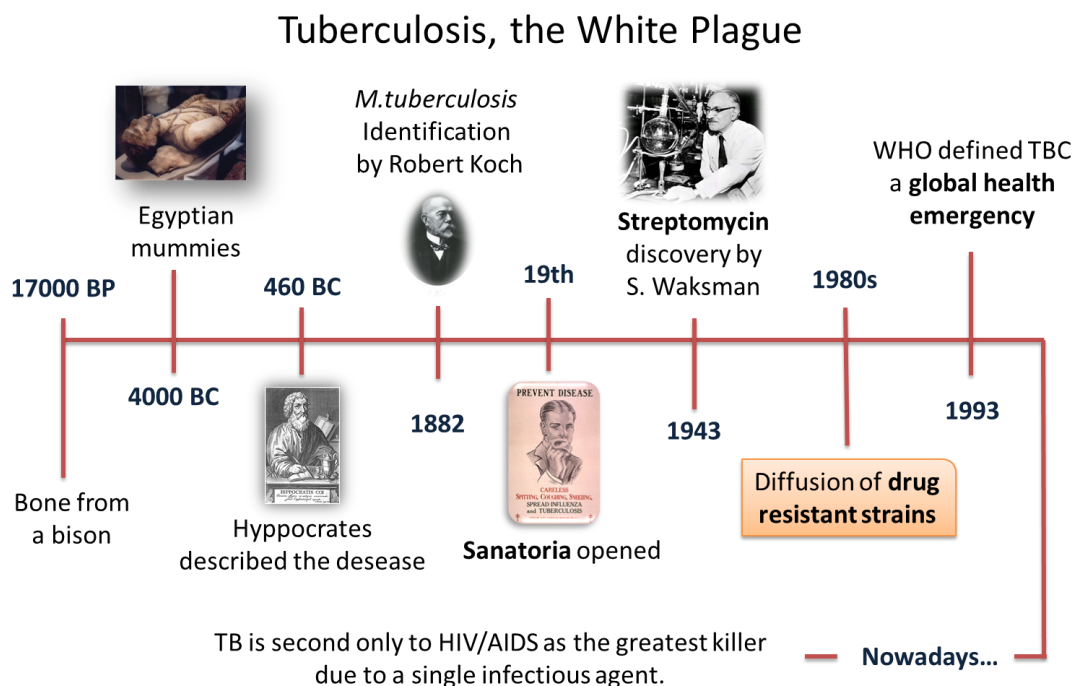


**Figure 10.** Historical events most important in tuberculosis infection diffusion.

However, due to the large use of this antibacterial drugs, in few decades drug resistant mycobacterium strains developed during antibiotics treatments. Synthetic drugs such as isoniazid, pyrazinimide, ethambutol and rifampicin were then used in combined administration to prevent drug resistant strains appearance. This treatment caused the decline of disease in industrialized countries while tuberculosis persisted in the third world regions such as Africa, Asia and Latin America [26]. In 1993 World Health Organization (WHO) declared tuberculosis a global public health emergency due to failures in health services, the diffusion of HIV/AIDS infection and appearance of multi-drug-resistant (MDR) strains [27].

Nowadays the increase of human migration and the development of extensively drug-resistant (XDR) strains led to a more dangerous context. Approximately 2 million people infected died each year and WHO estimates that between 2002 and 2020 approximately 1000 million people will be infected, 150 million people will become sick and 36 million will die of tuberculosis [28].

## 2.2 Mycobacterial infection and current therapies

Tuberculosis infection starts when bacteria are transported through the air and inhaled by an host organism. In this situation, MTB can incur into three different destinies depending on the host immune response, as shown in Figure 11.

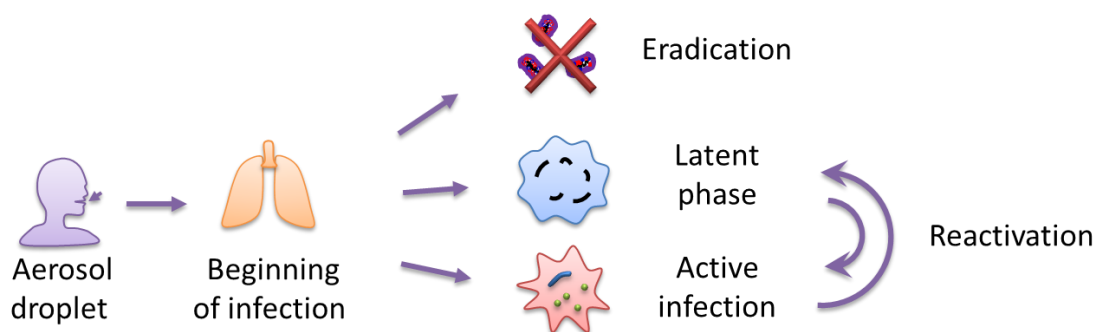


**Figure 11.** Tuberculosis infection schematization.

If the host's immune response is healthy enough to eradicate bacteria, a complete clearance of MTB will happen. If the immune response is compromised, MTB can replicate to cause a clinical disease called primary tuberculosis. Finally if the immune response is not able to strongly counteract bacterial invasion, MTB cells are confined within macrophages where they inhibit their fusion with lysosomes. In this site numerous types of cells such as lymphocytes, monocytes and neutrophils are engaged forming granuloma, a latent infection status without evident clinical manifestations. This phase can produce the so called post primary tuberculosis [29].

Current treatments against tuberculosis infection depends on the type of disease. Drug susceptible tuberculosis is treated with a combination of isoniazid, rifampicin, pyrazinamide and ethambutol (first-line drugs) for a period of six months. Multiple drug resistant tuberculosis strains are unaffected by at least isoniazid and rifampicin while extensively drug-resistant strains are cannot be treated with first and most part of the second line drugs and they cause an high rate of mortality [30]. The suggested procedure for resistant tuberculosis is a combination of at least four drugs choosing stepwise selection process [31].

### **2.3 Mycobacterium tuberculosis and alkylation response**

The appearance of drug resistant strains depends on the MTB capacity of adaptation to host environment and drugs treatments. Mutations in bacteria can be subordinated to selective pressure, horizontal gene transfer or recombination processes [32]. Macrophages defense human organisms at the same time by generating reactive species (oxygen and nitrogen classes), by changing pH, etc. In addition during detoxification processes, cellular components damaged by reactive species can be transformed in damaging molecules indirectly causing further damages to DNA [33].

Thereby, investigation of the mechanisms involved in DNA repair and protection is extremely interesting in the tuberculosis context because of their involvement in the drug resistant development. Moreover, proteins involved in these mechanisms represent excellent therapeutic targets because of the fundamental role

they play in bacterial survival and due to the absence of homologues in humans [34, 35].

The knowledge about MTB response systems to DNA alkylation is still poor because of experimental difficulties linked with pathogen slow-growing capability and most of the hypotheses formulated arise from homology studies. Nucleotide excision repair (NER), base excision repair (BER), recombination and SOS repair system genes were recognized in the MTB genome while mismatch repair (MMR) mechanism components could not be identified [36]. Recently the *ada* operon of MTB was preliminary characterized and AdaA, AlkA, AdaB/Ogt proteins were recombinantly expressed. Mingyi Yang et colleagues have demonstrated an effect of mutagenic but not cytotoxic inhibition executed by *ada* operon [37]. In contrast no literature data about AidB homologue in *M.tuberculosis* have been reported.

### 3. Aims

Alkylating molecules are exogenous or endogenous chemicals commonly capable to modify nucleic acids in all living organisms. DNA response mechanisms to alkylation damages are interesting target due to dangerous and often toxic effects caused to cellular life. Amongst alkylating species, monofunctional methylating agents such as methyl methane sulphonate preferentially induce the formation of 7MeG, 3MeA and O6MeG. Alkyl modifications are usually used as biomarkers and they are monitored by using several techniques such as  $^{32}\text{P}$  post-labeling and tandem mass spectrometry coupled with liquid chromatography.

Usually all organisms have developed several repair systems to counteract DNA alkylating modifications. In *Escherichia coli* AidB protein is involved in the adaptive response to alkylation stress in a still obscure fashion. The same mechanism is also present in the *Mycobacterium tuberculosis*, causing agent of tuberculosis. Host immune response usually defends humans by attacking bacterial systems which are essential for cells survival like the DNA alkylating response. A deep understanding of these mechanisms is then extremely important in order to identify new therapeutic drugs that might lead to novel therapeutic strategies against tuberculosis.

In this biological context, the study of DNA alkylation response processes in *E.coli* and *M.tuberculosis* was the main interest of this PhD thesis. The first part was principally addressed to complete the description of *E.coli* response to alkylation stress, while the second part was entirely focused on the MTB response to methylating molecules and finally in the third part a new tandem mass spectrometry approach was developed to detect and quantify methylating DNA extracted from bacterial cells upon dangerous effect.

In the first part a complete elucidation of DNA response to alkylation damages of *E.coli* was pursued because it represents a model organisms for all bacteria. This goal was achieved by using a proteomic approach in order to identify and functional analyze all the proteins differentially expressed in the presence and in the absence of methylating molecules. After that, a deep examination on the effects of methylating agents on cell-cell interactions was performed.



The second point of this thesis was focused on the exploration of MTB response to alkylation stress. Different clinical tubercular and non-tubercular strains were treated with alkylating agents in order to analyze sensitivity to stress conditions and morphological alterations. Observed effects on MTB cells suggested us to search for an AidB homologue, that was identified as the FadE8 protein *in silico*. The corresponding gene was cloned in several plasmidic vectors and then expressed in *E.coli*. The FadE8 protein was structurally and functionally characterized.

In the third part a Multiple Reaction Monitoring (MRM) tandem MS methodology was developed as a powerful tool to qualitative and quantitative analyze DNA modifications. Through this approach *E.coli* and MTB systems were eventually compared and the functional roles of homologues proteins involved were highlighted.

## **Chapter 2:**

### **Experimental section**

## **1. Identification of AidB molecular partners**

### **1.1 Escherichia coli Growths and Cell Extraction Preparation**

*E. coli* cells growths were transformed with the construct pET22b-AidB. Bacterial culture was grown overnight in LB medium at 37 °C and it was diluted 1:100 in fresh medium containing ampicillin (100 µg/mL) and riboflavin (100 µM). At an A600 nm of 0.4, the culture was divided in two aliquots and one of these was supplemented with 0.04% MMS (methyl methane sulfonate) that has been shown to induce the adaptive response. After one cell duplication cellular pellets were collected. The cells were resuspended in 20 mM Na<sub>2</sub>HPO<sub>4</sub>, 20 mM Imidazole, 500 mM NaCl, 1 mM PMSF (phenil methane sulphonyl fluoride) (pH = 7.4), disrupted by passage through a french press and centrifuged at centrifugal force of 14,000 x g for 15 min at 4 °C. The supernatant was collected and protein concentration was determined with the Bio-Rad protein assay, using bovine serum albumine as standard.

### **1.2 Pull-Down Experiments**

Isolation of AidB partners complex was performed by using His-Select<sup>TM</sup> Nickel (Sigma) containing Ni<sup>2+</sup> ions immobilized to bind His-tagged AidB. A control was carried out in order to discriminate between proteins that interact specifically with the Ni<sup>2+</sup> compared to those that bind in a nonspecific manner to the resin. For this reason, the stripping of the resin was executed by washing in 20 mM sodium phosphate, 0.5 M NaCl and 50 mM EDTA, for the purpose of removing Ni<sup>2+</sup> ions. In this way, the resin lost the ability to interact specifically with the tag of histidines, but it was still able to establish nonspecific interactions. At this point, the resin was washed with 20 mM sodium phosphate, 0.5 M NaCl and 20 mM imidazole pH 7.4. The two protein extracts (2.5 mg) were incubated for 16 h at 4 °C with 100 µL of resin without nickel ions in the precleaning step. The extracts were then recovered and incubated with His-Select<sup>TM</sup>

Nickel resin for 16 h at 4 °C to bind AidB by tag of histidines and to isolate its complexes. Both the precleaning and affinity chromatography resins were recovered and washed with 20 mM sodium phosphate, 0.5 M NaCl and 20 mM imidazole pH 7.4. The elution was performed with sample buffer. The samples were then subjected to SDS-PAGE (SDS-polyacrilamide gel electrophoresis).

### 1.3 In Situ Digestion and LC-MS/MS Analyses

Protein bands stained with Coomassie brilliant blue were excised from the gel and destained by repetitive washes with 0.1 M  $\text{NH}_4\text{HCO}_3$  (pH 7.5) and acetonitrile. Samples were reduced by incubation with 50  $\mu\text{L}$  of 10 mM DTT in 0.1 M  $\text{NH}_4\text{HCO}_3$  buffer (pH 7.5) and alkylated with 50  $\mu\text{L}$  of 55 mM iodoacetamide in the same buffer. Enzymatic digestion was carried out with trypsin (12.5 ng/ $\mu\text{L}$ ) in 10 mM ammonium bicarbonate (pH 7.8). Gel pieces were incubated at 4 °C for 2 h. Trypsin solution was then removed and a new aliquot of the digestion solution was added; samples were incubated for 18 h at 37 °C. A minimum reaction volume was used as to obtain the complete rehydration of the gel. Peptides were then extracted by washing the gel particles with 10 mM ammonium bicarbonate and 1% formic acid in 50% acetonitrile at room temperature.

Tryptic peptide mixtures obtained from in situ digestions were analysed by LC/MS/MS using an HPLC-Chip/Q-TOF 6520 (Agilent Technologies). The peptide mixtures were injected by auto sampler. They were sent to the enrichment column of the chip at flow rate of 4  $\mu\text{L}/\text{min}$ , in 98% water, 2% acetonitrile and 0.1% formic acid. Subsequently the peptides were eluted directly into the capillary column (C18 reversed phase), at a flow rate of 0.4  $\mu\text{L}/\text{min}$ . The chromatographic separation was carried out with a linear gradient in 95% acetonitrile, 5% water and 0.1% formic acid. The eluate was then introduced in the ESI source for the tandem analysis. In this way each mass spectrum (range 300-2,400  $m/z$ ) was followed by one or more tandem mass spectra (range 100-2,000  $m/z$ ), obtained by fragmenting the most intense ions in each fraction eluted chromatographic.

The acquired MS/MS spectra were transformed in Mascot generic file format and used for peptides identification with a licensed version of MASCOT (modular approach to software construction, operation and test, matrix science, USA), in a local database.

### **1.4 Construction of expression vectors, production and purification of recombinant proteins**

The UvrA, DeaD, RecA, TnaA and Ada genes of *E. coli* K12 were amplified from genomic DNA by PCR (polymerase chain reaction). To obtain proteins tagged with c-myc epitope, the corresponding amplification products were digested with BamHI and XhoI and cloned into the pET22b-c-myc vector [4], respectively. All plasmids containing the coding sequence for the corresponding recombinant protein fused to a 6X histidine tag to facilitate protein purification by Ni<sup>2+</sup> affinity chromatography. Plasmids construction was verified by automated DNA sequencing.

Recombinant cells were grown at 37 °C to an OD (optical density) at 600 nm of about 0.5, at which time 0.05 mM isopropyl-beta-D-thiogalactopyranoside (IPTG) was added in order to express UvrA, DeaD, RecA, TnaA and Ada genes. Selective antibiotic was used at concentration of 100 µg/mL ampicillin. After incubation, cells were harvested by centrifugation at centrifugal force of 5,000 x g for 15 min at 4 °C, resuspended in 50 mM Na<sub>2</sub>HPO<sub>4</sub>, 20 mM Imidazole, 500 mM NaCl, 1 mM PMSF (pH 7.4), disrupted by passage through a French press and centrifuged at centrifugal force of 14,000 x g for 30 min at 4 °C.

Recombinant proteins were purified by affinity chromatography on His-Select Nickel Affinity Gel (Sigma). After 1 min of incubation at 4 °C, the matrix was collected by centrifugation at centrifugal force of 11,000 x g for 1 min and washed three times with same equilibration buffer. The recombinant proteins were eluted with buffer containing 500 mM imidazole in 20 mM Na<sub>2</sub>HPO<sub>4</sub>, pH 7.4, 0.5 M NaCl. Protein concentration was estimated with Bradford reagent (Bio-Rad protein assay) and protein content was checked by SDS-PAGE.

## **1.5 Co-immunoprecipitation and Western Blotting**

For co-immunoprecipitations, *E. coli* strain C41 (DE3) was transformed with the following constructs: pET22b-c-myc-Ada, pET22b-c-myc-TnaA, pET22b-c-myc-DeaD, pET22b-c-myc-RecA and pET22b-c-myc-UvrA. After expression of the recombinant genes without induction, cells were harvested, suspended in 50 mM Na<sub>2</sub>HPO<sub>4</sub> (pH 7.4), disrupted by passage through a French press and centrifuged at centrifugal force of 14,000 x g for 30 min at 4 °C. The supernatants were used for the co-immunoprecipitation experiments.

Cell lysates (0.5 mg) were incubated with agarose-linked c-myc antibody (Bethyl) and with agarose beads only (control of the experiment) at 4°C overnight. The beads were then collected by centrifugation. Precipitates were washed several times, the bound proteins were eluted with 1 × SDS-PAGE sample buffer and subjected to SDS-PAGE followed by Western Blot Analysis that was performed by using anti-AidB antibody (Primm, Milano Italy) and anti-c-myc mouse antibody (Calbiochem) as first antibodies and anti-mouse IgG conjugated to peroxidase as a secondary antibody (Calbiochem).

## **2. DIGE analyses**

### **2.1 *Escherichia coli* growths**

MV1161 and  $\Delta$ aidB cells were grown overnight in LB medium at 37 °C and they were diluted 1:100 in fresh medium containing 5µg/mL tetracycline (only for  $\Delta$ aidB). At an A600 nm of 0.4, the cultures were divided in two aliquots and one of these was supplemented with 0.04% MMS (methyl methane sulfonate) or Busulfan. Cell debris was removed by centrifugation at 14,000 rpm at 4 °C for 30 min. The cell lysate supernatant was precipitated using a 2D clean up kit (GE Healthcare, Piscataway, NJ) and suspended in 100 µL 7 M urea, 2 M thiourea, 30 mM Tris-HCl pH 8.5, 4% CHAPS (w/v).

## 2.2 2D DIGE and image analysis

50 µg of lysates were labeled with 400 pmol of Cy3 or Cy5. Each Cy3/Cy5-labeled sample pair was mixed with a Cy2-labeled pooled standard sample containing an equal amount of all samples analyzed. The Cy2/Cy3/Cy5 labeled samples were run together on the same gel. Samples were fractionated on 18 cm IPG strips with 3–11NL, 3–5.6, 4–7 and 6–11 pH ranges. IPG strips were rehydrated, in the absence of protein samples, with 350 µL of rehydration buffer (350 µL DeStreak rehydration solution, 0.5% Pharmalyte and 0.5% IPG buffer) overnight at room temperature. The IPG strips were focused for 18h for a total of 60kV/h at 20 °C. Then, proteins were reduced with an equilibration buffer (6 M urea, 100 mM Tris pH 8.0, 30% glycerol (v/v), 2% SDS) containing 0.5% DTT for 15 min. Finally, proteins were alkylated for the same time with the buffer containing 4.5% IAA. After the equilibration step, the strips were overlaid onto 10% polyacrylamide gels (20 × 24 cm). The second dimension was carried out for 18 h at 2W per gel using an Ettan Dalt Twelve system (GE Healthcare, Piscataway, NJ).

After electrophoresis, gels were scanned in a Typhoon 9400 scanner (GE Healthcare, Piscataway, NJ). The images labeled with Cy2, Cy3 and Cy5 were acquired at excitation/emission values of 488/520, 532/580, 633/670nm, respectively.

Images were analyzed with the Decyder software version 5.2 (GE Healthcare, Piscataway, NJ) in batch processing mode. The maximum number of estimated spots per gel was fixed at 5000. Detection and quantification of protein spots were carried out by the differential in-gel (DIA) module, whereas protein-spot matching between different gels was obtained using the biological variation analysis (BVA) module. The DIA module was used for pairwise comparison of each sample (Cy3 and Cy5) with the Cy2 mixed standard present in each gel. In addition, DIA was used to detect spot boundaries and to calculate spot volume, normalized versus the volume of the corresponding spot present in the pool standard of the same gel. This analysis revealed the differentially expressed protein spots across six gels. The results from the intragel comparison for all dyes were imported into the BVA module. The Cy2 image containing the highest number of spots was designated the “master image” and used as template.

The protein spots belonging to the remaining internal standard images were

automatically matched with “master image”. Each spot intensity was then expressed as a mean value of the 6 gels, reducing intergel variation. Spot intensities were then compared in the two conditions: cell lines expressing TBX1 and control cells. Statistical significance of differences in spot intensity was determined with Student’s *t* test. Only protein spots with a change in size of at least 1.20 fold (*t* test:  $p \leq 0.05$ ) after normalization were considered significantly altered. We verified the validity of these changes and accuracy of spot matching by manual inspection of gels.

### **2.3 LC-MS/MS (Liquid Chromatography Tandem Mass Spectrometry) Analyses**

Tryptic peptide mixtures obtained from in situ digestions were analysed by LC/MS/MS using an HPLC-Chip/Q-TOF 6520 (Agilent Technologies). The peptide mixtures were injected by auto sampler. They were sent to the enrichment column of the chip at flow rate of 4  $\mu\text{L}/\text{min}$ , in 98% water, 2% acetonitrile and 0.1% formic acid. Subsequently the peptides were eluted directly into the capillary column (C18 reversed phase), at a flow rate of 0.4  $\mu\text{L}/\text{min}$ . The chromatographic separation was carried out with a linear gradient in 95% acetonitrile, 5% water and 0.1% formic acid. The eluate was then introduced in the ESI source for the tandem analysis. In this way each mass spectrum (range 300-2,400  $m/z$ ) was followed by one or more tandem mass spectra (range 100-2,000  $m/z$ ), obtained by fragmenting the most intense ions in each fraction eluted chromatographic. The acquired MS/MS spectra were transformed in Mascot generic file format and used for peptides identification with a licensed version of MASCOT (modular approach to software construction, operation and test, matrix science, USA), in a local database.



### **3. Biofilm production and Adhesion capability**

#### **3.1 Static biofilm assay**

The wells of a sterile 96-well flat-bottomed polystyrene plate (Falcon) were filled with 90 mL of the appropriate medium containing or not containing the inhibitors. 10 mL of overnight bacterial cultures grown in LB was added into each well. The plates were incubated aerobically with or without the enzyme for 24 h at 37 °C in the presence of either 0.04% MMS or Busulfan. Growth was monitored by measuring the OD<sub>600</sub>, and after 24 h incubation the ability of the *E.coli* strain to adhere to the polystyrene plates was tested. The content of the plates was then poured off and the wells washed with sterile distilled water. The plates were then stained with crystal violet for 5 min. Excess stain was rinsed off by placing the plate under running tap water. After the plates were air dried, the dye bound to the adherent cells was solubilized with 20% (v/v) glacial acetic acid and 80% (v/v) ethanol per well. The OD of each well was measured at 590 nm.

#### **3.2 Invasion assay**

HeLa cells, cultured in 24-well plates, were infected with 0.05 mL of logarithmically grown bacteria in the presence or in the absence of MMS as above described. The entry of MMS was tested by infecting cells for 1 h at 37 °C at an MOI of about 10 bacteria per cell. After incubation, the monolayers were washed with PBS and 0.5 mL of fresh medium containing 200 mg/mL of gentamicin was added to each well and maintained for 1 h at 37 °C to kill extracellular bacteria. Cells were then lysed by the addition of 0.025% Triton X-100 and plated on LB to count viable intracellular bacteria.

### **3.3 Adhesion assays**

Bacteria from 18 h cultures in BHI broth, grown in the absence of MMS were further subcultured up to OD<sub>600</sub> of 0.5 at 37 °C in BHI with or without MMS 0.04%. HeLa cells, cultured in 24-well plates (Falcon) to obtain semi-confluent monolayers (1x10<sup>5</sup> cells/well) were then inoculated with 0.05 mL of bacterial suspensions in logarithmic-phase growth at an MOI of about 10 bacteria per cell. The adhesion assay was carried out by keeping cells and bacteria in contact for 1 h at 37 °C. Loosely bound bacteria were removed from the cell monolayers by two washes with PBS. The cells were then lysed with 0.025% Triton X-100 and plated on LB agar to determine viable adherent bacteria. Adhesion efficiency was expressed as the percentage of the inoculated bacteria that adhered to HeLa cells.

## **4. Mycobacterial growths**

### **4.1 *M. smegmatis* growths**

Wild type cells were grown 3 days in LB medium at 37 °C and they were diluted 1:100 in fresh medium containing 100µg/mL ampicillin, 0.05% tween 80. At an A<sub>600</sub> nm of 0.4, the cultures were divided in aliquots and one of these was maintained as the untreated control while the others were supplemented with MMS or Busulfan in a 0.01-0.1% w/v range and the viability of bacterial cultures was monitored for 24 hs. Growing profiles were obtained by monitoring cells for 35 hours.

### **4.2 MTB growths**

Materials and Reagents used are following listed: Middlebrook 7H9 powder (Sigma), Middlebrook 7H11 powder (Sigma), Middlebrook, OADC Enrichment (Sigma), BD TB Quick Stain kit (BD Biosciences).

Culture were performed in 7H9 liquid medium. 1 frozen vial of 1 ml (450 million) MTB was suspended in 20 ml 7H9 liquid medium in T75 flask, culture

horizontally in incubator humidified at 37 °C without CO<sub>2</sub> for 14 days. OD at 600nm was measured every 48 hours. 0.03%, 0.015% MMS and reference concentration drug were singularly added on day 8. Viable MTB were counted by plating bacterial suspensions at different dilutions on Middlebrook 7H11 agar plates supplemented with OADC and counting colonies after two weeks.

Cells detection was performed by Ziehl-Neelsen acid-fast staining. 10 µl MTB culture were pipetted on glass microscopy slide, heated on top of bunsen flame until it totally dried to fix the bacteria. The slide was flood with carbol fuchsin stain and heated gently until it steams (about 5 min). The carbol fuchsin was poured off and the slide was washed thoroughly with tap water (about 5 min). Sample was decolorized with acid-alcohol (5 min). The slide was washed thoroughly with tap water (5 min) and flooded with methylene blue counterstain for 1 min. The slide was washed with tap water.

### **4.3 Construction of expression vectors**

The *fadE8* gene of *M. tuberculosis* was amplified from genomic DNA by PCR. To obtain protein tagged with c-myc epitope, the corresponding amplification product was digested with BamHI and XhoI and cloned into the pET22b-c-myc vector. Plasmid containing the coding sequence for the corresponding recombinant protein fused to a 6X histidine tag to facilitate protein purification by Ni<sup>2+</sup> affinity chromatography. Plasmids construction was verified by automated DNA sequencing.

The *aidB* gene of *E. coli* K12 was amplified from genomic DNA by PCR (polymerase chain reaction). Amplification product and *fadE8* gene were digested and cloned into the pTRC99a vector.

### **4.4 Production and purification of recombinant FadE8**

Bacterial culture was grown overnight in LB medium at 37 °C and it was diluted 1:100 in fresh medium containing ampicillin (100 µg/mL) and riboflavin (100 µM). Recombinant cells were grown at 25 °C to an OD (optical density) at 600 nm of about

0.5, at which time 0.05 mM isopropyl-beta-D-thiogalactopyranoside (IPTG) was added in order to express *fadE8* gene. After 16 hours of incubation, cells were harvested by centrifugation at centrifugal force of 5,000 x g for 15 min at 4 °C, resuspended in 50 mM Na<sub>2</sub>HPO<sub>4</sub>, 20 mM Imidazole, 500 mM NaCl, 1 mM PMSF (pH 7.4), disrupted by passage through a French press and centrifuged at centrifugal force of 14,000 x g for 30 min at 4 °C. Recombinant protein was purified by affinity chromatography on His-Select Nickel Affinity Gel (Sigma). After 1 min of incubation at 4 °C, the matrix was collected by centrifugation at centrifugal force of 11,000 x g for 1 min and washed three times with same equilibration buffer. The recombinant proteins were eluted with buffer containing 500 mM imidazole in 20 mM Na<sub>2</sub>HPO<sub>4</sub>, pH 7.4, 0.5 M NaCl. Protein concentration was estimated with Bradford reagent (Bio-Rad protein assay).

#### 4.5 Isovaleryl-CoA dehydrogenase activity assay.

Isovaleryl-CoA dehydrogenase activity assays were carried out at room temperature in 200 mM phosphate buffer, pH 8.0, and using purified recombinant proteins that had been dialyzed to remove imidazole. For routine assays, 2 mM isovaleryl-CoA (Sigma) was used as the substrate and 0.1 mM 2,6-dichlorophenolindophenol (DCPIP) was used as the terminal electron acceptor in a final volume of 300 µl. The change in absorbance at 600 nm was monitored by using a Beckman DU 7500 spectrophotometer, and the enzyme activity was calculated by assuming an extinction coefficient of 20.6 mM<sup>-1</sup> cm<sup>-1</sup> for DCPIP [38].

#### 4.6 Electrophoretic shift mobility assays.

Biotin-labeled DNA probes (fragments UP35 PaidB, UP35 Pada, UP35 PalkA, Neg PaidB) were used. Sense and antisense oligonucleotides were annealed by incubation at 95 °C for 5 min and successive gradual cooling to room temperature. Purified recombinant FadE8 was incubated with the probes for 20 min at room temperature in 20 µl of buffer Z (25 mM HEPES pH 7.6, 50 mM KCl, 12.5 mM MgCl<sub>2</sub>, 1 mM DTT, 20% glycerol, 0.1% triton). Protein–DNA complexes were separated on 5%

native polyacrylamide gel (29:1 cross-linking ratio) in 0.5 × TBE (45 mM Tris pH 8.0, 45 mM boric acid, 1 mM EDTA) at 200 V (20 V/cm) at room temperature. Afterwards, electrophoretic transfer to a nylon membrane was carried out in 0.5 × TBE at 380 mA for 45 min, and the transferred DNA was cross-linked to the membrane with UV light. After incubation in blocking buffer for 1 h at room temperature, the membrane was incubated with streptavidin–HRP conjugate (Sigma) for 30 min at room temperature. The membrane was washed and visualized with SuperSignal chemiluminescence reagent (Pierce).

## **5. Ethenobases analyses**

### **5.1 DNA extraction**

1 ml cell suspension was centrifuged at 8000g for 2 min. After removing the supernatant, the cells were washed with 400 µl STE Buffer (100 mM NaCl, 10 mM Tris/HCl, 1 mM EDTA, pH 8.0) twice. Then the cells were centrifuged at 8000g for 2 min. The pellets were resuspended in 200 µl TE buffer (10 mM Tris/HCl, 1 mM EDTA, pH 8.0). Then 100 µl Tris-saturated phenol (pH 8.0) was added to these tubes, followed by a vortex-mixing step of 60 s for bacteria, to lyse cells. The samples were subsequently centrifuged at 13 000g for 5 min at 4°C to separate the aqueous phase from the organic phase. 160 µl upper aqueous phase was transferred to a clean 1.5 ml tube. 40 µl TE buffer was added to make 200 µl and mixed with 100 µl chloroform and centrifuged for 5 min at 13 000g at 4°C. 160 µl upper aqueous phase was transferred to a clean 1.5 ml tube. 40 µl TE and 5 µl RNase (10 mg/ml) were added and incubated at 37 °C for 10 min to digest RNA. Then 100 µl chloroform was added to the tube, mixed well and centrifuged for 5 min at 13 000g at 4 °C. 150 µl upper aqueous phase was transferred to a clean 1.5 ml tube. The aqueous phase contained purified DNA and was directly used for the subsequent experiments or stored at -20°C. The purity and yield of the DNA were assessed spectrophotometrically by calculating the A260/A280 ratios and the A260 values to determine protein impurities and DNA concentrations

(Extremely rapid extraction of DNA from bacteria and yeasts, Hai-Rong Cheng<sup>1,2</sup> & Ning Jiang<sup>1</sup>,).

## **5.2 DNA hydrolyses and LC-MS/MS analyses**

The procedure involved incubation of DNA at pH 6 with phosphodiesterase II and nuclease P1, followed by treatment at pH 8 by phosphodiesterase I and alkaline phosphatase. The samples were transferred into an HPLC vial, and freeze dried. The resulting residue was dissolved in a 2 mM ammonium formate solution. The samples were then analyzed by reverse-phase HPLC associated with a Thermo Scientific TSQ Quantum Ultra used in the multiple reaction monitoring mode. The detection of methylated bases was achieved in the positive electrospray ionization mode. For all exocyclic adducts studied, the monitored transition corresponded to the loss of the 2-deoxyribose moiety from the protonated pseudo-molecular ion.

The column was maintained at 28 °C and eluted with a flow rate of 0.2ml/min starting with 100% ammonium formate 5mM (pH 6.5). The percentage of acetonitrile reached 15% in 25 min, whereas it reached 25% in 30 min. The column was then washed and equilibrated for 10 min with 100% of acetonitrile.

The amount of modified nucleoside was obtained by external calibration in the range of 20-200 fmol.

## **6. Methylated bases analyses**

### **6.1 DNA hydrolyses LC-MS/MS analyses**

The DNA solutions were subjected to acid hydrolysis in 0.1 M HCl at 80 °C for 30 min to obtain free bases. The samples were dried under vacuum and solubilized in 50 µL of 3% (v/v) methanol (MeOH)/0.1% (v/v) trifluoroacetic acid for methylated purine analysis. Standard methylated bases (Sigma-Aldrich) were solubilized in 3% (v/v) methanol (MeOH)/0.1% (v/v) trifluoroacetic acid [39]. Samples were then analyzed by reverse-phase HPLC associated with a Agilent Triple quadrupole 6420 used in the

multiple reaction monitoring mode. The C18 column was eluted with a flow rate of 0.2ml/min starting with 3% (v/v) MeOH/0.1% (v/v) formic acid. The column was delivered at 3% MeOH for 2 minutes. The percentage of MeOH reached 75% in 5 min and rapidly back to 3% MeOH.

The amount of methylated bases was obtained by external calibration in the range of 10-100 pg.

## **Chapter 3:**

### ***Escherichia coli* and methylation stress**



## **1. Molecular partners of *Escherichia coli* transcriptional regulator AidB**

### **1.1 Isolation of AidB Complexes in *E. coli* Upon Exposure to MMS**

Proteomic approaches were designed to shed some light on the mechanism of action of AidB through the identification of its protein partners *in vivo* [40]. The association of the protein with partners belonging to a particular mechanism will be strongly suggestive of its biological function. *In vivo* isolation of AidB containing protein complexes were performed by transforming *E. coli* C41 strain with the pET22b-AidB construct carrying the AidB gene fused to a six histidine tags. The strain was grown in the absence and in the presence of sub-inhibitory concentrations of the alkylating agent MMS. Isolation of AidB complexes was performed by IMAC (Ion Metal Affinity Chromatography). The total protein extracts from the two samples were first submitted to a pre-cleaning step by incubation with His-Select beads lacking nickel ions in order to remove non-specific proteins. Eluates from the pre-cleaning were then recovered and AidB containing complexes were isolated by IMAC on His Select beads. After extensive washing, the proteins specifically bound to the AidB bait were eluted with a strong ionic buffer containing 0.5 M imidazole and fractionated on SDS-PAGE stained with coomassie blue. Pre-cleaning samples were also eluted and used as control. Figure 12 shows the obtained Coomassie blue stained gel.

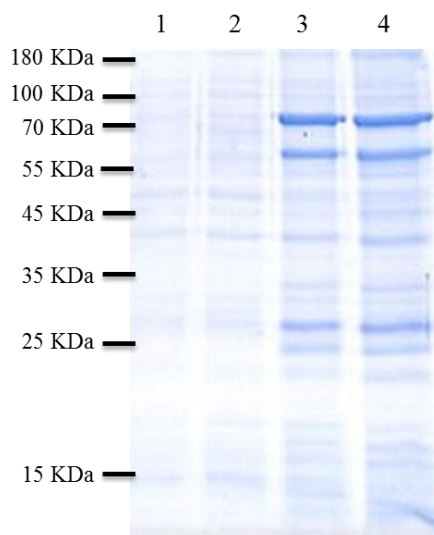


**Figure 12.** SDS-PAGE fractionation of AidB complexes. Lanes 1 and 2 pre-cleaning eluates. Lanes 3 and 4 AidB complexes in the absence and in the presence of MMS, respectively.

## 1.2 Identification of proteins specifically interacting with AidB

The entire lanes from both samples (3, 4) and controls (1, 2) were cut in 24 slices and each gel slice was in situ digested with trypsin and the corresponding peptide mixtures directly analysed by LC/MS/MS procedures. Tandem mass spectral analyses provided both the accurate molecular mass and sequence information from the daughter ion spectra of each peptide. These data were used for database search using a home version of the Mascot software leading to the identification of the proteins. Common proteins identified in both the sample and the control gel slices were ruled out and only those solely occurring in the samples were considered as putative AidB interactors thus greatly decreasing the number of false positives. Proteins identified in the proteomic experiments are listed in Tables 2 and 3 where the protein name, the corresponding Swiss Prot code and the number of identified peptides are reported. The presence of the AidB bait in both lists constituted a sort of internal control indicating the correctness of the pull down experiment.

A total of 73 proteins were identified by the proteomic procedure, 17 of which were found both in the presence and in the absence of the methylating agent. The results of the proteomic experiments are summarized in Tables 2 and 3.

**Table 2.** Proteins identified in the control sample.

In the absence of MMS	Swiss prot code	Peptides
2-oxoglutarate dehydrogenase E1 component (SucA)	P0AFG3	2
Dihydrolipoyllysine-residue acetyltransferase component of pyruvate dehydrogenase complex (AceF)	P06959	6
Phosphoenolpyruvate synthase (PpsA)	P23538	2
Bifunctional polymyxin resistance protein arnA (ArnA)	P77398	42
Glucosamine-fructose-6-phosphate aminotransferase [isomerizing] (GlmS)	P17169	10
Phosphoenolpyruvate-protein phosphotransferase (PtsI)	P08839	3
Protein AidB	P33224	20
Alkyl hydroperoxide reductase subunit F (AhpF)	P35340	7
Glycogen synthase (GlgA)	POA6U8	11
UDP-N-acetylmuramate: L-alanyl-gamma-D-glutamyl-meso-diaminopimelate ligase (mpl)	P37773	2
NADP-specific glutamate dehydrogenase (gdhA)	P00370	12
3-oxoacyl-[acyl-carrier-protein] synthase 2 (fabF)	P0AAI5	3
Transcriptional activator protein (lysR)	P03030	9
Ribosomal small subunit pseudouridine synthase A (rsuA)	P0AA43	11
UPF0011 protein yraL (yhbJ)	P67087	6
Enoyl-[acyl-carrier-protein] reductase [NADH] (fabI)	P0AEK4	2
Acyl-[acyl-carrier-protein]-UDP-N-acetylglucosamine O-acyltransferase (lpxA)	P0A722	2
FKBP-type 22 kDa peptidyl-prolyl cis-trans isomerase (fklB)	P0A9L3	6
Catabolite gene activator (crp)	P0ACJ8	22
UPF0011 protein yraL (yraL)	P67087	2
Uncharacterized protein yqjI (yqjI)	P64588	3
Uncharacterized protein ybgA (ybgA)	P24252	2
Ferric uptake regulation protein (fur)	P0A9A9	6
50S ribosomal protein L17 (rplQ)	P0AG44	3

**Table 3.** Proteins identified in the sample treated with 0.04% MMS.

In the presence of MMS	Swiss prot code	Peptides
UvrABC system protein A (UvrA)	P0A698	5
Aldehyde-alcohol dehydrogenase (AdhE)	P0A9Q7	2
Dihydrolipoyllysine-residue acetyltransferase component of pyruvate dehydrogenase complex (AceF)	P06959	5
Ribonucleoside-diphosphate reductase 1 subunit alpha (NrdA)	P00452	3
Maltodextrin phosphorylase (malP)	P00490	2
Bifunctional polymyxin resistance protein arnA (arnA)	P77398	37
Glucosamine-fructose-6-phosphate aminotransferase [isomerizing] (glmS)	P17169	20
Phosphoenolpyruvate-protein phosphotransferase (ptsI)	P08839	7
Cold-shock DEAD box protein A (DeaD)	P0A9P6	6
Succinate dehydrogenase flavoprotein subunit (sdhA)	P0AC41	3
GTP-binding protein typA/BipA (typA)	P32132	2
L-aspartate oxidase (NadB)	P10902	2
Chaperone protein hscA (hscA)	P0A6Z1	2
D-lactate dehydrogenase (dld)	P06149	2
Protein aidB (AidB)	P33224	19
Alkyl hydroperoxide reductase subunit F (ahpF)	P35340	9
Glucose-6-phosphate 1-dehydrogenase (zwf)	P0AC53	3
Glycogen synthase (glgA)	POA6U8	10
UDP-N-acetylmuramate: L-alanyl-gamma-D-glutamyl-meso-diaminopimelate ligase (mpl)	P37773	3
Tryptophanase (TnaA)	P0A853	2
NADP-specific glutamate dehydrogenase (gdhA)	P00370	24

3-oxoacyl-[acyl-carrier-protein] synthase 2 (fabF)	P0AAI5	4
3-oxoacyl-[acyl-carrier-protein] synthase 1 (fabB)	P0A953	5
Succinylornithine transaminase (astC)	P77581	13
UDP-N-acetylglucosamine 1-carboxyvinyltransferase (murA)	P0A749	11
Glutamate-1-semialdehyde 2,1-aminomutase (hemL)	P23893	4
S-adenosylmethionine synthetase (metK)	P0A817	5
Protein hflK (hflK)	P0ABC7	4
Isocitrate dehydrogenase [NADP] (icd)	P08200	2
Maltose/maltodextrin import ATP-binding protein malK (malK)	P68187	4
Transcription termination factor rho (rho)	P0AG30	3
ATP-dependent Clp protease ATP-binding subunit clpX (clpX)	P0A6H1	3
Cysteine desulfurase (iscS)	P0A6B8	3
Regulatory protein ada (ada)	P06134	9
Glycerol dehydrogenase (gldA)	P0A955	3
Acetylornithine deacetylase (arge)	P23908	4
Lactose operon repressor (laci)	P03023	3
Glutamate-1-semialdehyde 2,1-aminomutase (gsa)	P23893	2
USG-1 protein (usg)	P08390	2
Riboflavin biosynthesis protein RibD (RibD)	P25539	4
P-protein (pheA)	P0A9J8	3
UDP-4-amino-4-deoxy-L-arabinose—oxoglutarate aminotransferase (ArnB)	P77690	3
Glyceraldehyde-3-phosphate dehydrogenase A (gabA)	P0A9B2	13
Elongation factor Ts (tsf)	P0A6P1	8
UPF0042 nucleotide-binding protein yhbJ (yhbJ)	P0A894	6
Acetyl-coenzyme A carboxylase carboxyl transferase subunit beta (accD)	P0A9Q5	2
Aspartate carbamoyltransferase catalytic chain (pyrB)	P0A786	2
Ribosomal small subunit pseudouridine synthase A (rsuA)	P0AA43	12
Uncharacterized HTH-type transcriptional regulator yeiE (yeiE)	P0ACR4	10
UPF0042 nucleotide-binding protein yhbJ (yhbJ)	P0A894	11
Formyltetrahydrofolate deformylase (purU)	P0A440	10
UPF0011 protein yraL (yraL)	P67087	7
Enoyl-[acyl-carrier-protein] reductase [NADH] (fabI)	P0AEK4	2
Acyl-[acyl-carrier-protein]-UDP-N-acetylglucosamine O-acyltransferase (lpxA)	P0A722	3
D-methionine-binding lipoprotein metQ (metQ)	P28635	2
FKBP-type 22 kDa peptidyl-prolyl cis-trans isomerase (fklB)	P0A9L3	6
GTP cyclohydrolase 1 (folE)	P0A6T5	2
Catabolite gene activator (crp)	P0ACJ8	21
Translation initiation factor IF-3 (infC)	P0A707	2
Uncharacterized protein yqjI (yqjI)	P64588	3
UPF0227 protein ycfP (ycfP)	P0A8E1	3
50S ribosomal protein L6 (rplF)	P0AG55	2
UPF0304 protein yfbU (yfbU)	P0A8W8	2
Ferric uptake regulation protein (fur)	P0A9A9	8
50S ribosomal protein L27 (rpmA)	P0A7L8	2
30S ribosomal protein S15 (rpsO)	P0ADZ4	3

According to their reported biological activities, the putative interactors were grouped into different functional categories: metabolic pathways including several FAD and NAD<sup>+</sup> dependent dehydrogenases, stress response and transcription, translation and

processing of DNA/RNA. Among others, we focused our attention on the stress response proteins for further investigations.

### 1.3 Validation of Protein-protein Interactions by Co-immunoprecipitation Experiments

Putative protein-protein interactions detected by the proteomic experiments were validated by co-immunoprecipitation experiments. Proteins involved in pathways strictly connected with DNA repair and protection mechanisms were firstly examined. Each putative protein partner was recombinantly expressed as c-myc-tagged protein in *E. coli* C41 cells and the cell extracts were immunoprecipitated with anti-c-myc-conjugated antibody. Immunoprecipitates were fractionated by SDS-PAGE and stained by Western blot analysis using an anti-AidB antibody. Interaction of the individual partner with AidB was confirmed by the presence of a positive signal revealed by the western blot analysis. As an example, Figure 13 shows the Western Blot Analysis performed on the immunoprecipitate from *E. coli* cells expressing c-myc tagged UvrA.

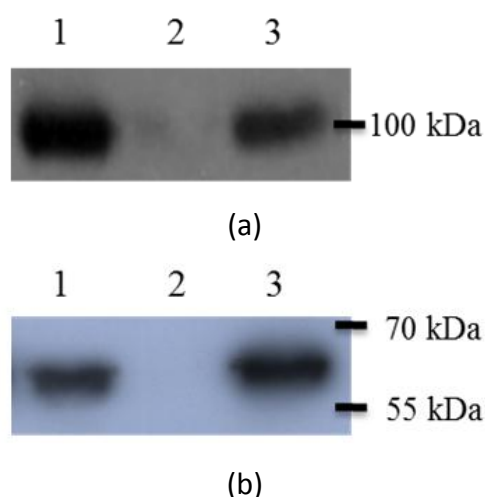


**Figure 13.** (a) Western blot analysis of the total cell extract from *E. coli* C41 cells producing c-myc-UvrA (lane 1) and the UvrA containing immunoprecipitate (lane 3). Lane 2 contains the precleaning; (b) Western blot analysis of the total cell extract from *E. coli* C41 cells (lane 1) and the UvrA immunoprecipitate revealed by the anti-AidB antibody (lane 3). Lane 2, precleaning.

Figure 13a shows the total cell extract (lane 1) and the corresponding

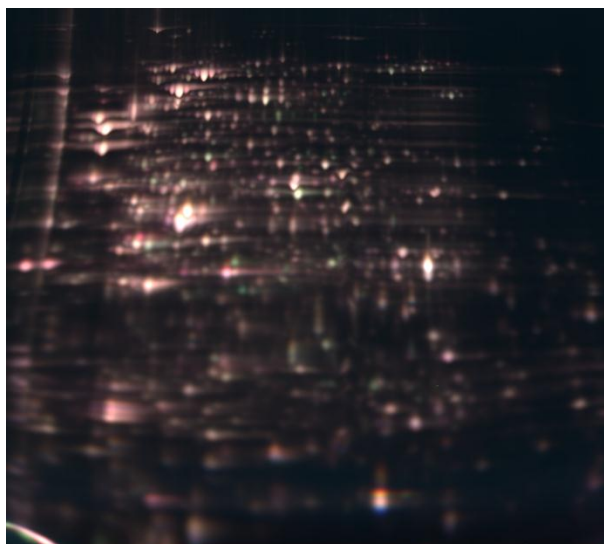
immunoprecipitate (lane 3) immunorevealed by anti c-myc antibody demonstrating that UvrA was expressed by the recombinant cells and immunoprecipitated by the antibody.

Figure 13b shows the positive signal detected when the UvrA immunoprecipitate was incubated with the anti-AidB antibody, demonstrating the presence of AidB in the sample and confirming the interaction.

Positive interactions of AidB with UvrA, DeaD and TnaA were identified, whereas no positive bands in the western blot could be detected when Ada and RecA proteins were tested. It should be underlined that both Cold-shock DEAD box protein A (DeaD) and Tryptophanase (TnaA) had already been identified in complex with AidB in the transcriptional machinery gathered at the *E. coli* *arnB* P1 promoter in the presence of MMS [19].

## **2. Differential proteomic approach to the study of *E.coli* upon exposure to methylating agent**

Differential in Gel Electrophoresis (DIGE) was used to deeply examine the effect of methylation stress on *Escherichia coli* proteome. MV1161 cells were grown in four replicates in LB medium to an optical density of 0.5 at 600 nm. Each culture was divided into two aliquots, one of them was treated with MMS 0.04% and the other one was kept untreated and used as control. Upon 20 minutes of exposure, cells were collected and washed with PBS. Cells were suspended in lysis buffer. Lysates from treated or untreated cells were labeled with Cy3 or Cy5 respectively []. Each Cy3/Cy5-labeled sample pair was mixed with a Cy2-labeled pooled standard sample containing an equal amount of both treated and untreated samples. The Cy2/Cy3/Cy5 labeled samples were run together on the same gel. After electrophoresis, gels were scanned in a Typhoon 9400 scanner. The images labeled with Cy2, Cy3 and Cy5 were acquired at excitation/emission values of 488/520, 532/580, 633/670nm respectively [41, 42]. The three images acquired at three different wavelengths were superimposed as shown in Figure 14.



**Figure 14.** Protein extracts of treated and untreated *E.coli* cells labeled with the three different fluorophores Cy2, Cy3, Cy5, and fractionated by 2D SDS-PAGE.

Images were used for pairwise comparison of each sample (Cy3 and Cy5) with the Cy2 mixed standard present in each gel. A specific software was used to detect spot boundaries and to calculate spot volume, normalized versus the volume of the corresponding spot present in the pool standard of the same gel. Statistical significance of differences in spot intensity was determined with Student's *t* test. Only protein spots with a change in size of at least 1.20 fold (*t* test:  $p \leq 0.05$ ) after normalization were considered significantly altered. We verified the validity of these changes and accuracy of spot matching by manual inspection of the gels.

The image analysis showed the occurrence of about 45 differently expressed protein spots. The spots of interest were picked, *in situ* hydrolyzed and the resulting peptide mixtures were analyzed by MS using the LC/MSD Trap XCT Ultra. Data analyses were performed through Mascot software selecting NCBI database. A total of 69 proteins were identified, 61 down and 8 up regulated. The comprehensive list is reported in Table 4.

**Table 4.** Differentially expressed proteins identified.

Av Ratio	Protein description	Gene Symbol	Swiss Prot
-5.78	N-acetylneuraminate lyase	nanA	<a href="#">P0A6L4</a>
-1.85	Formate dehydrogenase, nitrate-inducible, major subunit	fdnG	<a href="#">P24183</a>
-1.82	Fumarate reductase flavoprotein subunit	frdA	<a href="#">P00363</a>

### Chapter 3: *Escherichia coli* and methylation stress

-1.72	Tryptophanase	tnaA	<a href="#">P0A853</a>
	Bifunctional protein GlmU	glmU	<a href="#">P0ACC7</a>
-1.67	Oligopeptide transport ATP-binding protein OppD	oppD	<a href="#">P76027</a>
	Dihydroorotase	pyrC	<a href="#">P05020</a>
-1.65	2,3-bisphosphoglycerate-independent phosphoglycerate mutase	gpml	<a href="#">P37689</a>
	Aerobic glycerol-3-phosphate dehydrogenase	glpD	<a href="#">P13035</a>
-1.62	Fumarate hydratase class I, anaerobic	fumB	<a href="#">P14407</a>
-1.62	Cytidine deaminase	cdd	<a href="#">P0ABF6</a>
	Probable deferrochelataase/peroxidase YfeX	yfeX	<a href="#">P76536</a>
-1.61	UDP-glucose 4-epimerase	galE	<a href="#">P09147</a>
-1.53	Ribonuclease G	rng	<a href="#">P0A9J0</a>
	Bifunctional purine biosynthesis protein PurH	purH	<a href="#">P15639</a>
	Transcriptional regulatory protein TyrR	tyrR	<a href="#">P07604</a>
-1.53	PTS system mannose-specific EIIAB component	manX	<a href="#">P69797</a>
	L-threonine dehydratase catabolic TdcB	tdcB	<a href="#">P0AGF6</a>
-1.49	Anaerobic glycerol-3-phosphate dehydrogenase subunit A	glpA	<a href="#">P0A9C0</a>
-1.41	Glyceraldehyde-3-phosphate dehydrogenase A	gapA	<a href="#">P0A9B2</a>
-1.40	Trehalose-6-phosphate hydrolase	treC	<a href="#">P28904</a>
-1.38	Uncharacterized oxidoreductase YdgJ	ydgJ	<a href="#">P77376</a>
	Aspartate--ammonia ligase	asnA	<a href="#">P00963</a>
-1.32	Aminomethyltransferase	gcvT	<a href="#">P27248</a>
	Flagellar motor switch protein FliM	fliM	<a href="#">P06974</a>
-1.32	Probable acrylyl-CoA reductase AcuI	acuI	<a href="#">P26646</a>
-1.30	Phosphoenolpyruvate carboxykinase [ATP]	pckA	<a href="#">P22259</a>
	3-octaprenyl-4-hydroxybenzoate carboxy-lyase	ubiD	<a href="#">P0AAB4</a>
	Uncharacterized sulfatase YdeN	ydeN	<a href="#">P77318</a>
	Malate synthase A	aceB	<a href="#">P08997</a>
-1.30	Catalase-peroxidase	katG	<a href="#">P13029</a>
	Polyribonucleotide nucleotidyltransferase	pnp	<a href="#">P05055</a>
	Dihydrolipoyllysine-residue acetyltransferase component of pyruvate dehydrogenase complex	aceF	<a href="#">P06959</a>
-1.27	Threonine--tRNA ligase	thrS	<a href="#">P0A8M3</a>
-1.27	Phosphoenolpyruvate carboxykinase [ATP]	pckA	<a href="#">P22259</a>
	Malate synthase A	aceB	<a href="#">P08997</a>
-1.26	Chaperone protein ClpB	clpB	<a href="#">P63284</a>
	Elongation factor G	fusA	<a href="#">P0A6M8</a>
-1.26	UDP-glucose 4-epimerase	galE	<a href="#">P09147</a>



-1.26	HTH-type transcriptional regulator CysB	cysB	<a href="#">P0A9F3</a>
-1.25	Glycerol kinase	glpK	<a href="#">P0A6F3</a>
-1.21	Bifunctional protein FolC	folC	<a href="#">P08192</a>
	D-tagatose-1,6-bisphosphate aldolase subunit GatZ	gatZ	<a href="#">P0C8J8</a>
-1,2	Deoxyribose-phosphate aldolase	deoC	<a href="#">P0A6L0</a>
-1.19	tRNA-dihydrouridine synthase A	dusA	<a href="#">P32695</a>
-1.17	Trehalose-6-phosphate hydrolase	treC	<a href="#">P28904</a>
-1.17	Histidine--tRNA ligase	hisS	<a href="#">P60906</a>
-1.15	2,3-bisphosphoglycerate-dependent phosphoglycerate mutase	gpmA	<a href="#">P62707</a>
-1.12	Pyruvate kinase I	pykF	<a href="#">P0AD61</a>
	Ribose import ATP-binding protein RbsA	rbsA	<a href="#">P04983</a>
1,09	Glutamate decarboxylase beta	gadB	<a href="#">P69910</a>
	Bifunctional protein HldE	hldE	<a href="#">P76658</a>
1,11	Outer membrane protein assembly factor BamA	bamA	<a href="#">P0A940</a>
1,24	Phosphoglucomutase	pgm	<a href="#">P36938</a>
-2.76	Transketolase 2	tktB	<a href="#">P33570</a>
1,2	Methionine--tRNA ligase	metG	<a href="#">P00959</a>
-1.52	phosphoenolpyruvate carboxykinase	pck	<a href="#">P22259</a>
1,37	6-phospho-beta-glucosidase A	bglA	<a href="#">P24240</a>
	potassium transporter peripheral membrane protein	trkA	<a href="#">P0AGI8</a>
1,51	alkyl hydroperoxide reductase	ahpF	<a href="#">Q8XBT4</a>
-1.56	aldehyde dehydrogenase A, NAD-linked	aldA	<a href="#">P25553</a>
	aspartate ammonia-lyase	aspA	<a href="#">P0AC38</a>
-1.51	thymidine phosphorylase	deoA	<a href="#">P07650</a>
	6-phosphogluconate dehydrogenase	gnd	<a href="#">P00350</a>
-1.79	galactitol-1-phosphate dehydrogenase	gatD	<a href="#">P0A9S4</a>
-1.48	aldehyde reductase, NADPH-dependent	yqhD	<a href="#">Q46856</a>
	dihydro-orotase	pyrC	<a href="#">P05020</a>
-1.69	phenylalanine tRNA synthetase, alpha subunit	pheS	<a href="#">P08312</a>
-1.68	glucosamine-6-phosphate deaminase	nagB	<a href="#">P0A760</a>

The list of total proteins was submitted to Database for Annotation, Visualization and Integrated Discovery (DAVID) Bioinformatics Resources to obtain a functional organization. Proteins were then grouped according to their biological function as shown in Figure 15.

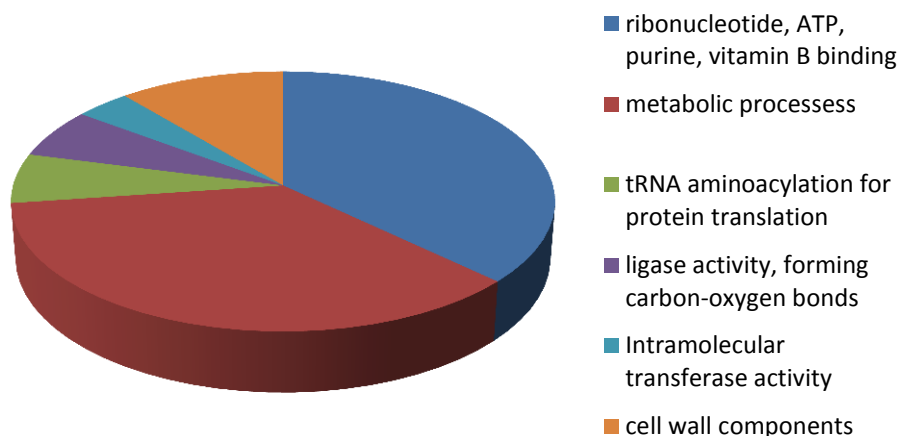


**Figure 15.** Clustered identified proteins are reported.

Most of the identified proteins were down regulated and belonged to metabolic processes, a result that confirmed the negative effect of methylating agents on cellular growths, as previously observed [2].

An interesting group is represented by cell wall components containing both proteins directly involved in cell wall structure and others belonging to biosynthetic pathways leading to the synthesis of cell wall components.

In particular, N-acetylneuraminase lyase (*nanA*) was part of this functional group and critically down regulated in the presence of MMS. In pathogen bacteria such as *Streptococcus pneumonia* NanA is involved in biofilm formation and in adhesion to host cells [43, 44, 45]. These data indicate that in the presence of methylating stress the substantial decreasing in NanA expression might affect *E. coli* cell-cell interaction capabilities. NanA down regulation in the presence of methylation stress was explored through *in vitro* and *in vivo* assays addressed to evaluate biofilm formation and adhesion abilities during a stage at Prof. Selan laboratory (Department of Public Health and Infectious Diseases, University La Sapienza of Rome).

### 3. Effect of methylating agent on bacterial biofilms formation and adhesion capability

Biofilms are surface attached polymeric matrices of cells having biological activities. This bacterial attachment mechanism is also required to adhere directly to host organism and it is involved in infectious processes for most pathogen microorganisms [46]. Static growth conditions were first optimized in order to obtain the maximum amount of attached cells to multiwell surface and to eventually evaluate biofilm formation. MV1161 (a wild type strain) and MV5924 (an *E. coli* strain missing the *aidB* gene, called  $\Delta aidB$ ) strains were inoculated on different sizes wells in the presence and in the absence of 0.5% and 1% glucose to promote biofilm formation. *In vitro* quantification of attached cells was evaluated after 24 hours of incubation at 37°C by crystal violet staining and subsequent measurement of the absorbance at 590 nm. Better results were obtained on bigger surfaces and following addition of 1% glucose that increased biofilm formation five times. Once defined the best experimental conditions, wild type and  $\Delta aidB$  strains were grown in the presence and in the absence either of 0.04% MMS or Busulfan. Figure 16 shows biofilm production for both strains.

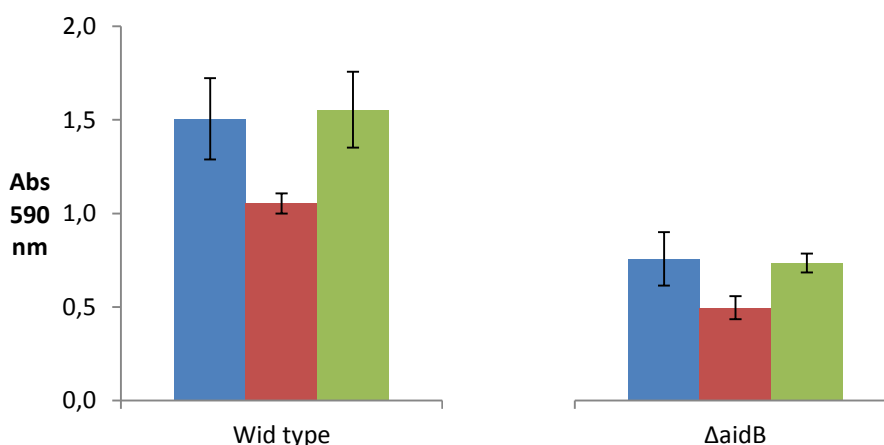


**Figure 16.** Biofilm formation for wild type (on the left) and  $\Delta aidB$  (on the right) *E. coli* strains untreated (blue), in presence of MMS (red) and Busulfan (green). Biofilm is reported by crystal violet absorbance at 590 nm. Data represent results obtained on three different independent experiments for both wild type and  $\Delta aidB$  strains.

Data obtained showed that wild type strain produces an amount of biofilm two times greater than  $\Delta aidB$  suggesting that the absence of *aidB* in the strain causes activation of pathways in layers accumulation capacity. The presence of MMS decreased biofilm formation in agreement with proteomic results that suggested a down regulation of processes linked to cellular wall formation. On the contrary, biofilm production is unaffected by the presence of Busulfan suggesting that *E.coli* responses are unable to counteract this kind of DNA modification in both wild type and  $\Delta aidB$ . These data support the occurrence of a connection between alkylation response and cellular cohesive properties.

Biofilm mechanisms are usually associated to cellular adhesion/invasion processes so further investigations were focused on deeply study this point. The capability of wild type *E. coli* strain to adhere and invade human HeLa cells was examined. Such cell type is an immortal line taken in 1951 and derived from Henrietta Lacks cervical cancer, and it was chosen because of its durability and proliferation. Bacteria invasion capability of *E. coli* was evaluated by using gentamycin invasion assay. Data obtained clearly showed that wild type was not able to invade HeLa cells. This result was expected because invasion property is commonly found in pathogenic rather than in non-pathogen bacteria and wild type *E. coli* belongs to the second group.

Adhesion capability was evaluated independently from invasion. After 0.04% MMS treatment, wild type cells were sub cultured and multiply diluted on HeLa cells in order to establish the best bacterial/eukaryotic cells ratio. Data obtained for one of the three cellular dilution realized are reported in Figure 17.

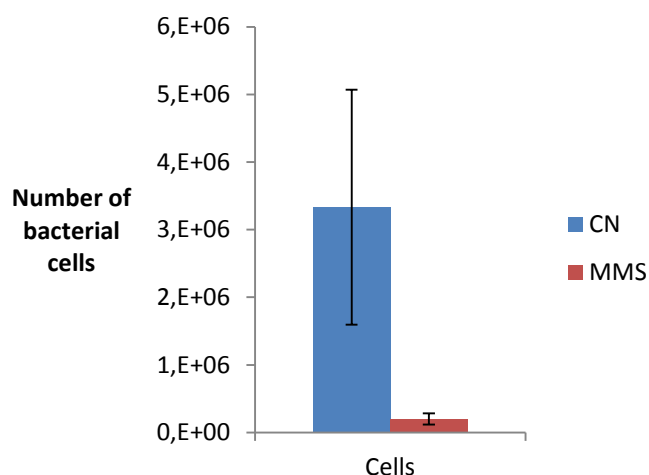


**Figure 17.** Number of bacterial cells adhered on HeLa cells is reported in presence and in absence of MMS 0.04%. Data represent the mean  $\pm$  SD of three independent experiments

*E. coli* adhesion on HeLa cells resulted drastically decreased in the presence of MMS demonstrating a functional correlation between methylation stress and cohesive cellular properties in agreement with proteomic data. In particular, the down regulation of NanA suggested that this protein might have a leading role in biofilm formation and adhesion processes not only in pathogenic bacteria but also in *E.coli*.

## **Chapter 4:**

### ***Mycobacterium tuberculosis* and alkylation stress**

## 1. Effect of alkylating agent on *M. tuberculosis* growth and morphology

### 1.1 MMS on *Mycobacterium smegmatis* cells

The investigation of the effect of DNA methylation on the cellular growth of MTB was performed to explore whether limited doses of alkylating agents might affect MTB cell viability. Methyl methanesulfonate (MMS) and the bi-functional chemotherapeutic drug Busulfan were used as methyl donors.

Preliminary experiments were carried out on *Mycobacterium smegmatis* to evaluate the lowest amount of reagent clearly affecting cells growth. *M.smegmatis* cells were grown in the presence and in the absence of different concentrations of MMS in a 0.01-0.1% w/v range and the viability of bacterial cultures was monitored for 24 hs. Figure 18 clearly shows a decrease in cell survival with increasing doses of MMS in comparison with untreated cells (CN).

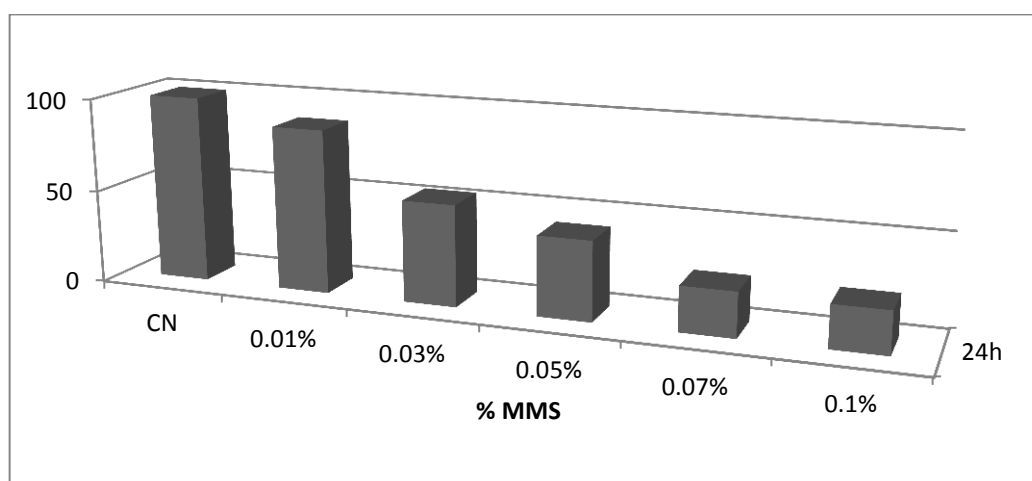


**Figure 18.** Cells survival rate after 24 hours from the exposure to MMS.

These data demonstrated that a 0.03% MMS concentration led to a decrease of about 50% in cell survival. This concentration was then selected for further experiments. First, the growth profiles of *M.smegmatis* in the absence and in the presence of 0.03% MMS were evaluated. Figure 19 clearly shows that treated cells

displayed a remarkable reduction in the growth profile as compared to the control, indicating that in these conditions *M.smegmatis* cultures were affected by DNA alkylation.

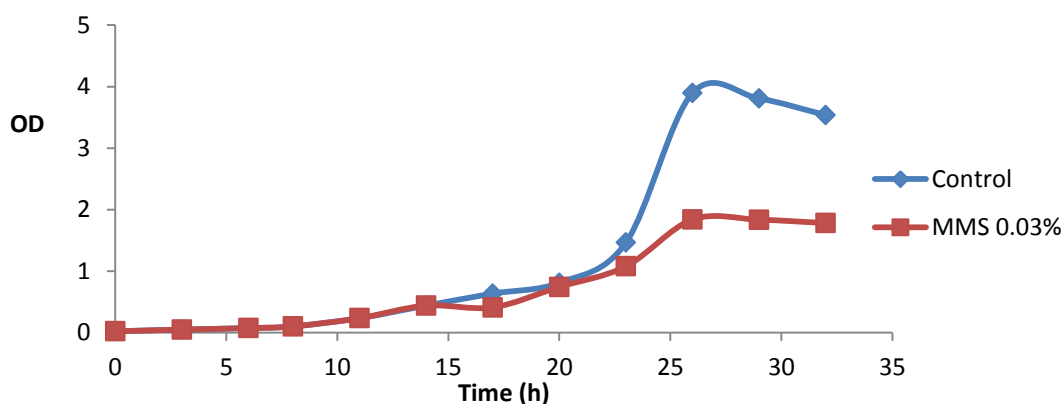


**Figure 19.** Growth profile of *M.smegmatis* cells in the presence (red) and in the absence (blue) of MMS 0.03%.

## 1.2) MMS on *M.tuberculosis* clinical strains

Alkylation experiments were then performed on two reference (H37Rv and H37Ra) and 8 clinical strains of the pathogen *Mycobacterium tuberculosis* during a stage at Prof. Zanetti laboratory (Department of Chemistry and Pharmacy, University of Sassari). Preliminarily, the Minimum inhibitory concentrations (MIC) of MMS for both reference strains were calculated by Resazurin Microtiter Assay (REMA). The MIC concentration values obtained for H37Rv and H37Ra were 0.10% and 0.05% respectively, slightly higher than those used for *M.smegmatis*. Finally, alkylation experiments were performed on 4 different tubercular strains that had developed drug resistance to isoniazid, streptomycin and both isoniazid and rifampicin and on 4 different non-tubercular (NTM) clinical strains of *M. tuberculosis* (*M. gordonae*, *M. szulgai*, *M. xenopi*, *M. chelonae*). Once these bacteria cultures were exposed to multiple MMS concentrations, seven out of eight strains appeared sensitive to MMS showing an extended cells death in these conditions. Interestingly, the MMS concentrations used resulted lower than the MIC previously determined for reference strains. As an example, figure 9 shows the growth profiles of the clinical strain resistant to isoniazid, in the presence of 0.03% and 0.015% w/v MMS in comparison with cells untreated or treated with the reference drug.



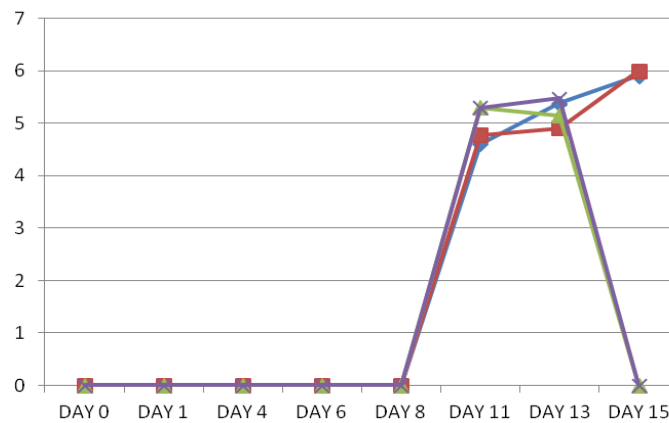


**Figure 20.** Growth profiles of the tubercular clinical strain resistant to isoniazid in the presence of isoniazid (red), MMS 0.03% (green), MMS 0.015% (violet) and in the absence of methylating compound (blue).

The viability of this strain was heavily affected by both MMS concentrations whereas bacterial cells are clearly resistant to the reference drug isoniazid. Optical microscopy images of mycobacterial cells were obtained in all conditions tested as shown in Figure 21.

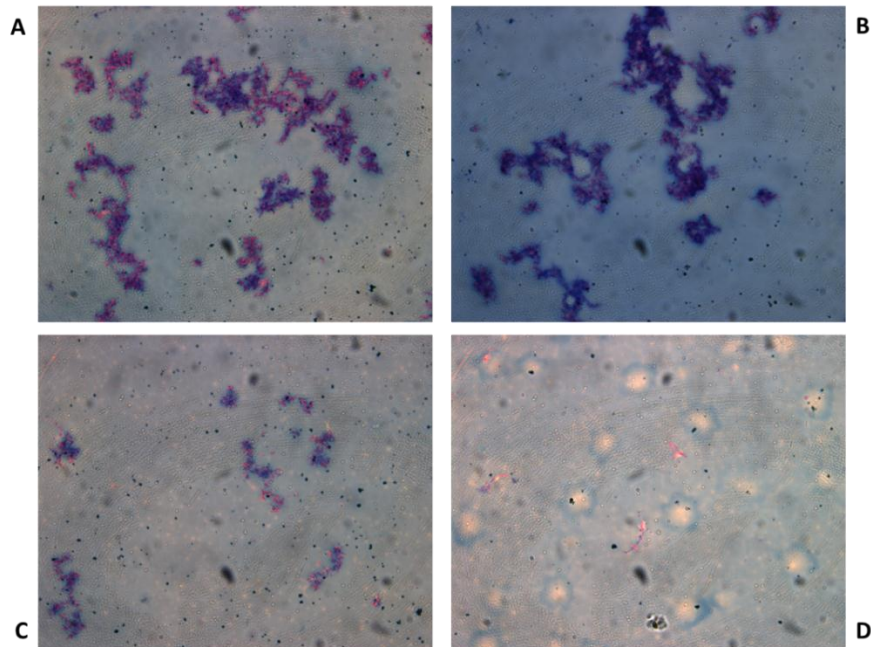


**Figure 21.** Optical microscopy images of the clinical strain resistant to isoniazid in the absence of methylating compounds (A), in the presence of isoniazid (B), MMS 0.015% (C) and MMS 0.03% (D).

A remarkable disappearance of typical cells clusters was clearly detected in the presence of both MMS concentrations (C and D) with respect to isoniazid treated cells (B) and control samples (A).

### 1.3 Busulfan on *M. smegmatis* cells

Since DNA methylation seems to impair *M.tuberculosis* cell viability, we evaluated the effect of a bi-functional methylating drug commonly used in cancer chemotherapy (Busulfan). The effect of this molecule was tested on *M.smegmatis* cells in a 0.01%-0.1% concentration range (w/v). Figure 22 shows the growth profile of *M.smegmatis* treated with 0.06% Busulfan where about 20% decrease in cells survival was clearly detected.

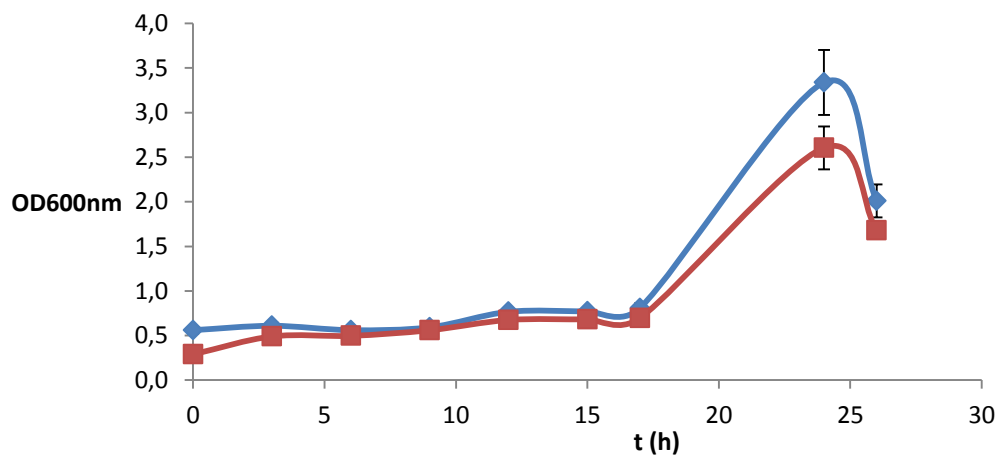


**Figure 22.** Growth profiles of *M.smegmatis* cells in the presence (red) and in the absence (blue) of Busulfan 0.06%.

## 2. Study of a *M.tuberculosis* protein potentially involved in alkylation response

### 2.1) *In silico* analysis of MTB putative AidB homologue

A mechanism of adaptive response to alkylation stress had already been reported in *M. tuberculosis* [37]. This process showed certain similarities to the homologous mechanism described in *E. coli*. Therefore, an *in silico* screening on the MTB protein database was carried out using the bioinformatics tool BLAST (Basic Local Alignment Search Tool) searching for putative proteins homologue to the *E.coli* adaptive response factors with particular emphasis on the AidB protein. The *E.coli* protein sequence was employed as a template to find regions of local similarity between protein sequences presenting in MTB database. Searching results produced a positive match with the putative acyl-CoA dehydrogenase FadE8 with an amino acid identity of 44% and a good percentage of positives substitutions. Figure 23 shows the sequence alignment between the two protein.

PROBABLE ACYL-CoA DEHYDROGENASE FADE8 (Acyl-CoA dehydrogenase, putative)

Sequence ID: [sp|O86368|O86368\\_MYCTU](#) Length: 542 Number of Matches: 1

Range 1: 3 to 514		<a href="#">GenPept</a>	<a href="#">Graphics</a>			<a href="#">Next Match</a>	<a href="#">Previous Match</a>
Score	Expect	Method	Identities	Positives	Gaps		
404 bits(1037)	4e-138	Compositional matrix adjust.	230/520(44%)	306/520(58%)	16/520(3%)		
Query 4	QTHIVFNQPIPLNNSNLYLSDGALCEAVTREGAGWSDFLASIGQQLGTAESELELGR	63					
	TH V NQ PL N N S L EA+ +EG W D + +G + ++ G LA+						
Sbjct 3	DIHVVTNQVPLENYPN-ASSPVLIEALIQEGGQWGLDEVNEVGASASCQAQRWGLAD	61					
Query 64	VNPPELLRYDAQGRRLDDVRFHPAWHLLMQALCTNRVHNLAWEEEDARSAGFVARAARFML	123					
	N P L +DA G R+D+V + PA+H LM+ T+ +H W +D R GA V RAA+ +						
Sbjct 62	RNRPIHLTHDAYGYRVDEVEYDPAYHELMRTAITHGMHAAPWADD-RPGAHVVRAAKTSV	120					
Query 124	HAQVEAGSLCPITMTFAATPLLL--QMLPAPFQDWTTPLLSDR-YDSHLLPGGQKRGILLI	180					
	VE G +CPI+MT+A P L I A ++ PLL+ R YD I P K G+						
Sbjct 121	WT-VEPGHICPISMTYAVVPALRYNSELAAYVE----PLITSREYDPELKPATTKAGITA	175					
Query 181	GMGMTEKQGGSDVMSNITRAERLEDGSYRLVGHKWFSSVPQSDAHLVLAQTAGGLSCFFV	240					
	GM MTEKQGGSDV + TT+A DGSY L GHKW F S P D LVLAQ GLSCF +						
Sbjct 176	GMSMTEKQGGSDVRAGTTQATPNADGSYSLTGHKWFSAAPMCDIFLVLAQAPDGLSCFLL	235					
Query 241	PRFLPDGQRNAILRLERLKDGLGNRSNASCEVEFQDAIGWLLGLEGEGIRLILKMGMGMR	300					
	PR LPDG RN + L+RLKDKLGN +NAS EVE+ A+ WL+G EG G+ I++M +TR						
Sbjct 236	PRVLPDGTNRNMFRLQRLKDKLGNHANASSEVEYDGAVANLVGEEGRGVPTIIEVMNLTRL	295					
Query 301	DCALGSHAMRRRAFLAIYHAHQHVFNGNPLIQQLMRHVLRSMAQLLEGQTALLFRLAR	360					
	DCALGS MR + A++HA R FG LI QPLMR+VL+ +A++ E T + R+A						
Sbjct 296	DCALGSATSMRTGLTRAVHHAQHRKAFGAYLIDQPLMRNVLADLAVEAEAAITVAMRMAG	355					
Query 361	AWDR--RADAKEALWARLFTPAKVFICKRGMPPFAEAMEVLGGIGYCEESELPRLYREM	418					
	A D R + EAL R+ AAK+ +CKR AEA+E LGG GY E+S +PRLYRE						
Sbjct 356	ATDNAVRGNETEALLRRIGLAAAKYVWCKRSTAHAAEALECLGGNGYVEDSGMPRLYREA	415					
Query 419	FVNSIWEGSGNIMCLDVLRLNKGAGVYDLLSEAFVEVKQGDYFDRVRRQLQQLRKPA	478					
	P+ IWEGSGN+ LD LR + + ++L + GQD D V RL+ QL						
Sbjct 416	PLMGIWEGSGNVSLDITLRAMATRPACVEVLFDELARSAGQDPRLDGHVERLRPQLGD-L	474					
Query 479	EELG---REITHQLFLGCGAQLKYASPPMAQAWCQVML	515					
	+ +G R+I + L G+ +++ P +A+A+ L						
Sbjct 475	DTIGYRARKIAEDICLALQSSLLVRHGHFAVAEAFATRL	514					

**Figure 23.** Sequence alignment between AidB from *E.coli* and FadE8 from MTB.

No information on FadE8 could be obtained from either the Swiss Protein Database or the recent literature. This protein was classified as a putative Acyl-CoA dehydrogenase on the basis of sequence similarity with other members of the Acyl-CoA dehydrogenase family.

An homology modeling of FadE8 was performed in collaboration with Dr. Rita Berisio of the National Research Council of Naples in order to evaluate common or different structural features with AidB. Figure 24 shows a ribbon representation of the general FadE8 fold. Two distinct domains encompassing the N - and C - terminal regions of the protein are reported in yellow and in purple respectively. The surface and cartoon representation of FadE8 is reported in Figure 25 where the putative DNA binding site is also indicated.

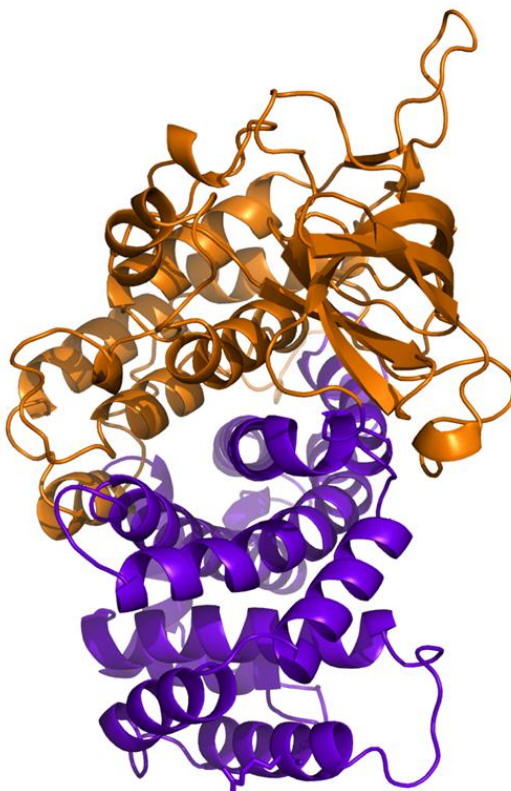


**Figure 24.** Ribbon representation of FadE8 homology model. The N - and C – terminal domains are depicted in yellow and purple respectively.

The structural model showed the same main features of the *E. coli* homologous AidB, where the putative DNA binding site seemed to be separated from the dehydrogenase

domain. Substrate is binding at the interface between the middle (orange) and the C-terminal (purple) domains as shown in Figure 25.

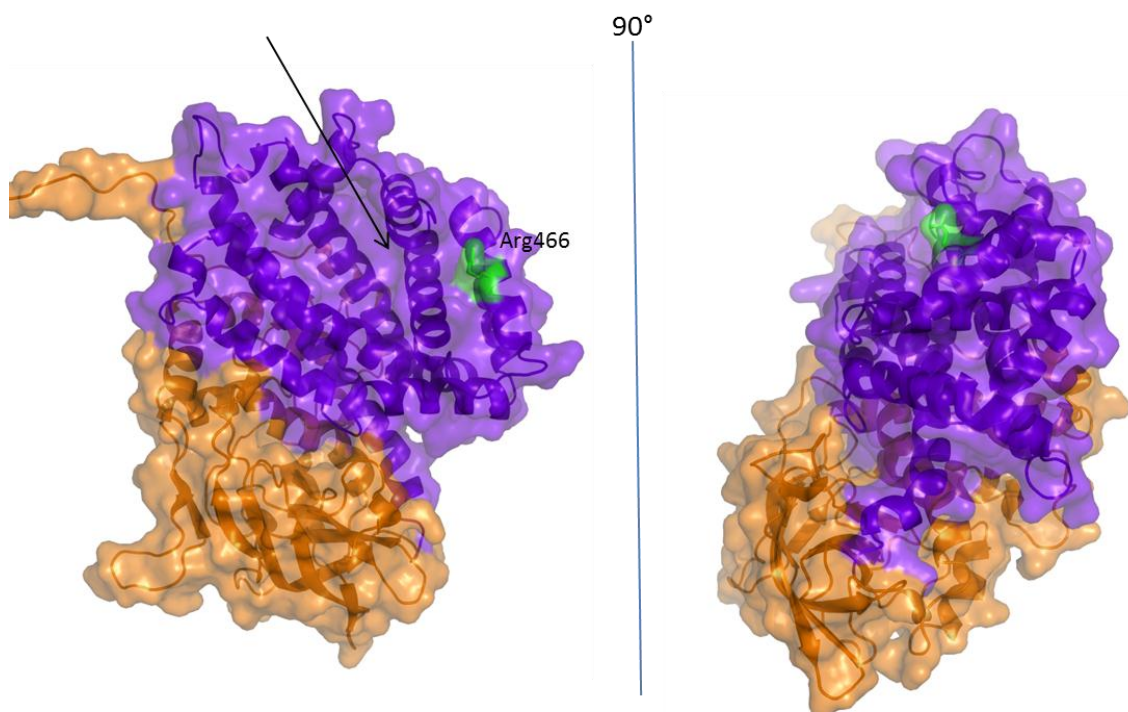


**Figure 25.** Surface and cartoon representation of FadE8. The putative DNA binding site is indicated by an arrow.

## 2.2 Heterologous expression of *fadE8* in *E.coli* and protein purification

*In silico* analyses indicate a possible functional homology between *E. coli* AidB and FadE8 from MTB. This hypothesis was verified by cloning and expressing *fadE8* gene in *E.coli*. The gene was amplified from MTB genome through PCR and cloned in a pET22b vector containing sequence coding a 6-His tag at the C-terminus of the protein. FadE8 production was obtained in C41 *E.coli* cells in the presence of 10mM riboflavin by 0.1mM IPTG induction by growing bacterial cells at 25°C for 16 hours. Cells were lysed and the insoluble fraction containing inclusion bodies was separated from the soluble fraction. Production and cellular localization of recombinant FadE8 were

evaluated through SDS-PAGE analysis. Figure 26 shows the gel fractionation of total *E. coli* extract (lane 1), solubilized inclusion bodies (lane 2) and the soluble fraction (lane 3). FadE8 was clearly produced in large amount but essentially confined in inclusion bodies.

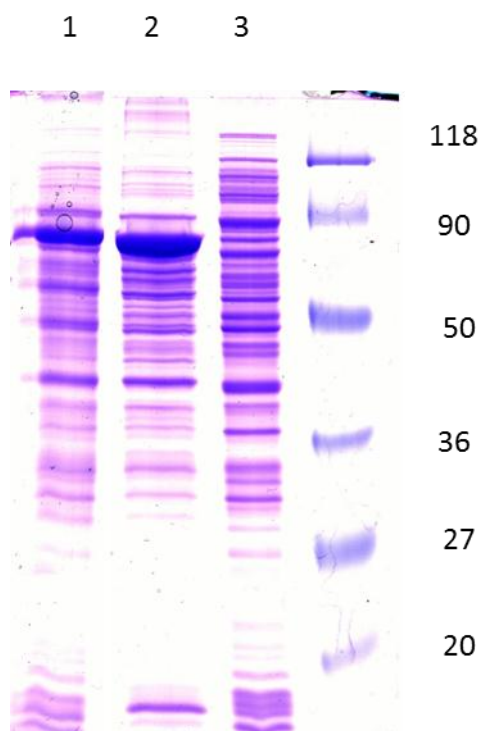


**Figure 26.** SDS-PAGE of the FadE8 production in *E.coli*. Total cells extract is loaded in lane 1, inclusion bodies in lane 2 and soluble fraction in lane 3.

Recombinant tagged FadE8 produced in *E.coli* cells was purified from soluble fraction by Immobilized Metal ion Affinity Chromatography (IMAC). This technique exploits the interaction between the histidine tag on the recombinant protein and  $\text{Ni}^{2+}$  ions coupled to highly cross-linked agarose beads. The eluted proteins were analysed by SDS-PAGE as reported in Figure 27.



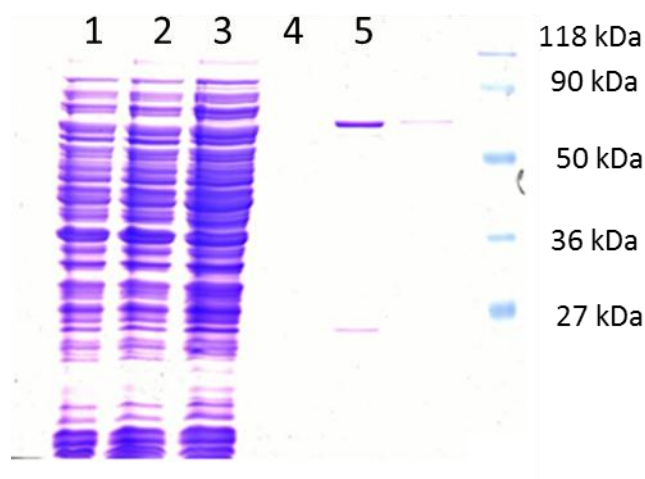


**Figure 27.** Total cells extract is loaded in lane 1, unbound fraction in lane 2, washings in lane 3 and 4, eluted FadE8 in lane 5.

### 2.3 FadE8 refolding processes

The FadE8 protein was purified to homogeneity but was obtained with a very low yield. Two different refolding approaches were then performed to increase the soluble amount of FadE8. Inclusion bodies were isolated after cells lysate and were solubilized in strong denaturants. Refolding of solubilized inclusion bodies was performed by both dialysis and dilution. Inclusion bodies were dissolved in denaturing conditions (6M guanidine hydrochloride, 50 mM Hepes pH 7.5, 25 mM dithiothreitol) and dialysed against decreasing concentrations of denaturant. This multistep treatment resulted in slow removal of the denaturing agent leaving the protein exposed to intermediate denaturant concentrations for long time. Alternatively, inclusion bodies were dissolved in denaturing conditions to a protein concentration of about 0.1 mM and then ten-fold diluted with non-denaturing buffer in a single step. Better results were obtained with the multistep dialyses method since no protein precipitation was observed. The refolding process of recombinant FadE8 protein was also investigated by adding different molecules into the refolding solution. Because of their ability to interact with hydrophobic molecules, cyclodextrins (CD) were selected and used in collaboration with Prof. Castronuovo (Department of Chemical Sciences, Federico II University). Two CDs were chosen, an  $\alpha$ -CD (six membered sugar ring molecule) and a synthetic  $\beta$ -CD (seven sugar ring molecule). In these experiments,

refolding was performed directly on the IMAC column; the denatured protein was first bound to the stationary phase through its histidine tag under denaturing conditions and then transferred into native conditions either washing directly with non-denaturing buffer or in multiple steps with decreasing concentrations of denaturant in the presence of CD. In both cases, the refolded protein yield was increased although the process is still far from being satisfactory suggesting that other factors should play a role in the refolding process.

#### 2.4 *In vivo* assisted FadE8 folding by GroEL/GroES complex

Because of the high amount of recombinant protein produced, cellular chaperones might be unable to mediate correct protein folding of newly synthesized proteins. The complex between molecular chaperones GroEL/GroES is one of the *E. coli* system that is usually responsible for facilitating correct folding processes. Recombinant overproducing FadE8 cells were co-transformed with a vector containing genes coding GroES and GroEL in order to increase the cellular amount of protein chaperones. Figure 28 shows that co-producing the recombinant protein with GroES and GroEL greatly increased the amount of soluble protein.

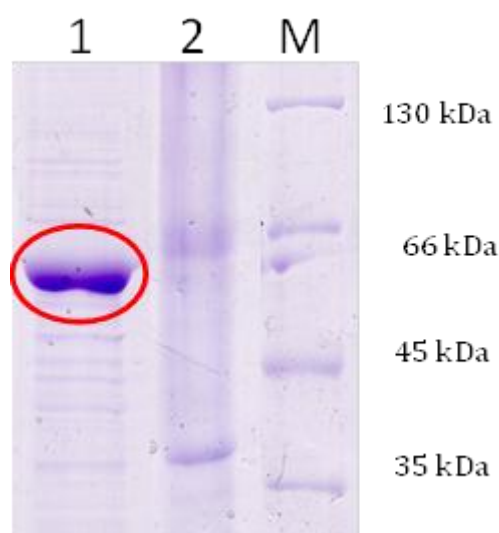


**Figure 28.** SDS-PAGE of FadE8 co-produced with GroES/GroEL chaperones. Soluble fraction is loaded in lane 1 and inclusion bodies in lane 2.



Unfortunately the complex formed by GroEL/GroES with FadE8 was very stable and difficult to dissociate. Several attempts were performed to affinity purify the recombinant protein by the IMAC method always resulting in FadE8 heavily contaminated by GroEL.

## 2.5 Recombinant FadE8 characterization

Structural and functional characterization of FadE8 were then performed by using the low amount of soluble protein purified in the absence of chaperones. The correct primary structure of recombinant FadE8 was proved by MALDI mass mapping. Purified FadE8 was analysed by SDS-PAGE and the corresponding protein band excised from the gel, reduced and alkylated with iodoacetamide to irreversibly block the cysteine residues and in situ enzymatically digested with trypsin. The resulting peptide mixture was then directly analysed by MALDI-MS using a reflectron instrument. The accurate mass values of the peptides in the mass spectrum was mapped onto the anticipated FadE8 sequence leading to a consistent coverage of the protein primary structure.

In order to evaluate if FadE8 was functionally homologue to AidB from *E.coli*, the DNA binding ability and the dehydrogenase activity of the protein were *in vitro* tested. Electrophoresis Mobility Shift Assay (EMSA) experiments were performed to investigate the possible binding of FadE8 with DNA. EMSA is an electrophoretic separation in native condition used to study protein-DNA interactions on polyacrylamide or agarose gel. A retardation in DNA electrophoresis mobility following incubation with a purified protein demonstrates the formation of a DNA-protein complex. Using different DNA sequences, EMSA can also indicate if these binding capabilities are sequence dependent.

FadE8 was incubated with a random DNA sequence and then analysed by EMSA experiments as shown in Figure 29 (lane 1). A clear retardation in the electrophoresis mobility of the DNA-protein complex was observed as compared to the DNA alone. Similarly to AidB, FadE8 was then capable to bind DNA. Further analyses were focused on the elucidation of the specificity of the interaction. Two different DNA regions of

aidB promoter (lane 2 and 3) were employed as probes using a random sequence as control (lane 4).

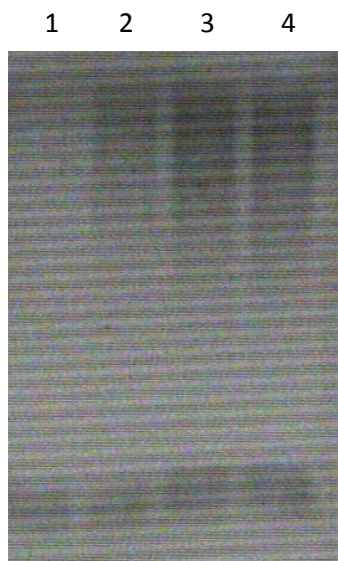


**Figure 29.** EMSA assay performed on FadE8 protein. DNA alone is loaded in lane 1, two different DNA regions of aidB promoter in lane 2 and 3, random sequence in lane 4.

EMSA experiments showed similar shifts in the electrophoresis mobility for all three DNA baits, indicating that FadE8 recognises DNA in a non-specific manner.

Specific enzymatic assays were performed to evaluate the dehydrogenase activity of FadE8. The reactions were carried out by using isovaleryl-CoA as substrate and 2,6-dichlorophenolindophenol (DCPIP) as the final electron acceptor. The change in absorbance at 600 nm was monitored over time. Purified AidB was used as positive control. Enzymatic activities obtained for AidB and FadE8 are reported in Table 5, in comparison with human isovaleryl-CoA dehydrogenase activity reported in literature [43].

**Table 5.** Dehydrogenase activities of AidB and FadE8.

Protein	Isovaleryl-CoA dehydrogenase activity
	( $\mu\text{mol min}^{-1} [\text{mg protein}]^{-1}$ )
AidB ( <i>E.coli</i> )	$0.12 \pm 0.01$
FadE8 ( <i>MTB</i> )	$0.30 \pm 0.01$
Human dehydrogenase	8.2 to 11.7

The results revealed a weak dehydrogenase activity of FadE8 very similar to AidB and much smaller than the human enzyme. These data suggested that the specific FadE8 substrate might be different from Acyl-CoA molecules as already reported for AidB [2].

**Chapter 5:**  
**Qualitative and quantitative analyses of DNA**  
**alkylation *in vivo***

## 1. Quantitative analysis of DNA ethenobases by LC-MS/MS

The mechanism of DNA protection exerted by AidB was investigated using a quantitative analysis based on liquid chromatography tandem mass spectrometry methodologies during a stage at Dr. Douki's laboratory, CEA Grenoble, France. AidB protects DNA from methylation but nothing was reported about protection of other alkyl lesion. This point was investigated by using an alkyl molecule known as chloroacetaldehyde (CAA) a metabolic intermediate of vinyl chloride that has been shown to give rise to DNA adducts. Upon alkylation with CAA, the purine bases are transformed into stable ethenobases [48].

Two *E. coli* strains, wild type and  $\Delta$ aidB, were individually engineered either with the gene encoding for AidB or FadE8, to generate wild type and  $\Delta$ aidB strains overproducing either AidB or FadE8. Exposure to CAA was performed on six different *E. coli* strains, three wild type (control, AidB and FadE8 overproducing) and three  $\Delta$ aidB strains (control, AidB and FadE8 overproducing). The six different strains were grown in the absence and in the presence of three different sub-inhibitory concentrations of CAA (1, 5, 10 mM). As an example the growth profiles of  $\Delta$ aidB overproducing AidB treated with different concentrations of CAA is shown in figure 30.

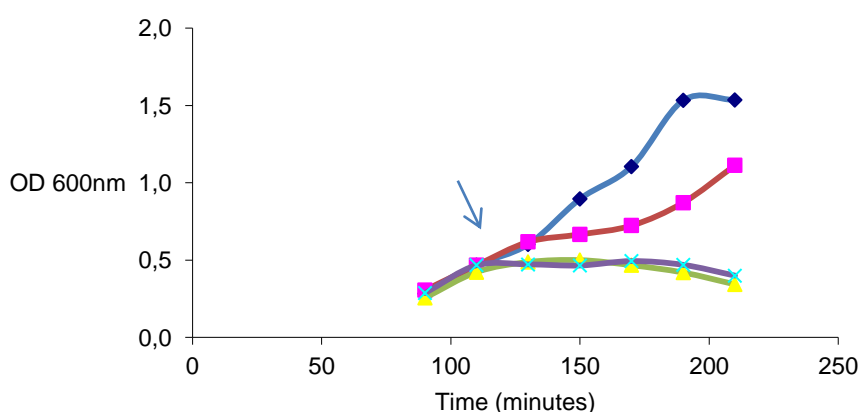


**Figure 30.** *Escherichia coli* cells growths in the absence of alkylating agent (blue), in the presence of 1 (purple), 5 (light blue), 10 (yellow) mM CAA.

Cellular pellets were collected during the exponential growth phase as indicated. Plasmidic DNAs were isolated from treated and untreated cells and digested with multiple enzymes to release single nucleosides. The mixture of alkylated and native nucleosides were eventually analysed by reverse-phase HPLC associated with a triple quadrupole mass spectrometer used in the multiple reaction monitoring mode (MRM). The molecular ions of ethenonucleosides and specific fragments were selectively recorded to identify and quantify the individual ethenoderivatives. Table 6 reports the scheme of MRM transitions monitored during the analyses. It should be underlined that this method could not distinguish between the two ethenoguanines.

**Table 6.** MRM transitions used for quantitative analyses.

Multiple Reaction Monitoring (MRM)		
Ethenonucleosides	Precursor ion (m/z)	Fragment ions (m/z)
$\epsilon$ dGua	292	176
$\epsilon$ dAdo	275	160

The monitored transition corresponded to the loss of 2-deoxyribose moiety from the protonated pseudo-molecular ion for all three modified bases [49]. The detection of ethenobases was realized in the positive electrospray ionization mode. Protonated nucleosides were isolated in the first quadrupole, whereas the corresponding protonated base was collected as a specific fragment in the third quadrupole following fragmentation of the parent ion in the collision cell.

Figure 31 shows the quantitative analysis of the ethenoguanines formed following alkylation of the six *E.coli* strains by different concentrations of CAA.

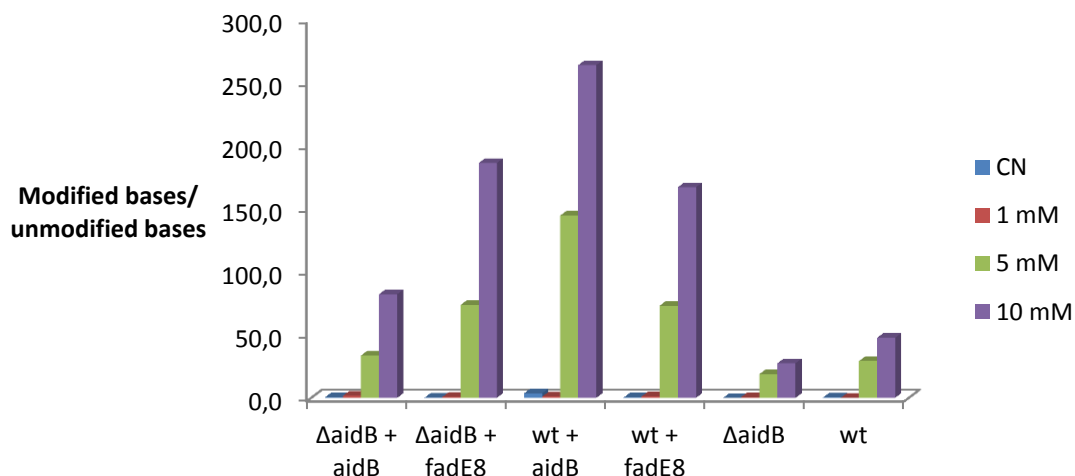


**Figure 31.** Methylations of plasmidic DNA are reported for ethenodeoxyguanines.

Data are reported as the ratio between modified and unmodified bases that were quantified by HPLC using their UV absorbance. As expected both wild type and  $\Delta$ aidB strains showed increasing DNA alkylation at increasing concentrations of CAA.  $\Delta$ aidB revealed only a slightly less amount of ethenoguanines as compared to wild type. Surprisingly, when the analysis was performed on both strains overproducing the protection protein AidB or FadE8, similar results were obtained. Alkylation of both engineered strains increased with increasing concentrations of CAA, suggesting that both AidB and FadE8 were unable to protect DNA from CAA alkylation.

## 2. Quantitative analysis of methylated DNA by LC-MS/MS

The ability of both AidB and FadE8 to protect DNA from methylating agents was investigated by developing a new method for the qualitative and quantitative measurements of methylated DNA bases. Analogously to ethenobases analysis, the new method was based on the exploitation of LC-MS/MS technology in the MRM mode. In preliminary experiments, standard methylated 7MeG, O6MeG, 3MeA were analysed in a triple quadrupole MS to define the appropriate transitions to be used in the MRM analysis. It has been reported, in fact, that the most commonly methylated

DNA bases *in vivo* by MMS are guanine and adenine to form N-7-methylguanine (N7MeG), O6-methylguanine (O6MeG) and N-3-methyladenine (N3MeA) [39].

The molecular ions of these bases were isolated in the first quadrupole and then fragmented in the collision cell. The most intense and specific fragments produced by each base were selected to identify and quantify the individual methylated bases. The MRM transitions used to develop the analytical method are reported in Table 7. It should be underlined that the developed method was able to discriminate between the two methylated guanines that share the precursor ion and one fragment but can be distinguished by the second MRM transition.

**Table 7.** MRM transitions used for quantitative analyses.

Multiple Reaction Monitoring (MRM)			
Methylated bases	Precursor ion (m/z)	Fragment ions (m/z)	Loss
O-6-methylguanine	166	134	CH <sub>3</sub> OH
		149	NH <sub>3</sub>
7-methylguanine	166	124	NH <sub>2</sub> CN
		149	NH <sub>3</sub>
3-methyladenine	150	108	CH <sub>3</sub> HCN
		123	HCN

Figure 32 shows the calibration curves that were obtained for each methylated base by using different amount of standards in the range 10-100 µg/L. Correlation coefficients resulted very close to 1 indicating a very good degree of linear dependence between the two variables.



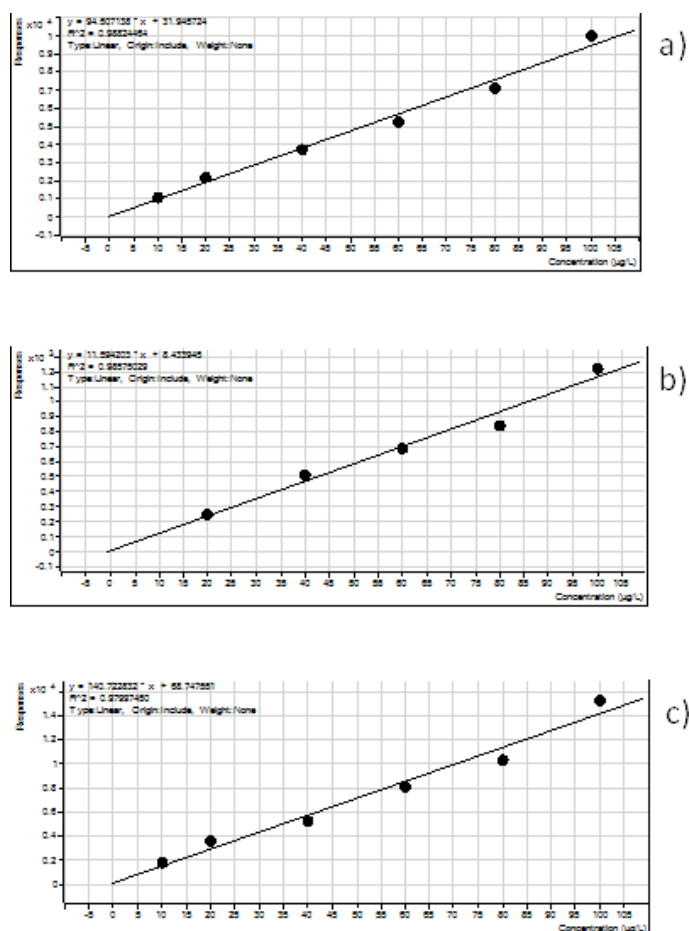


**Figure 32.** Calibration curves obtained by using 10, 20, 40, 60, 80, 100 µg/L of methylated standard bases N7MeG (a), O6MeG (b) and N3MeA (c).

The effect of alkylating molecules on *E. coli* DNA was first monitored on a time course basis by collecting sample from wild type cells at three different times (20, 40 and 60 minutes) following exposure to methylation stress. Two different alkylating agents were used: MMS and Busulfan at the same concentration (0.04%). Figure 33 summarizes the data.

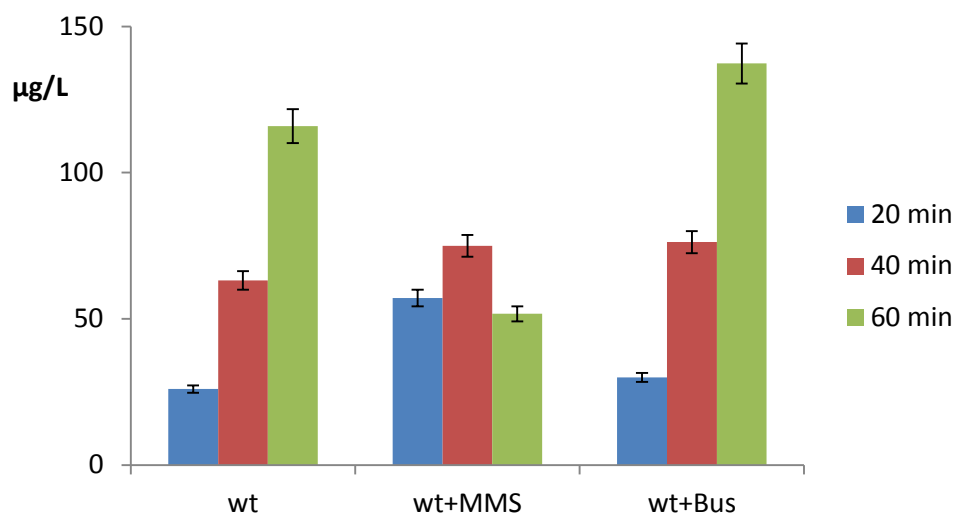


**Figure 33.** DNA methylations of wild type cells are reported in the absence and in the presence of MMS and Busulfan over three different times: 20 minutes (blue), 40 min (red) and 60 minutes (green).

In the absence of methylating agents, wild type cells showed increasing DNA methylation over time probably because cellular responses to methylation stress were not activated in these conditions. When *E. coli* cells were treated with MMS, an increasing in DNA methylation was first observed. However after 1 hour a clear decreasing in DNA methylation was detected according to the induction of the adaptive response. Finally, cells treated with Busulfan showed increasing DNA methylation over time suggesting that the cellular stress elicited by this reagent did not provide induction of the adaptive response. Busulfan is a bifunctional alkylating molecule that causes DNA intra- or inter-strands crosslinkings, leading to a covalent structure that probably cellular defenses are not capable to counteract.

Quantitative MRM tandem MS approach was also used to evaluate the biological roles exerted by AidB and FadE8 in the cellular response to alkylating agents.

Wild type and  $\Delta aidB$  strains engineered to produce the two proteins were grown in the presence and in the absence of MMS. DNA was extracted from cells in exponential growth phase, hydrolyzed in acidic conditions to obtain free bases and analysed by the MRM method developed. Figure 34 shows the results obtained in the absence of MMS.

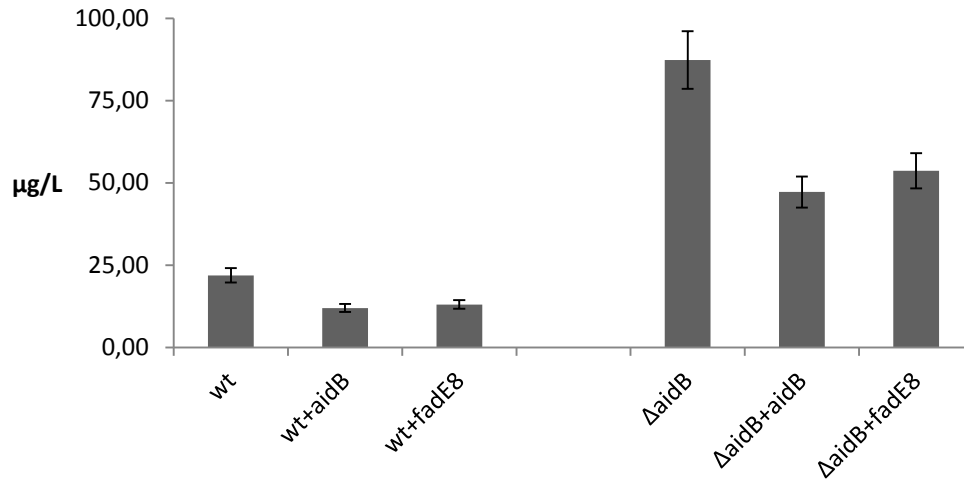


**Figure 34.** DNA methylations of wild type cells in presence and in the absence of AidB and FadE8 are reported in the absence of methylation stress.

As expected, the wild type strain resulted generally less methylated than  $\Delta aidB$  because of the presence of the DNA protecting protein AidB. The results obtained on both strains overproducing either AidB or FadE8 clearly showed a decrease in DNA methylation. These data demonstrated that both AidB and FadE8 are able to exert a protection effect on DNA methylation.

These results were supported by data obtained in the presence of MMS, reported in Figure 35.

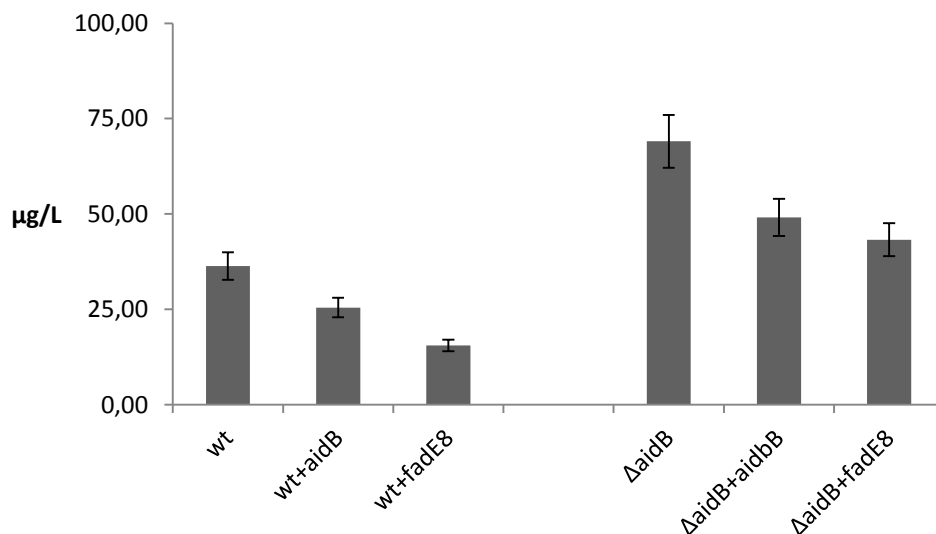


**Figure 36.** DNA methylations of wild type cells in presence and in the absence of AidB and FadE8 are reported in the presence of methylation stress.

Again  $\Delta$ aidB showed a higher level of DNA methylation as compared to wild type. The presence of either AidB or FadE8 decreased DNA methylation in both strains even in the presence of the methylating agent.

Quantitative data demonstrated that AidB and FadE8 are functionally homologs *in vivo* protecting DNA from methylation suggesting that FadE8 might be part of the adaptive response to methylating stress in *M.tuberculosis*.

## **Chapter 6:**

## **Discussion**

## Discussion

Alkylating stress is a widespread issue affecting living organisms, originated by both endogenous and exogenous chemicals. DNA alkylation causes several mutations and often cells death by blocking essential biological processes such as DNA replication and transcription [50, 51]. Therefore all the organisms developed different response systems to counteract these events either repairing the DNA molecule or degrading the alkylating molecules [52].

In *Escherichia coli*, sub inhibitory concentration of methylating agents induces the expression of four genes (ada, alka, alkB, aidB) involved in the direct repair of DNA alkylation damages [53]. Ada protein is the methylation sensor of this system known as the adaptive response. While the role of Ada, AlkA and AlkB, was clearly defined [54, 55], the involvement of AidB in this system has long been known but its specific role in the protection of DNA is still obscure. Previous data demonstrated that AidB interacts with DNA very likely to protect the nucleic acid from alkylating molecules but it is not able to repair the DNA molecule following alkylation [2]. In addition, the protective action of AidB is preferentially expressed on DNA regions containing upstream elements. This observation led to the hypothesis that AidB might belong to a putative pathway of degradation of alkylating agents through its FAD dependent dehydrogenase activity. Alternatively, AidB might protect these DNA regions by physically interact with them thus impairing the dangerous action of alkylating agents.

An homolog adaptive response was also found in *Mycobacterium tuberculosis*, the etiologic agent of tuberculosis [37]. During the infection, if the host immune response is not able to strongly counteract bacterial invasion, MTB cells are confined within macrophages and together with different cell types are enclosed in a granuloma, a latent infection status without evident clinical manifestations [56, 57]. During MTB infection, the host antimicrobial response generates several metabolically activated DNA alkylating agents leading to severe DNA-damaging injuries on MTB cells [58]. Protection of the bacterial DNA from host chemical damages then strictly depends on the MTB repair mechanisms including the adaptive response. Being this

mechanism fundamental for MTB viability whereas it is missing in human, this process may represent a putative therapeutic target to explore in search for new tuberculosis treatments.

In this biological contest, this PhD thesis was focused on the investigation of *E. coli* responses to methylation stress in order to obtain a global proteomic view of the changes induced by alkylating damages. Moreover *M. tuberculosis* responses to alkylation stress were analysed to obtain information concerning cellular and morphological modifications induced. Finally a deeply comparison between the two proteins *E.coli* AidB and its homologue MTB FadE8 was carried out in order to identify new therapeutic target.

Differential proteomic approaches were performed on *E.coli* in the presence and in the absence of MMS upon exposure of 20 minutes. This analysis allowed the identification of about 70 differentially expressed proteins between MMS treated and untreated conditions. In particular, the presence of methylating molecule caused a widespread down regulation in proteins expression. Metabolic processes were especially down regulated in according to data previously reported that showed growing profiles heavily affected by the presence of methylating molecules [2]. In particular, the massive down regulation of enzymes belonging to the glycolytic pathway and the fatty acids degradation strongly suggests a decrease of energy production in *E. coli* with concomitant difficulties in cell growth. Among the few up regulated proteins AhpF and GadB are reported to be involved in the response to stress conditions. GadB is part of the gad system that helps the cells to maintain a neutral intracellular pH when *E. coli* is exposed to extremely acidic conditions [59]. Alkyl hydroperoxide reductase subunit F, AhpF, is specifically involved in protecting cells against alkyl hydroperoxides that are capable to damage DNA [60, 61, 62]. This protein belongs to the glutathione-independent peroxidase system in *Escherichia coli* and *Salmonella typhimurium* with a protective role in limiting oxygen-linked DNA damage [63]. AhpF belongs to the family of pyridine nucleotide-disulfide oxidoreductases and functions as a channel electrons to produce a cascade of disulfide-exchange reactions [64, 65]. The general overview provided by the proteomic data suggests that following methylation stress *E. coli* is suffering a decrease in the

energetic metabolism, a situation that the cells is trying to counteract by producing defense proteins.

The emergency in energy production is supported also by the down regulation of proteins involved either in cell wall structure or in membrane biosynthesis components. Interestingly, the most down regulated protein is the lyase NanA that was reported to be involved in biofilm formation and in adhesion to host cells in pathogen bacteria such as *Streptococcus pneumonia* [66, 67, 68, 69]. Functional experiments performed on wild type *E. coli* demonstrated that both cellular properties are decreased by the presence of methylating molecule. The lack in energy production highlighted by the proteomic analyses might have impaired the synthesis of all the proteins and other macromolecules needed to form both biofilm and adhesion structures.

Since changes in the proteome are expected to require some time to become effective, it is reasonable that none adaptive response components were identify in the up regulated proteins. This finding was also supported by quantitative data of DNA methylation performed on cells treated with MMS. Time course analyses showed that an effective decreasing in DNA methylation occurred after one hour following exposure to MMS suggesting that the adaptive response needs at least three cellular duplications to become effective. Proteomic analyses were indeed performed on protein extracts obtained after only one cellular duplication, too early to induce expression of the adaptive response.

Functional proteomic approaches were designed to shed some light on the mechanism of action of AidB through the identification of its protein partners in vivo. AidB partners were isolated by immunoprecipitation procedures both in the absence and in the presence of MMS as alkylating agent and the individual protein components identified by mass spectrometry. Several proteins were identified in both conditions, although the number of AidB molecular partners is considerably higher in the presence of MMS. Surprisingly, AhpF protein was also found as AidB partner both in the presence and in the absence of MMS delineating a new possible role for the AidB protein in other stress mechanisms.

Proteins identified under methylating stress conditions were grouped in three large categories according to their reported biological activities, stress response,



energetic metabolic pathways, and nucleic acid metabolism (transcription, processing and translation). In particular, AidB was found to interact with UvrA whose expression is under the control of the SOS response system involved in DNA damages response [70]. This interaction was also validated by co-immunoprecipitation experiments confirming proteomic data. Interaction of these two proteins is very interesting since UvrA is part of the UvrABCD nucleotide excision system involved in removing modified nucleotides as a result of several different DNA modifications including formation of covalent bonds, local unfolding, abnormal folds and variations in charge distribution [71]. UvrA works in a multienzyme complex with the specific role of examining the DNA molecule in search for modifications in order to allow the other proteins of the complex to perform the excision of the damaged nucleotides [72]. This protein is generally present at very low concentrations within the cell but its expression strongly increases under stress conditions [73]. Interaction of AidB with UvrA and AhpF might then indicate that AidB is involved in different response complexes other than the Ada-dependent adaptive mechanism, suggesting new cellular strategies to minimize DNA damages.

*M. tuberculosis* response to alkylation damages was also deeply investigated. The effect of DNA alkylation was evaluated on the cellular growth of clinical tubercular and non-tubercular strains. Growth profiles showed that methylating donor can impair mycobacteria cell viability even at low concentrations whereas bacterial cells are clearly resistant to the reference drug isoniazid.

Optical microscopy images were also performed in order to estimate whether tubercular and non-tubercular strains could be morphological affected by the presence of methylating agent. In particular, cell wall MTB exterior is primary characterised by the presence of a glycolipid molecule, trehalose dimycolate, also known as cord factor [74]. These molecules bring to the arrangement of *M. tuberculosis* cells into long and thin structures named cord factors like the glycolipid component. This cellular formation is a key step in pathogenicity of tuberculosis infection because can affect immune response and granuloma production [75, 76]. Optical microscopy images of MMS treated and untreated MTB cells showed a remarkable disappearance of typical cord factors in cells treated with methylating molecule suggesting that alkylating stress might influence *in vivo* pathogenicity of MTB.

In addition anti-cancer chemotherapeutic drug Busulfan significantly affect *M. smegmatis* cells survival in concentrations lower than those commonly used in cancer treatments. These results confirmed mycobacterial sensitivity to methylation damages and promising the MTB adaptive response as a new putative therapeutic target against mycobacterial infection.

Investigations of *M. tuberculosis* responses mechanisms to DNA alkylation were also focused on molecular response by searching for an AidB homologue. *In silico* analysis identified the putative Acyl-CoA dehydrogenase FadE8 with an aminoacidic identity of 44%. Exhaustive structural and functional studies demonstrated that purified FadE8 showed functional homology to AidB displaying both DNA binding capability and isovaleryl-CoA dehydrogenase activity. In particular, experimental assays revealed a weak dehydrogenase activity versus isovaleryl-CoA very similar to AidB and much smaller than the human enzyme. These data suggested that the specific FadE8 substrates might be different molecules, as already reported for AidB, suggesting that methylating molecules could be degraded by an oxidative system. This putative degradation pathway might be similar to that occur inside the mitochondria by  $\beta$ -oxidation of fatty acids. In this process methylating molecule might play the role of fatty acid while either AidB or FadE8 might performed the leading step of oxidation by FAD.

This data were supported by *in vivo* tandem MS quantitative analyses performed on DNA extracted from *E. coli* wild type and  $\Delta$ aidB strains. As expected  $\Delta$ aidB resulted more methylated than wild type both in the absence and in the presence of MMS since the DNA protective protein AidB is absent. In addition the presence of either AidB or FadE8 decreased DNA methylation suggesting that both proteins are able to exert a protection effect on DNA damages.

Similar experiments were performed in the presence of different alkylating molecules such as chloroacetaldehyde, a metabolic derivative of polyvinyl chloride and the bi-functional drug Busulfan. Both wild type and  $\Delta$ aidB overproducing the protective proteins AidB and FadE8 showed increasing alkylation with increasing concentrations of CAA. These data clearly demonstrated that both AidB and FadE8 are unable to protect DNA from either CAA or Busulfan alkylation, suggesting that these proteins might exert their DNA protection effect selectively on methylated DNA. The similar

behavior shown by FadE8 and AidB, in DNA methylation processes demonstrated that FadE8 might be involved in the adaptive response of MTB by a still obscure mechanism of DNA protection.

In conclusion, even though *E. coli* and *M. tuberculosis* are far away in the evolutionary grade they seems to show similar behaviors in molecular responses to alkylation damages. *E. coli* is a facultative anaerobic that is capable to switch from aerobic to anaerobic respiration according to oxygen availability [77]. *M. tuberculosis* is highly aerobic requiring high levels of oxygen. It have an unusual cell wall, rich in lipids such as mycolic acid responsible for its resistance, pathogenicity and impediment to Gram staining. Moreover cell wall complexity causes *M. tuberculosis* divisions to be extremely slow, about every 24 hours compared to *E. coli* that divides every twenty minutes [78, 79].

In order to counteract DNA alkylation, *M. tuberculosis* shows the presence of several systems including nucleotide excision repair (NER), base excision repair (BER), recombination and SOS repair system genes while missing the mismatch repair (MMR) mechanism [80]. Recently the *ada* operon of MTB was preliminary characterized but none was reported about AidB homologue in *M. tuberculosis*. We demonstrated the existence in MTB of FadE8, a protein structurally and functionally homologue to AidB. Considering that FadE8 is involved in DNA protection and that the MTB cord factor disappears upon methylation stress, it is possible to imagine FadE8 as a new putative target against tuberculosis infection. Inhibition of FadE8 that is absent in human might reduce MTB survival upon exposure to human immune system that usually fight bacteria by damaging DNA.

All findings about DNA repair and protection systems, reported in this PhD thesis, can be gather together to a unique prospective. Methylation stress could be used as a new strategy to counteract mycobacterial infection either by strengthening human immune response by using exogenous methylating drugs or by weakening bacterial defenses by providing adaptive response inhibitor molecules.

## References

## References

1. Michael R Volkert\* and Paolo Landini, 2001. Transcriptional responses to DNA damage. *Current Opinion in Microbiology*, 4:178–185.
2. Valentina Rippa, Angela Duilio, Pamela di Pasquale, Angela Amoresano, Paolo Landini, Michael R. Volkert, 2011, Preferential DNA damage prevention by the *E. coli* AidB gene: A new mechanism for the protection of specific genes. *DNA repair*, 10:934– 941.
3. V. Lobo, A. Patil, A. Phatak, and N. Chandra, 2010. Free radicals, antioxidants and functional foods: Impact on human health. *Pharmacogn Rev.* 4(8): 118–126.
4. Hasan Koc, James A. Swenberg. Applications of mass spectrometry for quantitation of DNA adducts. *J. Chromatogr. B* 778, 323–343.
5. Dragony Fu, Jennifer A. Calvo & Leona D. Samson, 2002. Balancing repair and tolerance of DNA damage caused by alkylating agents. *Nat Rev Cancer* 12, 104–120.
6. NR JENA, 2012. DNA damage by reactive species: Mechanisms, mutation and repair. *J. Biosci.* 37(3), 503–517.
7. E. Dogliotti, 2006. Molecular mechanisms of carcinogenesis by vinyl chloride. *Ann Ist Super Sanità* vol. 42, no. 2: 163-169.
8. S J Sturla, 2007. DNA adduct profiles: chemical approaches to addressing the biological impact of DNA damage from small molecules. *Current Opinion in Chemical Biology*, 11:293–299.
9. Shrivastav N, Li D, Essigmann JM. Chemical biology of mutagenesis and DNA repair: cellular responses to DNA alkylation. *Carcinogenesis*. 2010; 31:59–70.
10. <http://www.what-is-cancer.com/papers/newmedicine/gompertz.htm>
11. <http://www.clinonc.com/content/drugdb/drug.cfm?DrugRef=552>

12. Chiung-Wen Hu & Chih-Ming Chen & Hsin Hui Ho & Mu-Rong Chao. 2012. Simultaneous quantification of methylated purines in DNA by isotope dilution LC-MS/MS coupled with automated solid-phase extraction. *Anal Bioanal Chem* 402:1199–1208
13. Hasan Koc, James A. Swenberg, 2002. Applications of mass spectrometry for quantitation of DNA adducts. *Journal of Chromatography B*, 778: 323–343
14. Hu CW, Chao MR, Sie CH, 2010. Urinary analysis of 8-oxo-7,8-dihydroguanine and 8-oxo-7,8-dihydro-2'-deoxyguanosine by isotope-dilution LC-MS/MS with automated solid-phase extraction: study of 8-oxo-7,8-dihydroguanine stability. *Free Radic Biol Med* 48:89–97
15. Thierry Douki, Francette Odin, Sylvain Caillat, Alain Fa Vier, And Jean Cadet, 2004, predominance of the 1,N<sup>2</sup>-propano 2'-deoxyguanosine adduct among 4-hydroxy-2-nonenal-induced DNA lesions. *Free Radical Biology & Medicine*, Vol. 37, No. 1, pp. 62 – 70.
16. P. Ø. FALNES, A. KLUNGLAND AND I. ALSETH, 2007. Repair of methyl lesions in DNA and RNA by oxidative demethylation. *Neuroscience* 145: 1222–1232
17. Pegg AE. 2000. Repair of O(6)-alkylguanine by alkyltransferases. *Mutat Res*. 2000 Apr;462(2-3):83-100.
18. Jadwiga Nieminuszczy and Elżbieta Grzesiuk, 2007. Bacterial DNA repair genes and their eukaryotic homologues: 3. AlkB dioxygenase and Ada methyltransferase in the direct repair of alkylated DNA. *Acta biochimica Polonica*, 54(3):459-68.
19. Bowles, Timothy; Metz, Audrey H; O'Quin, Jami; Wawrzak, Zdzislaw; Eichman, Brandt F, 2008. Structure and DNA binding of alkylation response protein AidB. *PNAS*, 105(40):15299-304.
20. Valentina Rippa, Angela Amoresano, Carla Esposito, Paolo Landini, Michael Volkert and Angela Duilio, 2010, Specific DNA Binding and Regulation of Its Own Expression by the AidB Protein in *Escherichia coli*, *Journal Of Bacteriology*, 192 (23): 6136–6142.

21. Hamill, Michael J; Jost, Marco; Wong, Cintyu; Elliott, Sean J; Drennan, Catherine L, 2011, Flavin-induced oligomerization in *Escherichia coli* adaptive response protein AidB. *Biochemistry*, 50(46):10159-69.
22. Mulrooney, Scott B; Howard, Michael J; Hausinger, Robert P, 2011, The *Escherichia coli* alkylation response protein AidB is a redox partner of flavodoxin and binds RNA and acyl carrier protein. *Archives of biochemistry and biophysics*. 513(2):81-6.
23. Valentina Rippa, Angela Duilio, Pamela di Pasquale, Angela Amoresano, Paolo Landini, Michael R. Volkert, 2011, Preferential DNA damage prevention by the *E. coli* AidB gene: A new mechanism for the protection of specific genes. *DNA repair*, 10:934– 941.
24. S.V. Vasilieva, D.A. Streltsova, E.Yu. Moshkovskaya, N.A. Sanina, S.M. Aldoshin, 2010, Fnr[4Fe-4S]<sub>2</sub><sup>+</sup> Protein Regulates the aidB Gene Expression in *Escherichia coli* Cultured under Anaerobic Conditions. *Doklady Biochemistry and Biophysics*, Vol. 433, pp. 179–182.
25. Bruce M. Rothschild, Larry D. Martin, Galit Lev, Helen Bercovier, Gila Kahila Bar-Gal, Charles Greenblatt, Helen Donoghue, Mark Spigelman, and David Brittain, 2001, Mycobacterium tuberculosis Complex DNA from an Extinct Bison Dated 17,000 Years before the Present. *Clinical Infectious Diseases*, 33:305–11.
26. E. Cambau and M. Drancourt, 2014, Steps towards the discovery of Mycobacterium tuberculosis by Robert Koch, 1882. *Clinical Microbiology and Infection*. 20 (3): 196–201.
27. Napier, Ruth J; Shinnick, Thomas M; Kalman, Daniel, 2012, Back to the future: host-targeted chemotherapeutics for drug-resistant TB. *Future microbiology*, 7(4):431-5.
28. <http://www.who.int/mediacentre/factsheets/who104/en/print.html>
29. <http://www.who.int/mediacentre/factsheets/who104/en/print.html>
30. Norbis, Luca; Miotto, Paolo; Alagna, Riccardo; Cirillo, Daniela M, 2013, Tuberculosis: lights and shadows in the current diagnostic landscape. *The new microbiologica*. 36(2):111-20.

31. Koul, Anil; Arnoult, Eric; Lounis, Nacer; Guillemont, Jerome; Andries, Koen, 2011, The challenge of new drug discovery for tuberculosis. *Nature*. 469(7331):483-90.
32. Caminero JA, Sotgiu G, Zumla A, Migliori GB, 2010, Best drug treatment for multidrug-resistant and extensively drug-resistant tuberculosis. *Lancet Infect* 10(9):621-9.
33. Dos Vultos, Tiago; Mestre, Olga; Tonjum, Tone; Gicquel, Brigitte, 2009, DNA repair in *Mycobacterium tuberculosis* revisited. *FEMS microbiology reviews*. 33(3):471-87.
34. Kurthkoti, Krishna; Varshney, Umesh, 2012, Distinct mechanisms of DNA repair in mycobacteria and their implications in attenuation of the pathogen growth. *Mechanisms of ageing and development*. 133(4):138-46.
35. Gorna, Alina E; Bowater, Richard P; Dziadek, Jaroslaw, 2010, DNA repair systems and the pathogenesis of *Mycobacterium tuberculosis*: varying activities at different stages of infection. *Clinical science*, 119(5):187-202.
36. Mizrahi V, Andersen SJ, 1998, DNA repair in *Mycobacterium tuberculosis*. What have we learnt from the genome sequence? *Mol Microbiol*, 29(6):1331-9.
37. Warner, Digby F; Mizrahi, Valerie, 2006. Tuberculosis chemotherapy: the influence of bacillary stress and damage response pathways on drug efficacy. *Clinical microbiology reviews*. 19(3):558-70.
38. Yang M, Aamodt RM, Dalhus B, Balasingham S, Helle I, Andersen P, Tønjum T, Alseth I, Rognes T, Bjørås M, 2011, The *ada* operon of *Mycobacterium tuberculosis* encodes two DNA methyltransferases for inducible repair of DNA alkylation damage. *DNA Repair (Amst)*. 10(6):595-602.
39. Engel, P. C. (1981). Butyryl-CoA dehydrogenase from *Megasphaera elsdenii*. *Methods Enzymol* 71, 359-366.
40. Hu, Chiung-Wen W; Chen, Chih-Ming M; Ho, Hsin H; Chao, Mu-Rong R, 2012, Simultaneous quantification of methylated purines in DNA by isotope dilution LC-MS/MS coupled with automated solid-phase extraction.
41. Pamela Di Pasquale, Angela Amoresano, Francesca De Maria and Angela Duilio, 2013, Molecular Partners of *Escherichia coli* Transcriptional Modulator AidB. *J. Chem. Chem. Eng.* 7: 876-884



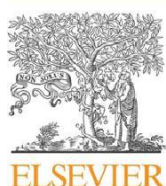
42. Marianna Caterino, Margherita Ruoppolo, Gabriella Fulcoli, Tuong Huynh, Stefania Orru`, Antonio Baldini and Francesco Salvatore, 2009, Transcription Factor TBX1 Overexpression Induces Downregulation of Proteins Involved in Retinoic Acid Metabolism: A Comparative Proteomic Analysis. *Journal of Proteome Research* 8, 1515–1526.
43. Marianna Caterino, Claudia Corbo, Esther Imperlini, Marta Armiraglio, Elisa Pavesi, Anna Aspesi, Fabrizio Loreni, Irma Dianzani and Margherita Ruoppolo, 2013 Differential proteomic analysis in human cells subjected to ribosomal stress. *Proteomics* 13: 1220–1227.
44. Brittan JL1, Buckeridge TJ, Finn A, Kadioglu A, Jenkinson HF. 2012, Pneumococcal neuraminidase A: an essential upper airway colonization factor for *Streptococcus pneumoniae*. *Mol Oral Microbiol.* 27(4):270-83.
45. Dominique H. Limoli, Julie A. Sladek, Lindsey A. Fuller, Anirudh K. Singh and Samantha J. King, 2011. BgaA acts as an adhesin to mediate attachment of some pneumococcal strains to human epithelial cells. *Microbiology*, 157, 2369–2381.
46. Satoshi Uchiyama, Aaron F. Carlin, Arya Khosravi, Shannon Weiman, Anirban Banerjee, Darin Quach, George Hightower, Tim J. Mitchell, Kelly S. Doran and Victor Nizet, 2009. The surface-anchored NanA protein promotes pneumococcal brain endothelial cell invasion. *J. Exp. Med.* Vol. 206 No. 9 1845–1852.
47. Trevor Roger Garrett; Manmohan Bhakoo; Zhibing Zhang, 2008, Bacterial adhesion and biofilms on surfaces, *Progress in Natural Science* 18: 1049–1056.
48. Battaile, K. P., McBurney, M., Van Veldhoven, P. P., and Vockley, J. *Biochimica et biophysica acta* 1390(3), 333–338 (1998).
49. Douki, Thierry; Odin, Francette; Caillat, Sylvain; Favier, Alain; Cadet, Jean, 2004, Predominance of the 1,N2-propano 2'-deoxyguanosine adduct among 4-hydroxy-2-nonenal-induced DNA lesions. *Free radical biology & medicine.* 37(1):62-70
50. C. Badouard, Y. M'en'ezo, G. Panteix , J.L. Ravanat , T. Douki , J. Cadet and A. Favier, 2008, Determination of new types of DNA lesions in human sperm. *Zygote* 16 (1), pp. 9–13.

51. Booth JA<sup>1</sup>, Thomassen GO, Rowe AD, Weel-Sneve R, Lagesen K, Kristiansen KI, Bjørås M, Rognes T, Lindvall JM, 2013, Tiling array study of MNNG treated *Escherichia coli* reveals a widespread transcriptional response. *Sci Rep.* 3:3053.
52. Rooney JP<sup>1</sup>, George AD, Patil A, Begley U, Bessette E, Zappala MR, Huang X, Conklin DS, Cunningham RP, Begley TJ, Systems based mapping demonstrates that recovery from alkylation damage requires DNA repair, RNA processing, and translation associated networks. *Genomics.* 93(1):42-51.
53. Salmelin C, Vilpo J, 2003. Induction of SOS response, cellular efflux and oxidative stress response genes by chlorambucil in DNA repair-deficient *Escherichia coli* cells (ada, ogt and mutS). *Mutat Res.* 522(1-2):33-44.
54. Volkert MR<sup>1</sup>, Gately FH, Hajec LI, 1989, Expression of DNA damage-inducible genes of *Escherichia coli* upon treatment with methylating, ethylating and propylating agents. *Mutat Res.* 217(2):109-15.
55. Baek JH<sup>1</sup>, Han MJ, Lee SY, Yoo JS, 2009, Transcriptome and proteome analyses of adaptive responses to methyl methanesulfonate in *Escherichia coli* K-12 and ada mutant strains. *BMC Microbiol.* 9:186.
56. Hamill MJ<sup>1</sup>, Jost M, Wong C, Bene NC, Drennan CL, Elliott SJ, 2012, Electrochemical Characterization of *Escherichia coli* Adaptive Response Protein AidB. *Int J Mol Sci.* 13(12):16899-915.
57. Shell SS<sup>1</sup>, Prestwich EG, Baek SH, Shah RR, Sassetti CM, Dedon PC, Fortune SM, 2013, DNA methylation impacts gene expression and ensures hypoxic survival of *Mycobacterium tuberculosis*. *PLoS Pathog.* 2013;9(7):e1003419.
58. Miggiano R<sup>1</sup>, Casazza V, Garavaglia S, Ciaramella M, Perugino G, Rizzi M, Rossi F. 2013, Biochemical and structural studies of the *Mycobacterium tuberculosis* O6-methylguanine methyltransferase and mutated variants. *J Bacteriol.* 2013 Jun;195(12):2728-36.
59. Muralidharan S<sup>1</sup>, Mandrekar P, 2013, Cellular stress response and innate immune signaling: integrating pathways in host defense and inflammation. *J Leukoc Biol.* 2013 Dec;94(6):1167-84.
60. Bekhit A<sup>1</sup>, Fukamachi T, Saito H, Kobayashi H, 2011, The role of OmpC and OmpF in acidic resistance in *Escherichia coli*. *Biol Pharm Bull.* 2011;34(3):330-4.

61. Poole LB1, Godzik A, Nayeem A, Schmitt JD, 2000, AhpF can be dissected into two functional units: tandem repeats of two thioredoxin-like folds in the N-terminus mediate electron transfer from the thioredoxin reductase-like C-terminus to AhpC. *Biochemistry*. 2000 Jun 6;39(22):6602-15.
62. Bieger B1, Essen LO, 2000, Crystallization and preliminary X-ray analysis of the catalytic core of the alkylhydroperoxide reductase component AhpF from *Escherichia coli*. *Acta Crystallogr D Biol Crystallogr*. 2000 Jan;56(Pt 1):92-4.
63. Higuchi M1, Yamamoto Y, Poole LB, Shimada M, Sato Y, Takahashi N, Kamio Y, 1999, Functions of two types of NADH oxidases in energy metabolism and oxidative stress of *Streptococcus mutans*. *J Bacteriol*. 1999 Oct;181(19):5940-7.
64. Jönsson TJ1, Ellis HR, Poole LB, 2007, Cysteine reactivity and thiol-disulfide interchange pathways in AhpF and AhpC of the bacterial alkyl hydroperoxide reductase system. *Biochemistry*. 2007 May 15;46(19):5709-21.
65. Roberts BR1, Wood ZA, Jönsson TJ, Poole LB, Karplus PA, 2005, Oxidized and synchrotron cleaved structures of the disulfide redox center in the N-terminal domain of *Salmonella typhimurium* AhpF. *Protein Sci*. 2005 Sep;14(9):2414-20.
66. Hall A1, Parsonage D, Horita D, Karplus PA, Poole LB, Barbar E, 2009, Redox-dependent dynamics of a dual thioredoxin fold protein: evolution of specialized folds. *Biochemistry*. 2009 Jun 30;48(25):5984-93.
67. Dane Parker, Grace Soong, Paul Planet, Jonathan Brower, Adam J. Ratner and Alice Prince, 2009. The NanA Neuraminidase of *Streptococcus pneumoniae* Is Involved in Biofilm Formation. *INFECTION AND IMMUNITY*, Vol. 77, No. 9: p. 3722–3730.
68. Gualdi L1, Hayre JK, Gerlini A, Bidossi A, Colomba L, Trappetti C, Pozzi G, Docquier JD, Andrew P, Ricci S, Oggioni MR, 2012, Regulation of neuraminidase expression in *Streptococcus pneumoniae*. *BMC Microbiol*. 2012 Sep 11;12:200.
69. Takao A1, Nagamune H, Maeda N, 2010, Sialidase of *Streptococcus intermedius*: a putative virulence factor modifying sugar chains. *Microbiol Immunol*. 2010 Oct;54(10):584-95.
70. Limoli DH1, Sladek JA, Fuller LA, Singh AK, King SJ, 2011, BgaA acts as an adhesin to mediate attachment of some pneumococcal strains to human epithelial cells. *Microbiology*. 2011 Aug;157(Pt 8):2369-81.

71. Sedgwick, B.; Lindahl, T. Recent Progress on the Ada Response for Inducible Repair of DNA Alkylation Damage. *Oncogene* 2002, 21, 8886-8894.
72. Croteau, D. L.; Della, V. M. J.; Perera, L.; Van, H. B. Cooperative Damage Recognition by UvrA and UvrB: Identification of UvrA Residues That Mediate DNA Binding. *DNA Repair* 2008, 7(3), 392-404.
73. Wagner, K.; Moolenaar, G. F.; Goosen, N. Role of the Insertion Domain and the Zinc-Finger Motif of *Escherichia coli* UvrA in Damage Recognition and ATP Hydrolysis. *DNA Repair* 2011, 10(5), 483-496.
74. Gu, C.; Zhang, Q.; Yang, Z.; Wang, Y.; Zou, Y.; Wang, Y. Recognition and Incision of Oxidative Intrastrand Cross-Link Lesions by UvrABC Nuclease. *Biochemistry* 2006, 45(35), 10739-10746.
75. McMullen AM, Hwang SA, O'Shea K, Aliru ML, Actor JK, 2013, Evidence for a unique species-specific hypersensitive epitope in Mycobacterium tuberculosis derived cord factor. *Tuberculosis (Edinb)*. 2013 Dec;93 Suppl:S88-93.
76. Welsh KJ1, Hunter RL, Actor JK, 2013, Trehalose 6,6'-dimycolate--a coat to regulate tuberculosis immunopathogenesis. *Tuberculosis (Edinb)*. 2013 Dec;93 Suppl:S3-9.
77. Lang R, 2013, Recognition of the mycobacterial cord factor by Mincle: relevance for granuloma formation and resistance to tuberculosis. *Front Immunol*. 2013 Jan 24;4:5.
78. Singleton P (1999). *Bacteria in Biology, Biotechnology and Medicine* (5th ed.). Wiley. pp. 444–454. ISBN 0-471-98880-4.
79. Ismael Kassim, Ray CG (editors) (2004). *Sherris Medical Microbiology* (4th ed.). McGraw Hill.
80. Murray PR, Rosenthal KS, Pfaller MA (2005). *Medical Microbiology*. Elsevier Mosby.
81. Warner DF1, Tønjum T, Mizrahi V, 2013, DNA metabolism in mycobacterial pathogenesis. *Curr Top Microbiol Immunol*. 2013;374:27-51.

## **Appendix A**



# Preferential DNA damage prevention by the *E. coli* AidB gene: A new mechanism for the protection of specific genes

Valentina Rippa<sup>a,b</sup>, Angela Duilio<sup>b</sup>, Pamela di Pasquale<sup>b</sup>, Angela Amoresano<sup>b</sup>, Paolo Landini<sup>c</sup>, Michael R. Volkert<sup>a,\*</sup>

<sup>a</sup> Department of Microbiology and Physiological Systems, University of Massachusetts Medical School, Worcester, MA 01655, USA

<sup>b</sup> Department of Organic Chemistry and Biochemistry, University Federico II of Naples, Naples, Italy

<sup>c</sup> Department of Biomolecular Sciences and Biotechnology, University of Milan, Milan, Italy

## article info

### Article history:

Received 24 February 2011

Received in revised form 1 June 2011

Accepted 7 June 2011

Available online 23 July 2011

### Keywords:

AidB protein

Alkylating agents

DNA protection

UP element

## abstract

aidB is one of the four genes of *E. coli* that is induced by alkylating agents and regulated by Ada pro-tein. Three genes (ada, alkA, and alkB) encode DNA repair proteins that remove or repair alkylated bases. However, the role of AidB remains unclear despite extensive efforts to determine its function in cells exposed to alkylating agents. The *E. coli* AidB protein was identified as a component of the protein complex that assembles at strong promoters. We demonstrate that AidB protein preferentially binds to UP elements, AT rich transcription enhancer sequences found upstream of many highly expressed genes, several DNA repair genes, and housekeeping genes. AidB allows efficient transcription from promoters containing an UP element upon exposure to a DNA methylating agent and protects downstream genes from DNA damage. The DNA binding domain is required to target AidB to specific genes preferentially protecting them from alkylation damage. However, deletion of AidB's DNA binding domain does not prevent its antimutagenic activity, instead this deletion appears to allow AidB to function as a cytoplasmic alkylation resistance protein. Our studies identify the role of AidB in alkylating agent exposed cells and suggest a new cellular strategy in which a subset of the genome is preferentially protected from damage by alkylating agents.

© 2011 Elsevier B.V. All rights reserved.

## 1. Introduction

The *E. coli* aidB gene is one of the four genes of the adaptive response to alkylation damage and is regulated by Ada protein (for review see: [1,2]). Ada protein is a methyltransferase that functions as a transcriptional activator after transfer of a methyl group from DNA to a cysteine residue in its amino terminal domain. The alkylation of Ada is stable and activates it to function as a transcriptional activator that induces expression of the ada–alkB operon, the alkA and aidB genes. Ada, AlkA and AlkB are enzymes that repair different alkyl lesions in DNA. Ada removes alkyl groups from O<sup>6</sup> alkylguanine, O<sup>4</sup> alkylthymine by transferring them to a cysteine residue in its C-terminal domain [3]. Its amino terminal domain is also a methyltransferase that repairs one stereoisomer of alkylated phosphates by transferring them to a cysteine residue in its N-terminal domain [4,5]. AlkA is a glycosylase that removes 6 different types of alkylated bases from DNA [6] and AlkB is an  $\alpha$ -ketoglutarate-

Fe(II)-dependent DNA dioxygenase that repairs 1-alkyladenine and 3-alkylcytosine lesions by oxidizing the alkyl groups to unstable derivatives that spontaneously decay restoring the bases to their original state [7,8].

The role for AidB in alkylated cells has remained an unsolved problem. AidB has similarity to the acyl-CoA dehydrogenase family of metabolic enzymes and has weak isovaleryl CoA-dehydrogenase activity [9,10]. AidB was also shown to be a flavoprotein that binds nonspecifically to double stranded DNA. This observation led to the suggestion that it might be a repair enzyme [9]. The recent crystal structure of AidB revealed that its flavin binding site lies within an interior channel, while its DNA binding site is accessible only from the exterior of the protein and is spatially distant from its flavin binding region. Based on these observations, it was suggested that AidB might instead bind and protect DNA by inactivating alkylators before they are able to react with DNA.

In this study we demonstrate that AidB has sequence specific DNA binding activity that targets AidB to UP element-containing genes. We propose the gene specific targeting of AidB protein to be a new cellular strategy that results in preferential protection from alkylation damage and counteracts transcription inhibition by alkylating agents at a subset of the genome, i.e., at genes controlled by promoters with UP elements.

\* Corresponding author at: Department of Microbiology and Physiological Systems, University of Massachusetts Medical School, Rm. S6-117, Worcester, MA 01655, USA. Tel.: +1 508 856 2314; fax: +1 508 856 5920.

E-mail address: [Michael.Volkert@umassmed.edu](mailto:Michael.Volkert@umassmed.edu) (M.R. Volkert).

## 2. Materials and methods

### 2.1. Bacterial strains and plasmids

The bacterial strains and plasmids used in this work are listed in Table 1.

### 2.2. Cloning of the aidB gene

The *E. coli* aidB gene was amplified from the bacterial chromosome by PCR using the primers listed in Table 2. The amplification product was digested with NdeI and HindIII (underlined in Table 2) and cloned into the pET22b (+) vector (Novagen) creating the plasmid pET22b-aidB. The resulting expression vector contains a 6X histidine tag to allow protein purification by Ni<sup>2+</sup> affinity chromatography. Plasmid construction was verified by automated DNA sequencing. The recombinant AidB protein was produced and purified as described previously [11].

### 2.3. Electrophoretic mobility shift assay (EMSA)

EMSA experiments were performed using rrnB P1<sub>wt</sub> as the biotin-labeled DNA probe. Sense and antisense oligonucleotides (Table 2) were annealed by incubation at 95 °C for 5 min and successive gradual cooling to room temperature. Purified recombinant AidB was incubated with 20 ng of biotinylated DNA rrnB P1<sub>wt</sub> for 20 min at room temperature in 20 l of buffer Z (25 mM HEPES pH 7.6, 50 mM KCl, 12.5 mM MgCl<sub>2</sub>, 1 mM DTT, 20% glycerol, 0.1% triton). Protein–DNA complexes were separated on 5% native poly-acrylamide gel (29:1 cross-linking ratio) in 0.5× TBE (45 mM Tris pH 8.0, 45 mM boric acid, 1 mM EDTA) at 200 V (20 V/cm) at room temperature. Afterwards, electrophoretic transfer to a nylon membrane was carried out in 0.5× TBE at 380 mA for 45 min, and the transferred DNA was cross-linked to the membrane with UV light. After incubation in blocking buffer for 1 h at room temperature, the membrane was incubated with streptavidin–HRP conjugate (Sigma) for 30 min at room temperature. The membrane was washed and visualized with SuperSignal chemiluminescence reagent (Pierce).

Competition experiments were performed using increasing quantities (100–500×) of either unlabelled rrnB P1<sub>wt</sub>, which contains its UP element used as a specific competitor or rrnB P1<sub>up</sub> is used as a non-specific competitor.

### 2.4. Construction of fusion plasmids for transcription assays

The lacZ gene was amplified from genomic DNA of *E. coli* by PCR using the primers listed in Table 2. The amplification product was digested with HindIII and XhoI (underlined in Table 2) and cloned into the pET22b (+) vector (Novagen) generating the plasmid pET22b-lacZ. The rrnB P1 promoter with (rrnB P1<sub>wt</sub>) and without its UP element (rrnB P1<sub>up</sub>), PleuA and PompF were amplified by PCR, digested with SphI and HindIII and inserted into pET22b-lacZ linearized with the same restriction enzymes. The resulting plasmids, designated as listed in Table 1, were verified by automated DNA sequencing.

### 2.5. In vivo transcription assays

MG1655 and MV5924 *E. coli* strains were individually transformed with pET22b-lacZ, pET22b-P rrnB P1<sub>wt</sub>-lacZ, pET22b-P rrnB P1<sub>up</sub>-lacZ, pET22b-PleuA-lacZ and pET22b-PompF-lacZ plasmids. These bacterial cultures grown overnight in LB medium at 30 °C, were diluted 1:100 in fresh medium. At an A<sub>600 nm</sub> of 0.4, the cultures were divided in four aliquots: one was not supplemented and the other three aliquots were supplemented with MNNG (5 g/ml), ENNG (5 g/ml), MMS 0.04%, respectively. Cellular pellets were collected during the exponential growth phase. Galactosidase activity from the promoter–lacZ fusions was determined by measuring ONPG-hydrolysis, as described by Miller [12] and was compared to the activity obtained using a promoterless lacZ gene.

### 2.6. Isolation of plasmid DNA and damage assay

The MG1655 and MV5924 *E. coli* strains bearing pET22b-lacZ were grown overnight in LB medium at 30 °C; these bacterial cultures were then diluted 1:100 in fresh medium. At an A<sub>600 nm</sub> of 0.4, the cultures were divided in four aliquots: one was not supplemented and the other three aliquots were supplemented with MNNG (5 g/ml), ENNG (5 g/ml), MMS 0.04%, respectively. After the addition of alkylating agent, the bacterial cells were allowed to grow for 3 h; the plasmid DNA was isolated and served as a probe for the estimation of alkylated bases. The plasmids were divided into 2 aliquots, one of which was treated with the *E. coli* AlkA (a kind gift from Patrick J. O'Brien) and AP Endo (NEB); the other aliquot did not receive further treatment (control). Treatment with AlkA

**Table 1**  
Bacterial strains and plasmids.

Strains/plasmids	Description	Reference or source
<b>Strains</b>		
MG1655	Wild-type; F <sup>-</sup> ilvG rfb50 rph1	[38]
MV5924	aidB ::TetR derivative of MG1655 in which the aidB gene is replaced by a tetracycline resistance cassette using the methods of Murphy and Campellone [39]	[11]
MV6774	ada-alkB 25::CmR alkA1 tag-1 aidB 35::TetR derivative of MV1161 [13]	This study
MV6780	ada-alkB 25::CmR alkA1 tag-1 aidB 35::TetR/pTrc99A	This study
MV6782	ada-alkB 25::CmR alkA1 tag-1 aidB 35::TetR/pMV435 (pTrc99A-AidB <sup>+</sup> )	This study
MV6790	ada-alkB 25::CmR alkA1 tag-1 aidB 35::TetR/pMV1526 (pTrc99A-AidB 440-451)	This study
<b>Plasmids</b>		
pET22b(+)	Carries an N-terminal pelB signal sequence for potential periplasmic localization, plus an optional C-terminal His-tag sequence	This study
pET22b-aidB	pET22b (NdeI–HindIII) (aidB gene)	This study
pET22b-lacZ	pET22b (HindIII–XhoI) (lacZ gene)	This study
pET22b-PrrnB(+UP)-lacZ	pET22b-lacZ (SphI–HindIII) PrrnB(+UP)	This study
pET22b-PrrnB(-UP)-lacZ	pET22b-lacZ (SphI–HindIII) PrrnB(-UP)	This study
pET22b-PleuA-lacZ	pET22b-lacZ (SphI–HindIII) PleuA	This study
pET22b-PompF-lacZ	pET22b-lacZ (SphI–HindIII) PompF	This study
pTrc99A	<i>E. coli</i> expression vector	[10]
pMV435	pTrc99A-AidB <sup>+</sup>	[10]
pMV1526	pTrc99A-AidB 440-541	This study

**Table 2**

Oligonucleotides.

aidB Fw	5 -ATACATATGGTGCCTGGCAAACTCA-3
aidB Rv	5 -ATAAAGCTTTAACACACACTCCCC-3
lacZ Fw	5 -TGTAAGCTTATAACAATTCACACAGGAA-3
lacZ Rv	5 -CGGCTCGAGTTATTTTGACACCAGAC-3
rrnB P1(+UP) Fw	5 -TAAAGCATGCTCAGAAAATTATTTTAAATTC-3
rrnB P1Rv	5 -ATTAAGCTTAGGAGAACCCCGCTGA-3
rrnB P1(-UP) Fw	5 -ATTTGCATGCCCTCTTGTGAGGCC-3
PleuA Fw	5 -ATAAGCATGCGGGACGTTTTTATTGCG-3
PleuA Rv	5 -AAGAAGCTTGATAAAGCGAACGATGTG-3
PompF Fw	5 -ATTTGCATGCACAAAGTTCCTTAAATTTTA-3
PompF Rv	5 -TAAAGCTTAATAAAAAATTACGGAACCTATTG-3
rrnB P1(+UP) Fw bio (emsa)	5 -bio-AGAAAATTATTTTAAATTCCTCTTGTGAGGCCGGAATAACTC CCTATAAT-3
rrnB P1(+UP) Rv (emsa)	5 -ATTATAGGGAGTTATTCGGCCCTGACAAGAGGAAATTTAAATAA TTTTCT-3
rrnB P1(+UP) Fw (emsa)	5 -AGAAAATTATTTTAAATTCCTCTTGTGAGGCCGGAATAACTCCCT ATAAT-3
rrnB P1(-UP) Fw (emsa)	5 -CCTCTTGTGAGGCCGGAATAACTCCCTATAAT-3
rrnB P1(-UP) Rv (emsa)	5 -ATTATAGGGAGTTATTCGGCCCTGACAAGAGG-3

was performed in 70 mM MOPS, pH 7.5, 1 mM EDTA, 1 mM DTT, 5% glycerol for 30 min at 37 °C, followed by treatment with AP Endo for 1 h at 37 °C. Then the samples were subjected to electrophoresis in 0.8% agarose gel for ~1 h at 80 V using 40 mM Tris, pH 7.8, 1 mM EDTA buffer.

### 2.7. Determination of DNA damage in the lacZ gene

MG1655 and MV5924 *E. coli* strains were individually trans-formed with pET22b-lacZ, pET22b-P rrnB P1<sub>WT</sub>-lacZ, pET22b-P rrnB P1<sub>UP</sub>-lacZ. These bacterial cultures grown overnight in LB medium at 30 °C were diluted 1:100 in fresh medium. At an A<sub>600 nm</sub> of 0.4, the cultures were divided in two aliquots, and one was supplemented with 0.04% MMS to activate the adaptive response. The bacterial cells were allowed to grow for 3 h. Then, the plasmids under study were isolated from these bacterial cells and were digested with HindIII and XhoI to release the lacZ fragment. To estimate the presence of alkyl lesions, the DNA fragments were treated or not with the AlkA and AP Endo proteins. The samples were then subjected to electrophoresis on alkaline agarose gels in 30 mM NaOH, 1 mM EDTA, pH 8 buffer, at 60 V for 3 h at 25 °C. The gel was neutralized by soaking in a solution containing 1.5 M NaCl and 1 M Tris-HCl, pH 7.6 for 1 h. Finally, the gel was stained in TE buffer (10 mM Tris-HCl, 1 mM EDTA, pH 7.4) containing SYBR<sup>®</sup> Gold for 30 min at 25 °C and the samples were then analyzed for single-strand DNA breaks.

### 2.8. Cell survival and mutagenesis

Cell survival was tested by growing cells to a density of  $1-3 \times 10^8$  cells/ml, treating with MNNG for 30 min, then diluting cells in phosphate buffered saline containing 4% Na<sub>2</sub>S<sub>2</sub>O<sub>3</sub> to inactivate residual MNNG [13], then plating cells on LB plates [13]. Mutation frequencies were determined using DSEM plates [13]. Cultures grown to approximately  $3 \times 10^8$  cells per ml then spread on alkylating agent containing plates and incubated for 3 days at 37 °C and Arg<sup>r</sup> mutant colonies counted. Since alkylating agents are relatively unstable, plates containing mutagens were made by first adding alkylators at volumes needed to attain the specified final concentration, then adding 25 ml cooled (50 °C) DSEM medium. The plates were cooled for 20 min, then dried by incubation at 37 °C for 20 min with covers removed and immediately inoculated. All mutagenesis measurements were made at sub-lethal doses of alkylators using strains deficient in most alkylation specific DNA repair mechanisms (ada-alkB 25::CmR alkA1 tag-1 aidB 35::TetR) carrying either the vector pTrc99A, or pTrc99A derivatives that express aidB alleles.

## 3. Results

To identify proteins that bind the upstream regions of strong promoters, we investigated the protein complex that assembles at the upstream elements of the rrnB P1 promoter (see [Supplemental Data and Supplemental Figure S1](#)) by comparing proteins that bind to a sequence containing the -35 region and the UP element, an A/T rich enhancer sequence that constitutes the upstream element of many genes [14–16], but not to a similar sequence lacking the UP element. The presence of the *E. coli* AidB protein among these proteins was unexpected, and suggested a possible regulatory role for AidB in transcription.

### 3.1. AidB preferentially binds DNA containing UP elements

**Fig. 1** shows that AidB protein binds to DNA containing the rrnB P1<sub>WT</sub> promoter retarding the fragment in an electrophoretic mobility shift experiment (EMSA). When rrnB P1<sub>WT</sub> DNA is used as competitor, there is a rapid loss of binding to the labeled DNA. However, when the rrnB P1<sub>UP</sub> promoter lacking the UP element is used as competitor, no inhibition of binding to the labeled rrnB P1<sub>WT</sub>

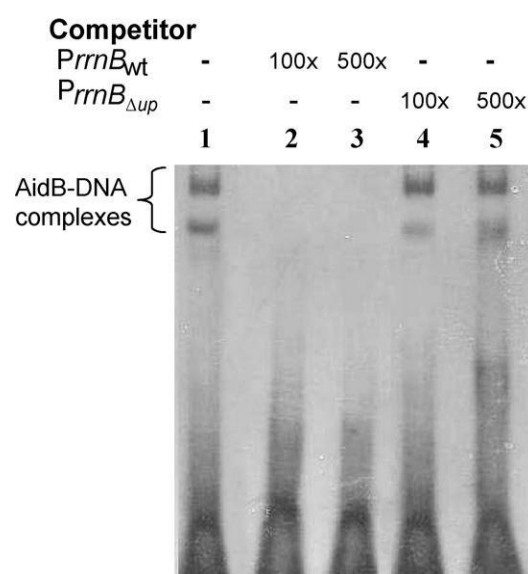


**Fig. 1.** Gel retardation. Experiments were performed by incubating the AidB protein with rrnB P1<sub>WT</sub>; competitors were included as indicated. Lane 1: AidB protein incubated with rrnB P1<sub>WT</sub>. Lanes 2–3: Competition assay with rrnB P1<sub>WT</sub> (100–500x) as specific competitor. Lanes 4–5: Competition assay with rrnB P1<sub>UP</sub> as non specific competitor (100–500x).



sequence is seen even when it is added at a 500-fold excess. This indicates that AidB protein preferentially binds to *rrnB* P1 promoter only when the UP element is present. Similar results were also seen when random DNA containing the same base pair composition was used as competitor (see supplemental data). The preferential binding is not restricted to the *rrnB* P1<sub>WT</sub> promoter, since binding of AidB to its own promoter also requires the presence of the UP element [11].

### 3.2. Functional analysis of AidB during transcription

In order to determine whether the presence of AidB at the *rrnB* P1 promoter might be of biological significance, we tested its effect on transcription from this promoter by in vivo transcription assays. In addition, we tested other promoters that differ with respect to presence or absence of an UP element, namely: (1) the *rrnB* p1 promoter with its UP element (*rrnB*<sub>WT</sub>), (2) the *rrnB* promoter deleted of its UP element (*rrnB*<sub>UP</sub>), (3) *PleuA*, which lacks an UP element and (4) *PompF*, which has an UP element. All promoters were individually fused to a promoterless lacZ gene contained in the reporter plasmid pET22b-lacZ. Both MG1655 (wild type) and MV5924 (*aidB*) *E. coli* strains were then transformed with the fusion plasmids and grown

in LB medium, either in the absence or in the presence of alkylating agents (MMS, MNNG, and ENNG). After 2 h incubation in the presence or absence of the alkylating agent, -galactosidase activity was measured during the exponential growth phase. As shown in Fig. 2A, wild type and *aidB* mutant strains not exposed to alkylators showed identical levels of -galactosidase activity, indicating that the presence of AidB has no effect on transcription in untreated cells experiencing normal growth.

When MG1655 cells are treated with MMS, MNNG, or ENNG, transcription is reduced by roughly 2-fold for all promoters tested. In contrast, the *aidB* mutant showed a much more severe reduction in transcription, especially at the *rrnB*<sub>WT</sub> and *PompF*, the two UP element containing promoters (Fig. 2). This suggests that the interaction of AidB protein with this class of promoters is of functional significance and that AidB prevents transcription block by alkylation stress. The smaller effect of the *aidB* deletion on the two promoters lacking UP elements is consistent with preferential binding of AidB to this region (Fig. 1). Taken together, these data strongly suggest that AidB is required for high levels of transcription during alkylation stress and that it has a more pronounced effect on transcription from promoters containing an upstream UP element sequence. While it is formally possible that AidB is a transcriptional

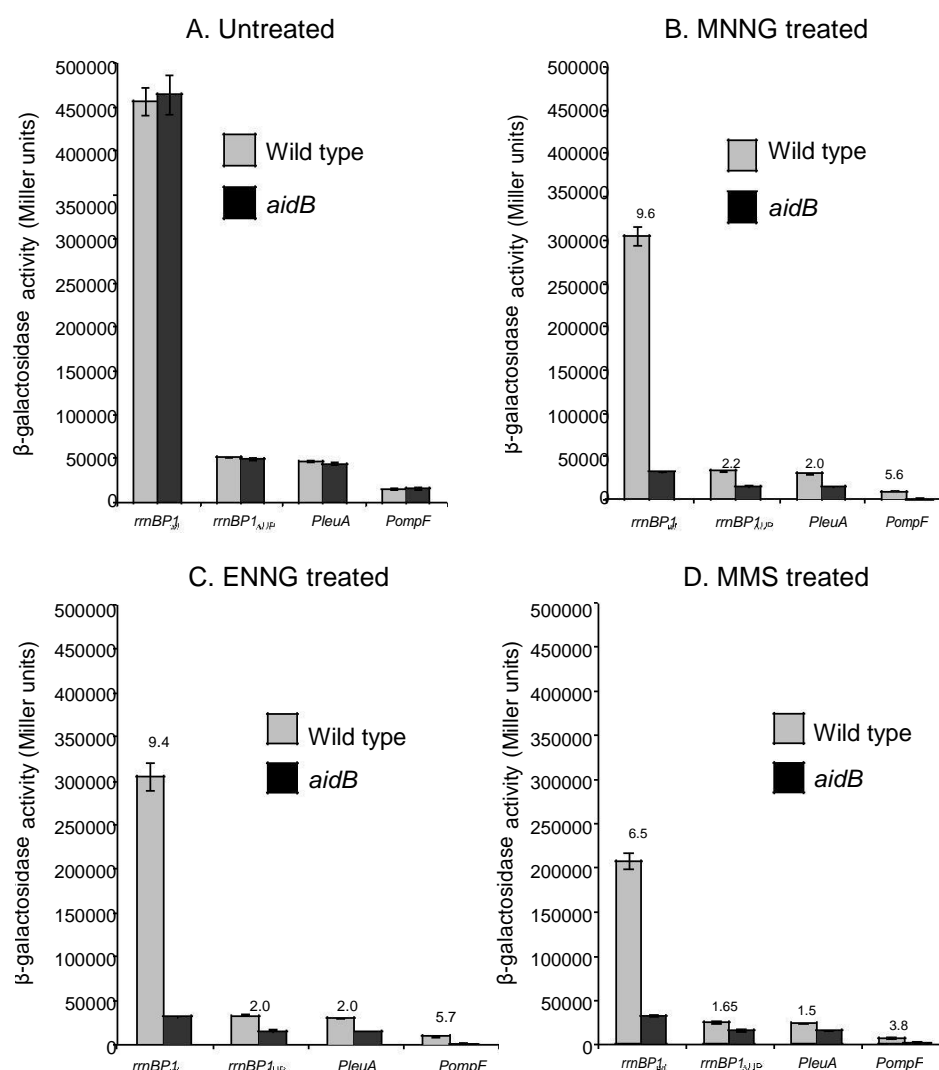


**Fig. 2.** In vivo transcription of lacZ fused to different promoters. The pET22b-P *rrnB* P1<sub>WT</sub>-lacZ, pET22b-P *rrnB* P1<sub>UP</sub>-lacZ, pET22b-*PleuA*-lacZ and pET22b-*PompF*-lacZ plasmids were individually introduced into MG1655 (wild type) and MV5924 (*aidB*) *E. coli* strains and the specific activity of -galactosidase was determined in the absence (A) and in the presence of MNNG (5 g/ml) (B), ENNG (5 g/ml) (C), MMS 0.04% (D). The activities of promoters are reported in Miller units; the activity obtained using a promoterless lacZ gene was subtracted. Numbers above bars refer to the ratio of the -galactosidase activity of the promoter measured in the wild type cells to the activity of that same promoter in the *aidB* mutant strain. Means and standard deviations have been calculated from four independent assays.

regulator of UP element containing genes when alkylating agents are present, a more likely explanation, based on its role as part of an alkylation inducible DNA repair response, is that AidB prevents or repairs DNA damage in specific regions of the genome, preferentially preserving the coding capacity of genes transcribed from UP element containing promoters.

### 3.3. AidB reduces the level of alkylation damage in DNA

To test directly if AidB might be able to prevent or repair alkylation damage to DNA the pET22b-lacZ plasmid was isolated from wild type and aidB mutant cells grown either in the absence or in the presence of alkylators (MMS, MNNG, and ENNG) and served as a probe for the estimation of alkylated bases in DNA. The plasmids were divided into 2 aliquots, one was treated with *E. coli* AlkA (a gift from Patrick J. O'Brien) and AP Endonuclease IV (AP Endo) (New England Biolabs); the other aliquot did not receive further treatment and served as a control. The AlkA glycosylase recognizes and removes a wide variety of alkylated bases converting them to abasic sites [6] and AP Endo is an apurinic/aprimidinic (AP) endonuclease that converts the abasic sites to nicks [17,18]. The combined action of these two enzymes on a damaged plasmid results in the conversion of the covalently closed circular (supercoiled) DNA to open circular and, if lesions are closely spaced, linear forms. AlkA treated and untreated plasmids were then subjected to electrophoresis on agarose gels and tested for the conversion of the supercoiled form to open circular and linear forms. As shown in Fig. 3A, alkyl lesions were not detected in plasmids isolated from bacteria grown in LB medium without the addition of alkylating agents, indicating there is no detectable endogenous damage or non-specific cleavage by

these enzymes in vitro. When plasmid DNA isolated from wild type cells exposed to alkylating agents was analyzed (Fig. 3B–D), treatment with AlkA and AP Endo did not result in nicking (Lane 2) indicating a lack of DNA damage, but when DNA isolated from the alkylating agent treated aidB mutant was analyzed, the supercoiled fraction was completely absent after AlkA/AP Endo treatment and there was an increase in both open circular and linear forms (Lane 4). These results indicate that the presence of AidB reduces the level of alkylation damage in plasmid DNA. Moreover, AidB protects DNA from all three alkylating agents tested, although they differ in the nature of DNA lesions they produce. Indeed, MNNG methylates and ENNG ethylates DNA more effectively at O<sup>6</sup>-G than MMS. In contrast MMS methylates double stranded DNA primarily at N<sup>7</sup>-G and N<sup>3</sup>-A sites and in single stranded DNA regions it also methylates N<sup>1</sup>-A and N<sup>3</sup>-C more efficiently than MNNG [19].

AidB preferentially protects DNA regions downstream of an UP element.

Since AidB appears to protect DNA from alkylating agents very effectively (Fig. 3), the lack of an alkylation sensitivity phenotype of aidB mutants remains a puzzle (see Fig. 5 and [13,20]). The observation that AidB protein allows more effective transcription of genes with UP element promoters in the presence of an alkylating agent (Fig. 2) and has a higher affinity for UP element containing promoters [11], suggests that AidB may not protect the entire genome equally and may show a preference for UP element containing regions of DNA. To test this possibility, we analyzed the effect of AidB on alkylation damage in vivo in the lacZ fragment. In this experiment, we used three plasmids, each carrying the lacZ gene fused to three different upstream sequences: the rrnB<sub>WT</sub> promoter, the rrnB<sub>UP</sub> promoter, and a third plasmid carrying a promoterless

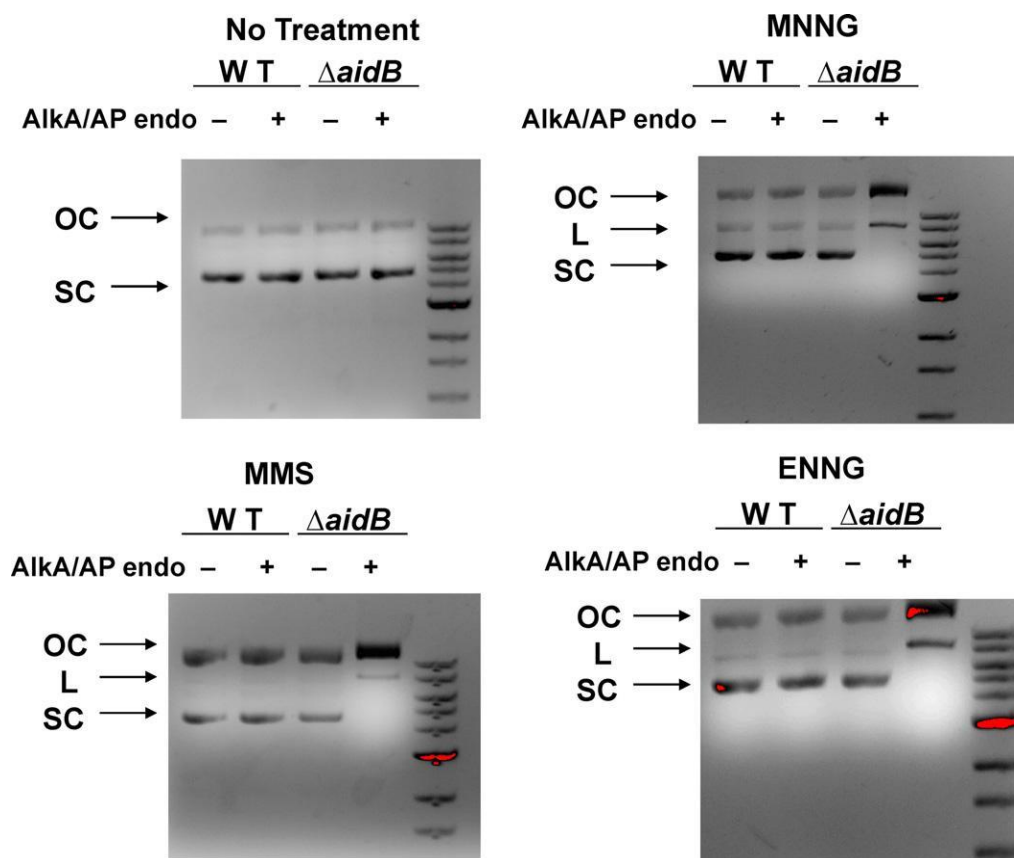


**Fig. 3.** Plasmid damage assay. The pET22b-lacZ DNA was isolated from wild type (Lanes 1–2) and aidB (Lanes 3–4) *E. coli* strains grown in the absence (A) or in the presence of MNNG (5 g/ml) (B), MMS 0.04% (C), ENNG (5 g/ml) (D), digested (Lanes 2, 4) or not (Lanes 1, 3) with AlkA and AP Endo and subjected to agarose gel electrophoresis. Lane 5, 1 kb DNA marker (NEB). OC: open circular; L: linear; SC: supercoiled.

lacZ gene. We investigated whether the presence of AidB might affect the content of alkyl lesions within the lacZ sequences. Wild type and aidB mutant cells containing these plasmids were first treated with MMS. After isolation, the plasmids were digested with restriction enzymes to release the lacZ fragment. The lacZ fragment was then purified by agarose gel electrophoresis and divided into two aliquots. One aliquot was treated with the AlkA/AP Endo to nick the DNA at the lesion sites. The samples were then subjected to electrophoresis on alkaline agarose gel to denature DNA and to separate nicked from full-length ssDNA fragments. Since only undamaged strands will run as full-length molecules, the fraction of strands containing lesions can be estimated by comparing the AlkA/AP Endo treated samples with controls not treated with AlkA/AP Endo. Fig. 4 shows that the aidB mutant cells are not able to protect the lacZ gene regardless of the upstream sequence present and all DNA samples are equally sensitive to AlkA/AP Endo treatment (Lanes 8, 10, and 12). In wild type cells, essentially all DNA from the rrnB<sub>WT</sub> bearing plasmid exposed to AlkA/AP Endo remains as full length (Fig. 4, compare Lanes 3 and 4). When lacZ is fused to the rrnB<sub>UP</sub> promoter, the sample treated with AlkA/AP Endo (Lane 6) shows a clear decrease in the amount of full-length fragments compared with the control DNA not treated with AlkA/AP Endo (Lane 5). Treatment of lacZ from the promoter-less plasmid with AlkA/AP Endo resulted in an almost complete loss of full-length DNA fragments indicating a higher level of damage (Compare Lanes 1 and 2), thus confirming that the presence of AidB is required for the protection against alkyl damage. It also suggests that transcription itself cannot be solely responsible for damage prevention, since transcription at the onset of damage is identical in wild type and the aidB mutant (Fig. 2). Additionally, there is no detectable difference in damage levels when DNA samples isolated from the aidB mutant are compared with one another despite the markedly higher level of transcription of the lacZ gene transcribed from the rrnB P1<sub>WT</sub> element versus the promoterless lacZ. By contrast, plasmids from MMS treated wild type cells show a clear difference in their levels of protection from alkylation damage. Fig. 4 shows that lacZ fused to the UP element containing the rrnB P1<sub>WT</sub> promoter is well protected from MMS exposure when compared, either to the samples from the aidB mutant, or lacZ fused to the rrnB promoter that lacks the UP element, or has no promoter.

These results demonstrate that AidB preferentially protects the DNA of genes transcribed from UP element-containing promoters

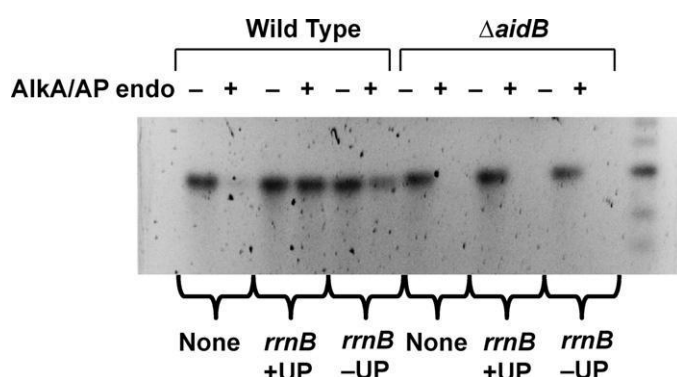


**Fig. 4.** AidB preferentially protects DNA regions containing an UP element. The pET22b-lacZ, pET22b-P rrnB P1<sub>WT</sub>-lacZ and pET22b-P rrnB P1<sub>UP</sub>-lacZ plasmids were isolated from wild type (Lanes 1–6) and aidB (Lanes 7–12) *E. coli* strains grown in the presence of MMS 0.04% and digested to release and purify the lacZ fragment. The lacZ containing DNA fragments were untreated (Lanes 1, 3, 5, 7, 9, 11) or treated (Lanes 2, 4, 6, 8, 10, 12) with AlkA and AP Endo and subjected to electrophoresis on alkaline agarose gel. Lanes 1, 2, 7, 8: lacZ lacking a promoter; Lanes 3, 4, 9, 10: lacZ fused to the rrnB P1<sub>WT</sub> promoter with its UP element; Lanes 5, 6, 11, 12: lacZ fused to the rrnB P1<sub>UP</sub> promoter without its UP element; Lane 13: 1 kb DNA marker (NEB).

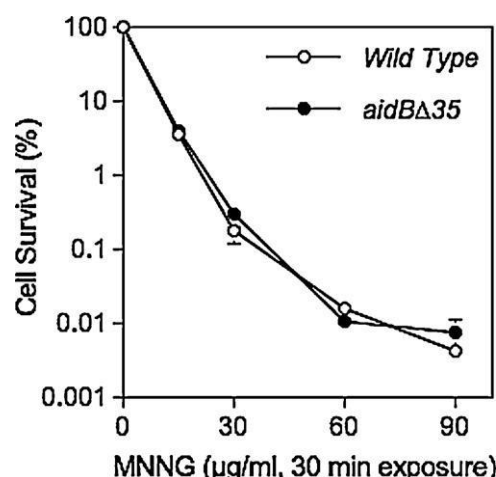


**Fig. 5.** Alkylating agent sensitivity of strains deficient in adaptive response genes. Cells were grown to a density of approximately  $1-3 \times 10^8$  cells/ml and treated with MNNG as indicated. Wild type (MG1655), aidB 35::TetR (MV5924). Each data point represents 3 (15, 90 g/ml) or 6 repetitions (0, 30 and 60 g/ml). Standard errors of the mean are shown where visible beyond the data point.

to a greater extent than DNA fragments bearing promoters lacking an UP element.

### 3.4. AidB does not confer cellular resistance to alkylation damage

The aidB mutant strain MV5924 was tested for its sensitivity to MNNG damage. Fig. 5 shows that even a complete deletion of aidB results in little or no sensitivity to MNNG when compared with its isogenic wild type. The aidB mutation also does not affect MMS sensitivity (Figure S3, supplementary material). These results are consistent with previous observations that mutants carrying insertions in the aidB gene show no increase in sensitivity to alkylating agents [13]. A lack of alkylation sensitivity of the aidB deletion mutant is inconsistent with a general DNA damage prevention mechanism, since the ability to prevent damage throughout the genome should result in increased resistance. However, protection of only some DNA regions would prevent damage to only those genes that are targets for AidB protein and is unlikely to have a major effect on overall survival.

Based on the 3-dimensional structure of AidB protein, it has been suggested that AidB is unlikely to function as a DNA repair protein. Instead it may bind DNA and enzymatically inactivate alkylators as they approach the DNA. This notion is based on the observation that the dehydrogenase active site of AidB is spatially distant from its DNA binding face and accessible only from the exterior of the protein [23]. Since a DNA repair protein predicts that the DNA binding domain will be required for activity, we constructed an AidB mutant that lacks the entire DNA binding domain (aidB 440–541). This mutant has previously been shown to have IVD activity identical to the wild type, but no detectable DNA binding activity [11]. Since wild type AidB protein functions as an antimutator when cells are grown in the presence of MNNG, we tested if the DNA binding deficient AidB mutant protein retains the antimutator activity. Fig. 6 shows that the aidB 440–541 mutant allele is as active as the wild type allele in the antimutator assay, indicating that DNA binding is not required for the alkylation resistance function of AidB and suggesting DNA binding instead serves to target AidB to specific genes.

## 4. Discussion

The biological role of AidB has long been uncertain. Our data demonstrate that AidB prevents DNA damage by alkylating agents

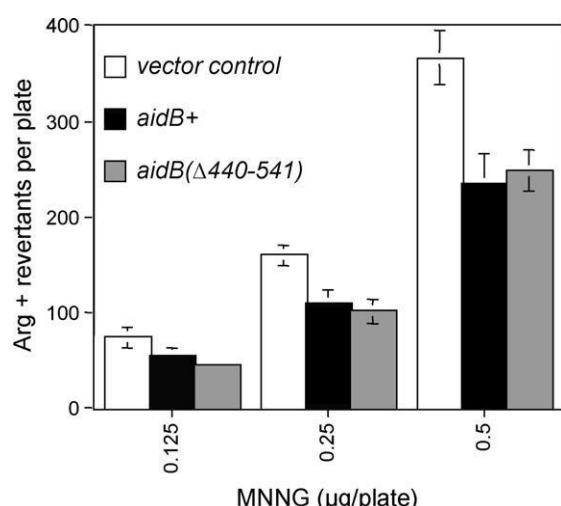


**Fig. 6.** Antimutagenic activity of wild type and AidB( 440-541). Cells were grown to a density of approximately  $3 \times 10^8$  cells per ml and undiluted cultures were spread on DSEM plates  $\pm$  alkylating agents and mutation frequencies determined. All mutagenesis experiments were conducted at sublethal doses of alkylating agents using strains deficient in most alkylation specific DNA repair mechanisms: aidB<sup>+</sup> (MV6782, ada-alkB 25::CmR alkA1 tag-1 aidB 35::TetR/pTrc99A-AidB<sup>+</sup>); aidB 440-541 (MV6790, ada-alkB 25::CmR alkA1 tag-1 aidB 35::TetR/pTrc99A-AidB 440-451); vector control (MV6780, ada-alkB 25::CmR alkA1 tag-1 aidB 35::TetR/pTrc99A).

and counteracts the block to transcription that results upon exposure to alkylating agents, especially in genes that are transcribed from promoters containing UP elements. These effects are seen after treatment with MMS, MNNG and ENNG, three alkylating agents that produce different DNA lesions or damage spectra [24]. The result that ENNG damage is also prevented is especially interesting since ENNG lesions are repaired not only by adaptive response repair system, but also by nucleotide excision repair in *E. coli* [25].

The result that AidB can prevent DNA damage seems inconsistent with the result that loss of AidB function by a complete deletion has little or no effect on MMS or MNNG sensitivity of the mutant strain (Fig. 5 and S3). However, effects of an aidB mutation on DNA damage and mutagenesis were seen at sublethal doses of alkylating agents (Figs. 3–6). Since Ada dependent aidB induction is relatively weak compared to that of other adaptive response genes [13,20], it is possible that AidB protein levels are too low to provide adequate protection against lethal doses of alkylating agents. The primary function of AidB may be to protect DNA from the low levels of alkylators that are produced as by-products of stationary phase metabolism [26–29], a possibility that is consistent with the observation that aidB is induced and expressed at elevated levels in stationary phase [10,30,31].

The result that the AidB protein specifically binds to DNA sequences that include the UP element [11] (see also Fig. 1), suggests that the lack of increased sensitivity to high levels of alkylating agents in the aidB mutant (Fig. 5) may also be due to the fact that AidB only protects a subset of the genome, leaving other genes, including essential ones, exposed to DNA damage. The aidB mutant phenotype is consistent with targeted repair or damage prevention and is analogous to the effect seen in strains that lack the ability to carry out transcription-coupled repair (TCR) of UV damage, the only other gene specific repair or damage prevention system currently known. A TCR deficient mfd mutant shows only a modest decrease in cellular resistance to UV, but a dramatic reduction in the rate at which repair of active genes occurs [32–34]. Thus, the AidB prevention mechanism appears to be a cellular strategy to preferentially protect a subset of genes. In this case the genes

include ones important for basic metabolic processes and key DNA repair genes. AidB is targeted towards genes whose promoters have upstream UP elements. This includes genes such as most of the ribosomal RNA genes and many tRNA genes as well as several key DNA repair genes required for recovery from alkylation damage such as recA, polA, sulA, recN the ada-alkB operon, and aidB itself [14,35,36].

The presence of a functional aidB gene protects UP element genes from alkylation damage and results in more efficient transcription in the presence of alkylating agents. lacZ fused to the two UP element containing rrn and ompF promoters are transcribed 10- and 6-fold more efficiently in the presence of an alkylating agent than lacZ fused to an rrn promoter whose UP element has been deleted, or the leuA promoter, which has no UP element. Although it is possible that AidB has regulatory effects on these genes, a lower level of template damage should clearly contribute to the transcription efficiency.

Promoters lacking an UP element, and thus not efficiently bound by AidB protein still show a slightly higher level of transcription in wild type versus aidB mutants upon alkylation (2.2- and 2-fold enhancement for rrn<sub>UP</sub> and P<sub>leu</sub>, Fig. 2). It is unclear if this aidB-dependent enhancement of transcription in the presence of an alkylating agent represents some direct protection by aidB, or is an indirect effect of the elevated levels of ribosomes, tRNAs and possibly other components of the translational machinery that are transcribed at a higher levels in the aidB<sup>+</sup> strain under these conditions. The observation that the protection of lacZ fused to the rrn promoter lacking an UP element and the observation that plasmid DNA shows better protection in wild type than in an aidB mutant strain (Fig. 4), suggests that there may be some general protection resulting from the presence of aidB, especially when it is highly expressed, or induced for a long period of time as in these experiments. Under these conditions AidB may initially protect the genes preferentially targeted, followed by other parts of the genome if AidB protein accumulates to sufficiently high levels. The precise mechanism of action of AidB remains to be determined, though it is possible that it provides the protection of DNA adjacent to its preferred binding site, either by simply inactivating alkylating agents and reducing the local concentration, or by polymerizing into multimers that extend from the initial binding site. In the latter case, it is likely to protect both by shielding the DNA and by inactivating alkylators.

However, the MNNG resistance resulting from expression of the DNA binding deficient aidB mutant protein, AidB( 440-541) indicates that the mutant lacking DNA binding activity still functions to prevent alkylation mutagenesis. This observation makes it unlikely that AidB functions by simply binding and coating the DNA, thus preventing access by alkylators. The ability of the DNA binding defective AidB protein to prevent mutagenesis suggests that AidB is not a DNA repair protein, since DNA repair would be inhibited by lack of DNA binding activity. Instead, AidB is more likely to function to prevent damage by detoxifying alkylating agents, which could reduce DNA alkylation even in the absence of DNA binding activity by reducing the intracellular concentration of active alkylators. A role for AidB in alkylating agent detoxification is also consistent with earlier work on AidB and analysis of the structural features of the protein [10,23]. Determination of the precise mechanism by which AidB may inactivate alkylating agents requires further work to examine the chemistry of the hypothetical process.

It is unclear how widespread preferential damage prevention mechanisms such as AidB are, if other prokaryotes and eukaryotes have similar damage prevention proteins, or if the strategy of preferential DNA protection extends to mechanisms that prevent damage by other agents. In *E. coli* the dps gene is highly expressed in stationary phase and prevents oxidative DNA damage. Unlike AidB,



however, this protein is produced at very high levels and appears to function as a genome wide protective protein. It is unclear if it may also have a preference for specific sequences when it is expressed at lower levels [37].

### Conflict of interest statement

The authors have no conflicts of interest.

### Acknowledgements

We thank Patrick J. O'Brien (University of Michigan) for AlkA protein. This work was funded in part by NIH Grant CA100122 to MRV, Italian MIUR PRIN 2008 and FIRB 2007 Italian Human Pro-teoNet grants to AD.

### Appendix A. Supplementary data

Supplementary data associated with this article can be found, in the online version, at [doi:10.1016/j.dnarep.2011.06.001](https://doi.org/10.1016/j.dnarep.2011.06.001).

### References

- [1] M.R. Volkert, P. Landini, Transcriptional responses to DNA damage, *Curr. Opin. Microbiol.* 4 (2001) 178–185.
- [2] P. Landini, M.R. Volkert, Regulatory responses of the adaptive response to alkylation damage: a simple regulon with complex regulatory features, *J. Bacteriol.* 182 (2000) 6543–6549.
- [3] T.V. McCarthy, P. Karran, T. Lindahl, Inducible repair of O-alkylated DNA pyrimidines in *Escherichia coli*, *EMBO J.* 3 (1984) 545–550.
- [4] I. Teo, B. Sedgwick, M.W. Kilpatrick, T.V. McCarthy, T. Lindahl, The intracellular signal for induction of resistance to alkylating agents in *E. coli*, *Cell* 45 (1986) 315–324.
- [5] Y. Nakabeppu, M. Sekiguchi, Regulatory mechanisms for induction of synthesis of repair enzymes in response to alkylating agents: Ada protein acts as a transcriptional regulator, *Proc. Natl. Acad. Sci. U.S.A.* 83 (1986) 6297–6301.
- [6] P.J. O'Brien, T. Ellenberger, The *Escherichia coli* 3-methyladenine DNA glycosylase AlkA has a remarkably versatile active site, *J. Biol. Chem.* 279 (2004) 26876–26884.
- [7] S.C. Trewick, T.F. Henshaw, R.P. Hausinger, T. Lindahl, B. Sedgwick, Oxidative demethylation by *Escherichia coli* AlkB directly reverts DNA base damage, *Nature* 419 (2002) 174–178.
- [8] P.O. Falnes, R.F. Johansen, E. Seeberg, AlkB-mediated oxidative demethylation reverses DNA damage in *Escherichia coli*, *Nature* 419 (2002) 178–182.
- [9] M.S. Rohankhedkar, S.B. Mulrooney, W.J. Wedemeyer, R.P. Hausinger, The AidB component of the *Escherichia coli* adaptive response to alkylating agents is a flavin-containing, DNA-binding protein, *J. Bacteriol.* 188 (2006) 223–230.
- [10] P. Landini, L.I. Hajec, M.R. Volkert, Structure and transcriptional regulation of the *Escherichia coli* adaptive response gene *aidB*, *J. Bacteriol.* 176 (1994) 6583–6589.
- [11] V. Rippa, A. Amoresano, C. Esposito, P. Landini, M. Volkert, A. Duilio, Specific DNA binding and regulation of its own expression by the AidB protein in *Escherichia coli*, *J. Bacteriol.* 192 (2010) 6136–6142.
- [12] J.H. Miller, *Experiments in Molecular Genetics*, Cold Spring Harbor Laboratories, Cold Spring Harbor, 1972.
- [13] M.R. Volkert, D.C. Nguyen, Induction of specific *Escherichia coli* genes by sublethal treatments with alkylating agents, *Proc. Natl. Acad. Sci. U.S.A.* 81 (1984) 4110–4114.
- [14] R.L. Gourse, W. Ross, T. Gaal, UPs and downs in bacterial transcription initiation: the role of the alpha subunit of RNA polymerase in promoter recognition, *Mol. Microbiol.* 37 (2000) 687–695.
- [15] S.T. Estrem, T. Gaal, W. Ross, R.L. Gourse, Identification of an UP element consensus sequence for bacterial promoters, *Proc. Natl. Acad. Sci. U.S.A.* 95 (1998) 9761–9766.
- [16] W. Ross, K.K. Gosink, J. Salomon, K. Igarashi, C. Zou, A. Ishihama, K. Severinov, R.L. Gourse, A third recognition element in bacterial promoters: DNA binding by the alpha subunit of RNA polymerase, *Science* 262 (1993) 1407–1413.
- [17] S. Ljungquist, T. Lindahl, Relation between *Escherichia coli* endonucleases specific for apurinic sites in DNA and exonuclease III, *Nucleic Acids Res.* 4 (1977) 2871–2879.
- [18] S. Ljungquist, A new endonuclease from *Escherichia coli* acting at apurinic sites in DNA, *J. Biol. Chem.* 252 (1977) 2808–2814.
- [19] B. Singer, The chemical effects of nucleic acid alkylation and their relation to mutagenesis and carcinogenesis, *Prog. Nucleic Acid Res. Mol. Biol.* 15 (1975) 219–284.
- [20] M.R. Volkert, D.C. Nguyen, K.C. Beard, *Escherichia coli* gene induction by alkylation treatment, *Genetics* 112 (1986) 11–26.
- [23] T. Bowles, A.H. Metz, J. O'Quin, Z. Wawrzak, B.F. Eichman, Structure and DNA binding of alkylation response protein AidB, *Proc. Natl. Acad. Sci. U.S.A.* 105 (2008) 15299–15304.
- [24] B. Singer, D. Grunberger, *Molecular Biology of Mutagens and Carcinogens*, Plenum Press, New York, 1983.
- [25] K. Bonanno, J. Wyrzykowski, W. Chong, Z. Matijasevic, M.R. Volkert, Alkylation resistance of *E. coli* cells expressing different isoforms of human alkyladenine DNA glycosylase (hAAG), *DNA Rep.* 1 (2002) 507–517.
- [26] G.W. Rebeck, L. Samson, Increased spontaneous mutation and alkylation sensitivity of *Escherichia coli* strains lacking the *ogt* O6-methylguanine DNA repair methyltransferase, *J. Bacteriol.* 173 (1991) 2068–2076.
- [27] B. Sedgwick, Nitrosated peptides and polyamines as endogenous mutagens in O6-alkylguanine-DNA alkyltransferase deficient cells, *Carcinogenesis* 18 (1997) 1561–1567.
- [28] P. Taverna, B. Sedgwick, Generation of endogenous methylating agents by nitrosation in *Escherichia coli*, *J. Bacteriol.* 178 (1996) 5105–5111.
- [29] B. Sedgwick, Oxidation of methylhydrazines to mutagenic methylating derivatives and inducers of the adaptive response of *Escherichia coli* to alkylation damage, *Cancer Res.* 52 (1992) 2693–2697.
- [30] P. Landini, L.I. Hajec, L.H. Nguyen, R.R. Burgess, M.R. Volkert, The leucine-responsive protein (Lrp) acts as a specific repressor for *s*<sup>+</sup>-dependent transcription of the *Escherichia coli* *aidB* gene, *Mol. Microbiol.* 20 (1996) 947–955.
- [31] M.R. Volkert, L.I. Hajec, Z. Matijasevic, F. Fang, R. Prince, Induction of the *Escherichia coli* *aidB* gene under oxygen limiting conditions requires a functional *ropS* (*katF*) gene, *J. Bacteriol.* 176 (1994) 7638–7645.
- [32] C.P. Selby, A. Sancar, Mechanisms of transcription–repair coupling and mutation frequency decline, *Microbiol. Rev.* 58 (1994) 317–329.
- [33] C.P. Selby, A. Sancar, Molecular mechanism of transcription–repair coupling, *Science* 260 (1993) 53–58.
- [34] C.P. Selby, E. Witkin, A. Sancar, *Escherichia coli* *mfd* mutant deficient in “mutation frequency decline” lacks strand-specific repair: in vitro complementation with purified coupling factor, *Proc. Natl. Acad. Sci. U.S.A.* 88 (1991) 11478–11574.
- [35] W. Ross, S.E. Aiyar, J. Salomon, R.L. Gourse, *Escherichia coli* promoters with UP elements of different strengths: modular structure of bacterial promoters, *J. Bacteriol.* 180 (1998) 5375–5383.
- [36] P. Landini, M.R. Volkert, RNA polymerase alpha subunit binding site in positively controlled promoters: a new model for RNA polymerase/promoter interaction and transcriptional activation in the *E. coli* *ada* and *aidB* genes, *EMBO J.* 14 (1995) 4329–4335.
- [37] A. Martinez, R. Kolter, Protection of DNA during oxidative stress by the nonspecific DNA-binding protein Dps, *J. Bacteriol.* 179 (1997) 5188–5194.
- [38] K.F. Jensen, The *Escherichia coli* K-12 “wild types” W3110 and MG1655 have an *rph* frameshift mutation that leads to pyrimidine starvation due to low *pyrE* expression levels, *J. Bacteriol.* 175 (1993) 3401–3407.
- [39] K.C. Murphy, K.G. Campellone, Lambda Red-mediated recombinogenic engineering of enterohemorrhagic and enteropathogenic *E. coli*, *BMC Mol. Biol.* 4 (2003) 11.

## **Appendix B**

# Molecular Partners of *Escherichia coli* Transcriptional Modulator AidB

Pamela Di Pasquale, Angela Amoresano, Francesca De Maria and Angela Duilio\*

Department of Chemical Sciences, University Federico II of Naples, Naples 80126, Italy

Received: May 29, 2013 / Accepted: June 17, 2013 / Published: September 25, 2013.

**Abstract:** The AidB protein is involved in the adaptive response to DNA alkylation damages in *Escherichia coli*. Functional proteomic experiments were designed to elucidate AidB biological functions in the presence and in the absence of methyl methanesulfonate as methylating agent. Several proteins were identified in both conditions and according to their reported biological activities, the inter-actors were grouped into three different functional categories: stress response, energetic metabolic pathways and nucleic acid metabolism. Particularly, the interaction between AidB and UvrA, a member of the UvrABCD nucleotide excision system, suggested a new interesting putative role for AidB.

**Key words:** AidB protein, adaptive response, UvrA protein, DNA alkylation damages, functional proteomics.

## 1. Introduction

DNA modifications by alkyl molecules can cause cytotoxic and mutagenic lesions in all living organisms. Several repair mechanisms able to remove alkyl groups and restore genetic information occur in microorganisms to counteract DNA chemical damages. Furthermore, bacteria exhibit the adaptive response by which cellular resistance enhances with increasing doses of methylating agents [1]. This response in *Escherichia coli* involves the presence of the acyl-CoA dehydrogenase AidB, among others. AidB consists of two domains, the N-terminal region responsible of the dehydrogenase activity, and the C-terminal domain exhibiting DNA binding capability [2]. Unlike all the other proteins of the adaptive response, AidB seems to act as a DNA protective protein and it is not endowed with DNA repair capabilities.

Moreover, in the presence of methylating agents, AidB allows efficient transcription from promoters containing an UP element, AT rich transcription

enhancer sequences and protects downstream genes from chemical damages [3, 4]. Even though the mechanism of DNA protection exerted by AidB is still obscure, this protein might prevent alkyl damage either by binding and physically hiding the DNA molecule or by inactivating alkylating agents thus reducing their local concentration.

This paper focused on the elucidation of AidB biological role at the molecular level by functional proteomic approaches addressed to the identification of AidB protein partners. Since it is now clear that relevant biological mechanisms involve multi-protein complexes, the association of AidB with partners belonging to a particular mechanism will be strongly suggestive of its biological function. Isolation of AidB multi-protein complexes was performed *in vivo* by pull down strategies using a His-tagged form of the protein as bait in the presence and in the absence of methyl-methane sulfonate as methylating agent.

Authors identified several proteins involved in different biological mechanisms including various response complexes thus suggesting that AidB is endowed with different functions indicative of new cellular strategies to counteract alkylation stresses.

---

\*Corresponding author: Angela Duilio, Associate Professor, research fields: microbiology, DNA repair mechanisms and M. tuberculosis. E-mail: anduilio@unina.it.

## 2. Experimental Sections

Proteomic grade trypsin, DTT (dithiothreitol), HEPES, KCl, MgCl<sub>2</sub>, glycerol, ammonium bicarbonate and triton were purchased from Sigma. All used solvents were of the highest purity available from Romil.

### 2.1 *Escherichia Coli* Growths and Cell Extraction Preparation

*E. coli* cells growths were transformed with the construct pET22b-AidB. Bacterial culture was grown overnight in LB medium at 37 °C and it was diluted 1:100 in fresh medium containing ampicillin (100 µg/mL) and riboflavin (100 µM). At an A<sub>600 nm</sub> of 0.4, the culture was divided in two aliquots and one of these was supplemented with 0.04% MMS (methyl methane sulfonate) that has been shown to induce the adaptive response. After one cell duplication cellular pellets were collected. The cells were resuspended in 20 mM Na<sub>2</sub>HPO<sub>4</sub>, 20 mM Imidazole, 500 mM NaCl, 1 mM PMSF (phenil methane sulphonyl fluoride) (pH = 7.4), disrupted by passage through a french press and centrifuged at centrifugal force of 14,000 x g for 15 min at 4 °C. The supernatant was collected and protein concentration was determined with the Bio-Rad protein assay, using bovine serum albumine as standard.

### 2.2 Pull-Down Experiments

Isolation of AidB partners complex was performed by using His-Select<sup>TM</sup> Nickel (Sigma) containing Ni<sup>2+</sup> ions immobilized to bind His-tagged AidB. A control was carried out in order to discriminate between proteins that interact specifically with the Ni<sup>2+</sup> compared to those that bind in a nonspecific manner to the resin. For this reason, the stripping of the resin was executed by washing in 20 mM sodium phosphate, 0.5 M NaCl and 50 mM EDTA, for the purpose of removing Ni<sup>2+</sup> ions. In this way, the resin lost the ability to interact specifically with the tag of

histidines, but it was still able to establish nonspecific interactions. At this point, the resin was washed with 20 mM sodium phosphate, 0.5 M NaCl and 20 mM imidazole pH 7.4. The two protein extracts (2.5 mg) were incubated for 16 h at 4 °C with 100 µL of resin without nickel ions in the precleaning step. The extracts were then recovered and incubated with His-Select<sup>TM</sup> Nickel resin for 16 h at 4 °C to bind AidB by tag of histidines and to isolate its complexes. Both the precleaning and affinity chromatography resins were recovered and washed with 20 mM sodium phosphate, 0.5 M NaCl and 20 mM imidazole pH 7.4. The elution was performed with sample buffer. The samples were then subjected to SDS-PAGE (SDS-polyacrilamide gel electrophoresis).

### 2.3 *In Situ* Digestion

Protein bands stained with Coomassie brilliant blue were excised from the gel and destained by repetitive washes with 0.1 M NH<sub>4</sub>HCO<sub>3</sub> (pH 7.5) and acetonitrile. Samples were reduced by incubation with 50 µL of 10 mM DTT in 0.1 M NH<sub>4</sub>HCO<sub>3</sub> buffer (pH 7.5) and alkylated with 50 µL of 55 mM iodoacetamide in the same buffer. Enzymatic digestion was carried out with trypsin (12.5 ng/µL) in 10 mM ammonium bicarbonate (pH 7.8). Gel pieces were incubated at 4 °C for 2 h. Trypsin solution was then removed and a new aliquot of the digestion solution was added; samples were incubated for 18 h at 37 °C. A minimum reaction volume was used as to obtain the complete rehydration of the gel. Peptides were then extracted by washing the gel particles with 10 mM ammonium bicarbonate and 1% formic acid in 50% acetonitrile at room temperature.

### 2.4 LC/MS/MS (Liquid Chromatography Tandem Mass Spectrometry) Analyses

Tryptic peptide mixtures obtained from *in situ* digestions were analysed by LC/MS/MS using an HPLC-Chip/Q-TOF 6520 (Agilent Technologies).

The peptide mixtures were injected by auto sampler.



They were sent to the enrichment column of the chip at flow rate of 4  $\mu\text{L}/\text{min}$ , in 98% water, 2% acetonitrile and 0.1% formic acid. Subsequently the peptides were eluted directly into the capillary column (C18 reversed phase), at a flow rate of 0.4  $\mu\text{L}/\text{min}$ . The chromatographic separation was carried out with a linear gradient in 95% acetonitrile, 5% water and 0.1% formic acid. The eluate was then introduced in the ESI source for the tandem analysis. In this way each mass spectrum (range 300-2,400  $m/z$ ) was followed by one or more tandem mass spectra (range 100-2,000  $m/z$ ), obtained by fragmenting the most intense ions in each fraction eluted chromatographic. The acquired MS/MS spectra were transformed in Mascot generic file format and used for peptides identification with a licensed version of MASCOT (modular approach to software construction, operation and test, matrix science, USA), in a local database.

### 2.5 Construction of Expression Vectors

The bacterial strains and plasmids used in this work are all reported in Table 1. The UvrA, DeaD, RecA, TnaA and Ada genes of *E. coli* K12 were amplified from genomic DNA by PCR (polymerase chain reaction). To obtain proteins tagged with c-myc epitope, the corresponding amplification products were digested with BamHI and XhoI and cloned into the pET22b-c-myc vector [4], respectively. All plasmids (Table 1) containing the coding sequence for

the corresponding recombinant protein fused to a 6X histidine tag to facilitate protein purification by  $\text{Ni}^{2+}$  affinity chromatography. Plasmids construction was verified by automated DNA sequencing.

### 2.6 Production and Purification of Recombinant Proteins

Recombinant cells were grown at 37 °C to an OD (optical density) at 600 nm of about 0.5, at which time 0.05 mM isopropyl-beta-D-thiogalactopyranoside (IPTG) was added in order to express UvrA, DeaD, RecA, TnaA and Ada genes. Selective antibiotic was used at concentration of 100  $\mu\text{g}/\text{mL}$  ampicillin. After incubation, cells were harvested by centrifugation at centrifugal force of 5,000  $\times g$  for 15 min at 4 °C, resuspended in 50 mM  $\text{Na}_2\text{HPO}_4$ , 20 mM Imidazole, 500 mM NaCl, 1 mM PMSF (pH 7.4), disrupted by passage through a French press and centrifuged at centrifugal force of 14,000  $\times g$  for 30 min at 4 °C. Recombinant proteins were purified by affinity chromatography on His-Select Nickel Affinity Gel (Sigma). After 1 min of incubation at 4 °C, the matrix was collected by centrifugation at centrifugal force of 11,000  $\times g$  for 1 min and washed three times with same equilibration buffer. The recombinant proteins were eluted with buffer containing 500 mM imidazole in 20 mM  $\text{Na}_2\text{HPO}_4$ , pH 7.4, 0.5 M NaCl.

Protein concentration was estimated with Bradford reagent (Bio-Rad protein assay) and protein content

**Table 1 Bacterial strains and plasmids used.**

Strains/plasmids	Description	Reference or source
Strains		
C41 (DE3)	Strain that derives from BL21 [ <i>F<sub>ompT</sub> hsdSB (r<sub>B</sub>-m<sub>B</sub><sup>-</sup>) gal dcm</i> (DE3)]. This strain has at least one uncharacterized mutation that prevents cell death associated with expression of many toxic recombinant proteins.	Ref. [3]
Plasmids		
pET22b(+)	Carries an N-terminal <i>pelB</i> signal sequence for potential periplasmic localization, plus an optional C-terminal His-tag sequence	Novagen
pET22b-Ada	pET22b $\Delta$ (BamHI-XhoI) $\Omega$ (Ada gene)	This work
pET22b-DeaD	pET22b $\Delta$ (BamHI-XhoI) $\Omega$ (DeaD gene)	This work
pET22b-TnaA	pET22b $\Delta$ (BamHI-XhoI) $\Omega$ (TnaA gene)	This work
pET22b-UvrA	pET22b $\Delta$ (BamHI-XhoI) $\Omega$ (UvrA gene)	This work
pET22b-RecA	pET22b $\Delta$ (BamHI-XhoI) $\Omega$ (RecA gene)	This work

was checked by SDS-PAGE.

### 2.7 Co-Immunoprecipitation and Western Blotting

For co-immunoprecipitations, *E. coli* strain C41 (DE3) was transformed with the following constructs: pET22b-c-myc-Ada, pET22b-c-myc-TnaA, pET22b-c-myc-DeaD, pET22b-c-myc-RecA and pET22b-c-myc-UvrA. After expression of the recombinant genes without induction, cells were harvested, suspended in 50 mM Na<sub>2</sub>HPO<sub>4</sub> (pH 7.4), disrupted by passage through a French press and centrifuged at centrifugal force of 14,000 x g for 30 min at 4 °C. The supernatants were used for the co-immunoprecipitation experiments.

Cell lysates (0.5 mg) were incubated with agarose-linked c-myc antibody (Bethyl) and with agarose beads only (control of the experiment) at 4°C overnight. The beads were then collected by centrifugation. Precipitates were washed several times, the bound proteins were eluted with 1 × SDS-PAGE sample buffer and subjected to SDS-PAGE followed by Western Blot Analysis that was performed by using anti-AidB antibody (Primm, Milano Italy) and anti-c-myc mouse antibody (Calbiochem) as first antibodies and anti-mouse IgG conjugated to peroxidase as a secondary antibody (Calbiochem).

## 3. Results and Discussion

### 3.1 Isolation of AidB Complexes in *E. coli* Upon Exposure to MMS

*In vivo* isolation of AidB containing protein complexes were performed by transforming *E. coli* C41 strain with the pET22b-AidB construct carrying the AidB gene fused to a six histidine tags. The strain was grown in the absence and in the presence of sub-inhibitory concentrations of the alkylating agent MMS. Isolation of AidB complexes was performed by IMAC (ion metal affinity chromatography). The total protein extracts from the two samples were first submitted to a pre-cleaning step by incubation with

His-Select beads lacking nickel ions in order to remove non-specific proteins. Eluates from the pre-cleaning were then recovered and AidB containing complexes were isolated by IMAC on His Select beads. After extensive washing, the proteins specifically bound to AidB bait were eluted with a strong ionic buffer containing 0.5 M imidazole and fractionated on SDS-PAGE stained with coomassie blue. Pre-cleaning samples were also eluted and used as control. Fig. 1 shows the obtained Coomassie black stained gel.

### 3.2 Identification of Proteins Specifically Interacting with AidB

The entire lanes from both samples (3, 4) and controls (1, 2) were cut in 24 slices and each gel slice was *in situ* digested with trypsin and the corresponding peptide mixtures directly analysed by LC/MS/MS procedures. Tandem mass spectral analyses provided both the accurate molecular mass

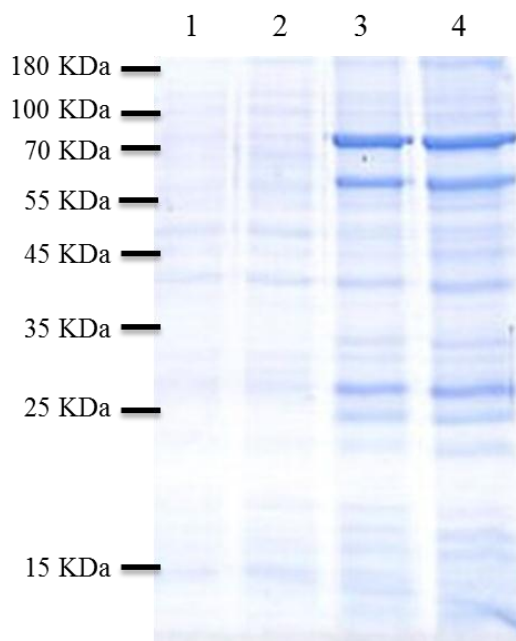


**Fig. 1** SDS-PAGE fractionation of AidB complexes. Lanes 1 and 2 pre-cleaning eluates. Lanes 3 and 4 AidB complexes in the absence and in the presence of MMS, respectively.

and sequence information from the daughter ion spectra of each peptide. These data were used for database searches using a home version of the Mascot

software leading to the identification of the proteins.

Common proteins identified in both the sample and the control gel slices were ruled out and only those solely occurring in the samples were considered as putative AidB inter-actors thus greatly decreasing the number of false positives. Proteins identified in the proteomic experiments are listed in Tables 2 and 3 where the protein name, the corresponding Swiss Prot code and the number of identified peptides are reported. The presence of the AidB bait in both lists constituted a sort of internal control indicating the correctness of the pull down experiment.

A total of 73 kinds of proteins were identified by the proteomic procedure, 17 of which were found both in the presence and in the absence of the methylating proteomic experiments are summarized in Tables 2 and 3. According to their reported biological activities, these identified inter-actors were grouped into different functional categories: metabolic

pathways including several FAD and NAD<sup>+</sup> dependent dehydrogenases, stress response and transcription, translation and processing of DNA/RNA. Among others, we focused our attention on the stress response proteins for further investigations.

### 3.3 Validation of Protein-protein Interactions by Co-immunoprecipitation Experiments

Putative protein-protein interactions detected by the proteomic experiments were validated by co-immunoprecipitation experiments. Proteins involved in pathways strictly connected with DNA repair and protection mechanisms were firstly examined. Each putative protein partner was recombinantly expressed as c-myc-tagged protein in *E. coli* C41 cells and the cell extracts were immunoprecipitated with anti-c-myc-conjugated antibody. Immunoprecipitates were fractionated by

**Table 2** Proteins identified in the control sample.

In the absence of MMS	Swiss prot code	Peptides
2-oxoglutarate dehydrogenase E1 component (SucA)	P0AFG3	2
Dihydrolipoyllysine-residue acetyltransferase component of pyruvate dehydrogenase complex (AceF)	P06959	6
Phosphoenolpyruvate synthase (PpsA)	P23538	2
Bifunctional polymyxin resistance protein <i>arnA</i> (ArnA)	P77398	42
Glucosamine-fructose-6-phosphate aminotransferase [isomerizing] (GlmS)	P17169	10
Phosphoenolpyruvate-protein phosphotransferase (PtsI)	P08839	3
Protein AidB	P33224	20
Alkyl hydroperoxide reductase subunit F (AhpF)	P35340	7
Glycogen synthase (GlgA)	POA6U8	11
UDP-N-acetylmuramate: L-alanyl-gamma-D-glutamyl-meso-diaminopimelate ligase ( <i>mpl</i> )	P37773	2
NADP-specific glutamate dehydrogenase ( <i>gdhA</i> )	P00370	12
3-oxoacyl-[acyl-carrier-protein] synthase 2 ( <i>fabF</i> )	P0AAI5	3
Transcriptional activator protein ( <i>lysR</i> )	P03030	9
Ribosomal small subunit pseudouridine synthase A ( <i>rsuA</i> )	P0AA43	11
UPF0011 protein <i>yraL</i> ( <i>yhbJ</i> )	P67087	6
Enoyl-[acyl-carrier-protein] reductase [NADH] ( <i>fabI</i> )	P0AEK4	2
Acyl-[acyl-carrier-protein]-UDP-N-acetylglucosamine O-acyltransferase ( <i>lpxA</i> )	P0A722	2
FKBP-type 22 kDa peptidyl-prolyl cis-trans isomerase ( <i>fkIB</i> )	P0A9L3	6
Catabolite gene activator ( <i>crp</i> )	P0ACJ8	22
UPF0011 protein <i>yraL</i> ( <i>yraL</i> )	P67087	2
Uncharacterized protein <i>yqjI</i> ( <i>yqjI</i> )	P64588	3
Uncharacterized protein <i>ybgA</i> ( <i>ybgA</i> )	P24252	2
Ferric uptake regulation protein ( <i>fur</i> )	P0A9A9	6
50S ribosomal protein L17 ( <i>rplQ</i> )	P0AG44	3

**Table 3** Proteins identified in the sample treated with 0.04% MMS.

In the presence of MMS	Swiss prot code	Peptides
UvrABC system protein A (UvrA)	P0A698	5
Aldehyde-alcohol dehydrogenase (AdhE)	P0A9Q7	2
Dihydrolipoyllysine-residue acetyltransferase component of pyruvate dehydrogenase complex (AceF)	P06959	5
Ribonucleoside-diphosphate reductase 1 subunit alpha (NrdA)	P00452	3
Maltodextrin phosphorylase (malP)	P00490	2
Bifunctional polymyxin resistance protein arnA (arnA)	P77398	37
Glucosamine-fructose-6-phosphate aminotransferase [isomerizing] (glmS)	P17169	20
Phosphoenolpyruvate-protein phosphotransferase (ptsI)	P08839	7
Cold-shock DEAD box protein A (DeaD)	P0A9P6	6
Succinate dehydrogenase flavoprotein subunit (sdhA)	P0AC41	3
GTP-binding protein typA/BipA (typA)	P32132	2
L-aspartate oxidase (NadB)	P10902	2
Chaperone protein hscA (hscA)	P0A6Z1	2
D-lactate dehydrogenase (dld)	P06149	2
Protein aidB (AidB)	P33224	19
Alkyl hydroperoxide reductase subunit F (ahpF)	P35340	9
Glucose-6-phosphate 1-dehydrogenase (zwf)	P0AC53	3
Glycogen synthase (glgA)	POA6U8	10
UDP-N-acetylmuramate: L-alanyl-gamma-D-glutamyl-meso-diaminopimelate ligase (mpl)	P37773	3
Tryptophanase (TnaA)	P0A853	2
NADP-specific glutamate dehydrogenase (gdhA)	P00370	24
3-oxoacyl-[acyl-carrier-protein] synthase 2 (fabF)	P0AAI5	4
3-oxoacyl-[acyl-carrier-protein] synthase 1 (fabB)	P0A953	5
Succinylornithine transaminase (astC)	P77581	13
UDP-N-acetylglucosamine 1-carboxyvinyltransferase (murA)	P0A749	11
Glutamate-1-semialdehyde 2,1-aminomutase (hemL)	P23893	4
S-adenosylmethionine synthetase (metK)	P0A817	5
Protein hflK (hflK)	P0ABC7	4
Isocitrate dehydrogenase [NADP] (icd)	P08200	2
Maltose/maltodextrin import ATP-binding protein malK (malK)	P68187	4
Transcription termination factor rho (rho)	P0AG30	3
ATP-dependent Clp protease ATP-binding subunit clpX (clpX)	P0A6H1	3
Cysteine desulfurase (iscS)	P0A6B8	3
Regulatory protein ada (ada)	P06134	9
Glycerol dehydrogenase (glgA)	P0A9S5	3
Acetylornithine deacetylase (arge)	P23908	4
Lactose operon repressor (laci)	P03023	3
Glutamate-1-semialdehyde 2,1-aminomutase (gsa)	P23893	2
USG-1 protein (usg)	P08390	2
Riboflavin biosynthesis protein RibD (RibD)	P25539	4
P-protein (pheA)	P0A9J8	3
UDP-4-amino-4-deoxy-L-arabinose—oxoglutarate aminotransferase (ArnB)	P77690	3
Glyceraldehyde-3-phosphate dehydrogenase A (gabA)	P0A9B2	13
Elongation factor Ts (tsf)	P0A6P1	8
UPF0042 nucleotide-binding protein yhbJ (yhbJ)	P0A894	6
Acetyl-coenzyme A carboxylase carboxyl transferase subunit beta (accD)	P0A9Q5	2
Aspartate carbamoyltransferase catalytic chain (pyrB)	P0A786	2
Ribosomal small subunit pseudouridine synthase A (rsuA)	P0AA43	12

(Table 3 continued.)

In the presence of MMS	Swiss Prot code	Peptides
Uncharacterized HTH-type transcriptional regulator yeiE (yeiE)	P0ACR4	10
UPF0042 nucleotide-binding protein yhbJ (yhbJ)	P0A894	11
Formyltetrahydrofolate deformylase (purU)	P0A440	10
UPF0011 protein yraL (yraL)	P67087	7
Enoyl-[acyl-carrier-protein] reductase [NADH] (fabI)	P0AEK4	2
Acyl-[acyl-carrier-protein]-UDP-N-acetylglucosamine O-acyltransferase (lpxA)	P0A722	3
D-methionine-binding lipoprotein metQ (metQ)	P28635	2
FKBP-type 22 kDa peptidyl-prolyl cis-trans isomerase (fkIB)	P0A9L3	6
GTP cyclohydrolase 1 (folE)	P0A6T5	2
Catabolite gene activator (crp)	P0ACJ8	21
Translation initiation factor IF-3 (infC)	P0A707	2
Uncharacterized protein yqjI (yqjI)	P64588	3
UPF0227 protein ycfP (ycfP)	P0A8E1	3
50S ribosomal protein L6 (rplF)	P0AG55	2
UPF0304 protein yfbU (yfbU)	P0A8W8	2
Ferric uptake regulation protein (fur)	P0A9A9	8
50S ribosomal protein L27 (rpmA)	P0A7L8	2
30S ribosomal protein S15 (rpsO)	P0ADZ4	3

SDS-PAGE and stained by Western blot analysis using an anti-AidB antibody. Interaction of the individual partner with AidB was confirmed by the presence of a positive signal revealed by the western blot analysis.

As an example, Fig. 2 shows the Western Blot Analysis performed on the immunoprecipitate from *E. coli* cells expressing c-myc tagged UvrA. Fig. 2a shows the total cell extract (lane 1) and the corresponding immunoprecipitate (lane 3) immunorevealed by anti c-myc antibody demonstrating that UvrA was expressed by the recombinant cells and immunoprecipitated by the antibody. Fig. 2b shows the positive signal detected when the UvrA immunoprecipitate was incubated with the anti-AidB antibody, demonstrating the presence of AidB in the sample and confirming the interaction.

Positive interactions of AidB with UvrA, DeaD and TnaA were identified, whereas no positive bands in the western blot could be detected when Ada and RecA proteins were tested.

It should be underlined that both Cold-shock DEAD box protein A (DeaD) and Tryptophanase (TnaA) had already been identified in complex with AidB in the

transcriptional machinery gathered at the *E. coli* *arnB* P1 promoter in the presence of MMS [4].

### 3.4 Discussion

The biological mechanism underlying the adaptive response to DNA alkylation damages in *E. coli* was extensively described. Sub inhibitory concentration of

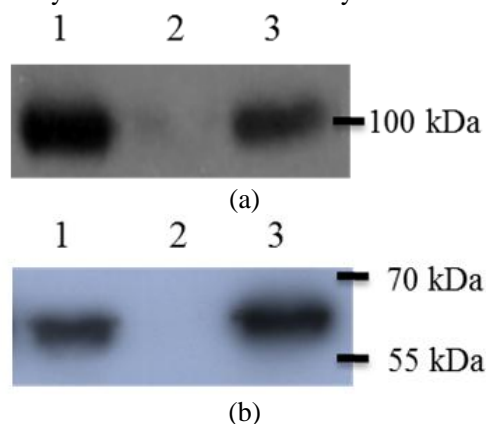


**Fig. 2** (a) Western blot analysis of the total cell extract from *E. coli* C41 cells producing c-myc-UvrA (lane 1) and the UvrA containing immunoprecipitate (lane 3). Lane 2 contains the precleaning; (b) Western blot analysis of the total cell extract from *E. coli* C41 cells (lane 1) and the UvrA immunoprecipitate revealed by the anti-AidB antibody (lane 3). Lane 2, precleaning.

methylating agents induces the expression of four genes (Ada, AlkA, AlkB, AidB) involved in the direct

repair of DNA alkylation damages. While the role of the first three proteins, Ada, AlkA and AlkB, was clearly defined [5], the involvement of AidB in this system has long been known but its specific role in the protection/repair of DNA is still obscure. Previous data demonstrate that AidB interacts with DNA very likely to protect the nucleic acid from alkylating molecules but it is not able to repair the DNA molecule following alkylation [4]. In addition, the protective action of AidB is preferentially expressed on DNA regions containing upstream elements. This observation led to the hypothesis that AidB might belong to a putative pathway of degradation of alkylating agents through its FAD dependent dehydrogenase activity. Alternatively, AidB might protect these DNA regions by physically interact with them thus impairing the dangerous action of alkylating agents.

Proteomic approaches were designed to shed some light on the mechanism of action of AidB through the identification of its protein partners *in vivo*. AidB partners were isolated by immunoprecipitation procedures both in the absence and in the presence of MMS as alkylating agent and the individual protein components identified by mass spectrometry. Several proteins were identified in both conditions, although the number of AidB molecular partners is considerably higher in the presence than in the absence of MMS.

Proteins identified under methylating stress conditions were grouped in three large categories according to their reported biological activities, stress response, energetic metabolic pathways, and nucleic acid metabolism (transcription, processing and translation). In particular, AidB was found to interact with UvrA whose expression is under the control of the SOS response system involved in DNA damages response [6]. This interaction was also validated by co-immunoprecipitation experiments confirming proteomic data. Interaction of these two proteins is very interesting since UvrA is part of the UvrABCD

nucleotide excision system involved in removing modified nucleotides as a result of several different DNA modifications including formation of covalent bonds, local unfolding, abnormal folds and variations in charge distribution [7]. UvrA works in a multienzyme complex with the specific role of examining the DNA molecule in search for modifications in order to allow the other proteins of the complex to perform the excision of the damaged nucleotides [8]. This protein is generally present at very low concentrations within the cell but its expression strongly increases under stress conditions [9]. Interaction of AidB with UvrA might then indicate that AidB is involved in different response complexes other than the Ada-dependent adaptive mechanism, suggesting new cellular strategies to minimize DNA damages.

In the presence of MMS, several other proteins belonging to metabolic pathways were identified suggesting a general mechanism of energy production developed by *E. coli* to counteract stress conditions. Among these, many AidB inter-actors are involved in the biosynthesis of fatty acids, indicating the occurrence of a possible mechanism of cell wall repair. It is likely, in fact, that besides DNA modifications, alkylating agents might produce damages to cell wall components thus inducing a specific response from the microorganism that enhances the metabolic synthesis of fatty acids in an attempt to repair or replace damaged membrane components thus strengthening the physical defenses of the cell.

#### 4. Conclusions

In conclusion, the data reported in this paper identified a novel interaction between AidB and UvrA which is a component of the UvrABCD system involved in DNA repair under several stress conditions delineating a new possible role for the AidB protein. Moreover, the identification of several proteins belonging to the fatty acid biosynthetic

pathway as AidB partners pointed out to a mechanism of cell wall consolidation as a new defense strategy of the cell against the poisonous effect of methylating agents.

## Acknowledgments

This paper was in part supported by PON01\_01802 and MIUR FIRB “Italian Human Proteome Net” RBRN07BMCT grants.

## References

- [1] Landini, P.; Hajec, L. I.; Volkert, M. R. Structure and Transcriptional Regulation of the *E. coli* Adaptive Response Gene AidB. *J. Bacteriol* **1994**, *176*, 6583-6589.
- [2] Bowles, T.; Metz, A. H.; Quin, J. O.; Wawrzak, Z.; Eichman, B. F. Structure and DNA Binding of Alkylation Response Protein AidB. *PNAS* **2008**, *105*, 15299-15304.
- [3] Rippa, V.; Duilio, A.; Pasquale, P.; Amoresano, A.; Landini, A.; Volkert, M. R. Preferential DNA Damage Prevention by the *E. coli* AidB Gene: A New Mechanism for Protection of Specific Genes. *DNA Repair* **2011**, *10*, 934-941.
- [4] Rippa, V.; Amoresano, A.; Esposito, C.; Landini, P.; Volkert, M.; Duilio, A. Specific DNA Binding and Regulation of Its Own Expression by the AidB Protein in *Escherichia coli*. *J. Bacteriol* **2010**, *192*(23), 6136-6142.
- [5] Miroux, B.; Walker, J. E. Over-Production of Proteins in *Escherichia coli*: Mutant Hosts That Allow Synthesis of Some Membrane Proteins and Globular Proteins at High Levels. *J. Mol. Biol.* **1996**, *260*, 289-298.
- [6] Sedgwick, B.; Lindahl, T. Recent Progress on the Ada Response for Inducible Repair of DNA Alkylation Damage. *Oncogene* **2002**, *21*, 8886-8894.
- [7] Croteau, D. L.; Della, V. M. J.; Perera, L.; Van, H. B. Cooperative Damage Recognition by UvrA and UvrB: Identification of UvrA Residues That Mediate DNA Binding. *DNA Repair* **2008**, *7*(3), 392-404.
- [8] Wagner, K.; Moolenaar, G. F.; Goosen, N. Role of the Insertion Domain and the Zinc-Finger Motif of *Escherichia coli* UvrA in Damage Recognition and ATP Hydrolysis. *DNA Repair* **2011**, *10*(5), 483-496.
- [9] Gu, C.; Zhang, Q.; Yang, Z.; Wang, Y.; Zou, Y.; Wang, Y. Recognition and Incision of Oxidative Intrastrand Cross-Link Lesions by UvrABC Nuclease. *Biochemistry* **2006**, *45*(35), 10739-10746.

## Ringraziamenti

E così, quasi all'improvviso, è arrivata la conclusione di questo lungo e articolato percorso. Guardandomi indietro vedo tante persone che, nel bene e nel male, hanno contribuito a rendermi la persona che sono oggi e mi sembra doveroso, per questo, rendere giustizia ad ognuno di voi. All'interno del gruppo BMA il mio cammino si è diviso tra i due mondi della spettrometria di massa e della biologia molecolare, con lo scopo di raggiungere una contaminazione reciproca; chi lo avrebbe mai ritenuto possibile?

Questo spunto mi permette di cominciare col ringraziare i miei capi, i Proff. Angela Duilio e Piero Pucci. Avete avuto fiducia in me fin dall'inizio, mi avete permesso di esplorare in piena libertà questi due mondi, permettendo la mia crescita scientifica e personale, nonostante i miei aculei! Posso vantare, come pochi, di avere avuto due mentori, che mi hanno insegnato come deve ragionare uno scienziato e come si può... allestire una scena del crimine! Potrebbe sempre tornarmi utile....

Francesca, il mio periodo di dottorato è stato contraddistinto dalla presenza quotidiana della tua confusionaria solarità. Sei stata la mia compagna di lavoro, insieme abbiamo diviso ogni momento, dalle lunghe ore in attesa che l'a-mycò crescesse, alle docce ghiacciate estive, dai battibecchi tanto esilaranti da richiamare pubblico, alla vetreria da lavare... no, quella è toccata solo a me! Dunque, vetreria a parte, grazie. Senza di te, sarebbe stato tutto più difficile, perché sei riuscita con la tua forza a rendere ogni istante migliore.

Gemma, la storia è iniziata con un armadietto in condivisione, è proseguita con una comunicazione assente e sembrava essersi conclusa con una certa autoclave della discordia. Viste le premesse, non avrei mai immaginato di trovarmi in tua compagnia ad arrampicarmi nel deposito plasticherie o a smontare, di notte, l'Explorer pezzo per pezzo. E così, a gran sorpresa, sei diventata un sostegno per me, una spalla vera su cui poter contare. Grazie per aver scelto, in questi anni, di appoggiarmi e di essermi accanto.

Quanti studenti mi sono trovata davanti... Siete troppi da elencare, ma meritate comunque un ringraziamento, siete stati in grado di darmi una motivazione in più. Avete reso la mia vita da dottoranda sempre movimentata e ricca di soddisfazioni.



Francesca Picca, sei stata la prima a lavorare con me al QQQ, grazie per avermi controllato nella compilazione della worklist. Michela Inverso, grazie per i pranzi esagerati che abbiamo diviso e per la presenza, a volte ingombrante, ma costante. Maura ed Angela, siete arrivate da poco, ma più di altri avete pagato lo scotto del mio squilibrio di fine dottorato. Un ringraziamento speciale è per Rossella, la mia vittima preferita. Sei una persona unica nel suo genere, sei riuscita a complicarmi la vita, ma alla fine, mi hai resa fiera di te.

Tutti voi ragazzi del gruppo BMA (stanze dei freddi, funghi, elettroforesi), avete arricchito ogni giornata trascorsa in questi laboratori che sono diventati una seconda casa per me. Passate e nuove generazioni di “massofili”, vi siete occupati di far crescere l’altra parte di me non solo dal punto di vista personale, ma anche dal punto di vista scientifico, per le ore di tempo macchina che mi avete regalato. Roberto, grazie per tutte le pause trascorse insieme, per tutte le volte che mi hai fatto arrabbiare, per tutto quello che è stato. Sei riuscito dove molti hanno fallito... mi hai reso caffeinomane.

Vorrei ringraziare Marianna Caterino del CEINGE di Napoli, il cui contributo scientifico è stato fondamentale per lo svolgimento dell’analisi DIGE.

Durante questi anni ho avuto la possibilità di svolgere diverse esperienze lontano da Napoli che hanno lasciato un segno indelebile nella mia vita. Innanzitutto devo ringraziare Thierry Douki del CEA di Grenoble, per la sua ospitalità e disponibilità durante il mio periodo trascorso all’estero. Insieme a lui, devo ringraziare il gruppo LAN ed in particolare Viviana De Rosa che mi ha aiutato con l’ostico francese.

Devo ringraziare ancora la Prof.ssa Zanetti del Dipartimento di Scienze Biomediche dell’Università di Sassari e tutto il suo gruppo. Un ringraziamento speciale a Paola Molicotti, Sara Cannas, Melania Ruggeri e Marina Cubeddu, perché mi avete mostrato quanto possa essere grande ed unica l’ospitalità sarda.

Voglio ringraziare anche il gruppo della Prof.ssa Laura Selan del Dipartimento di Sanità Pubblica e Malattie Infettive della Sapienza di Roma ed in particolar modo Rosanna Papa e Andrea Cellini, per la grande disponibilità mostratami nel periodo trascorso con voi.

Devo ringraziare ancora una triade di persone, che sono riuscite a starmi accanto, anche da chilometri di distanza.

Francesca, questo viaggio lo avremmo dovuto compiere insieme, ma il destino ci ha beffato, allontanandoti da Napoli. Siamo comunque riuscite a fare buon viso a cattivo gioco e la tua amicizia è, oggi come ieri, una solida certezza per me. Grazie delle interminabili discussioni telefoniche, scientifiche e non solo, che mi hai regalato.

Gabriella, grazie per le chiacchiere scambiate e per i consigli che mi hai dato. Anche se non sempre li ho seguiti, ti assicuro che ne ho fatto buon uso lo stesso.

Ilaria, sei sempre stata molto più di una sorella, la mia prima amica, l'unica persona capace di capire fino in fondo il mio essere. Grazie per l'appoggio e per le avventure vissute insieme.

I miei genitori, siete gli ultimi che voglio ringraziare, perché con voi tutto ha avuto inizio. Mi avete sostenuto quotidianamente, sopportato nei momenti di difficoltà e mostrato il modo giusto di intraprendere la vita. Non avete mai dubitato di me, grazie a voi.